MATERIALS DATA HANDBOOK

Stainless Steel Alloy A-286

Prepared by

R. F. Muraca
J. S. Whittick

June 1972

CR-123776

Prepared for

National Aeronautics and Space Administration
George C. Marshall Space Flight Center
Marshall Space Flight Center, Alabama 35812

Contract NAS8-26644

WESTERN APPLIED RESEARCH & DEVELOPMENT, INC.

1403-07 Industrial Road San Carlos, California 94070

PREFACE

This Materials Data Handbook on stainless steel alloy A-286 was prepared by Western Applied Research & Development, Inc. under contract with the National Aeronautics and Space Administration, George C. Marshall Space Flight Center, Marshall Space Flight Center, Alabama.

It is intended that this Handbook present, in the form of a single document, a summary of the materials property information presently available on alloy A-286.

The Handbook is divided into twelve (12) chapters. The scope of the information presented includes physical and mechanical property data at cryogenic, ambient, and elevated temperatures, supplemented with useful information in such areas as material procurement, metallurgy of the alloy, corrosion, environmental effects, fabrication and joining techniques. Design data are presented, as available, and these data are complemented with information on the typical behavior of the alloy. The major source used for the design data is the Department of Defense document, Military Handbook-5A.

Information on the alloy is given in the form of tables and figures, supplemented with descriptive text as appropriate. Source references for the information presented are listed at the end of each chapter.

Throughout the text, tables, and figures, common engineering units (with which measurements were made) are accompanied by conversions to International (SI) Units, except in the instances where double units would over-complicate data presentation, or where SI units are impractical (e.g., machine tools and machining). In these instances, conversion factors are noted. A primary exception to the use of SI units is the conversion of 1000 pounds per square inch to kilograms per square millimeter rather than newtons, in agreement with the ASTM that this unit is of a more practical nature for worldwide use.

ACNOWLEDGMENTS

This "Materials Data Handbook: Stainless Steel Alloy A-286" was prepared by Western Applied Research & Development, Inc. under Contract No. NAS8-26644 for the George C. Marshall Space Flight Center of the National Aeronautics and Space Administration. The work was administered under the technical direction of the Astronautics Laboratory, Materials Division of the George C. Marshall Space Flight Center with Mr. Wayne R. Morgan acting as Project Manager.

Sincere appreciation is tendered to the many commercial organizations and Government agencies who have assisted in the preparation of this document.

TABLE OF CONTENTS

TABULAR ABSTRACT

Stainless Steel Alloy A-286

TYPE:

Precipitation hardening, heat treatable, austenitic stainless steel

NOMINAL COMPOSITION:

Fe-15Cr-25Ni-2.1Ti-1.2Mo-0.2Al

AVAILABILITY:

Sheet, plate, bar, tubing, forgings, castings, wire, rivets, bolts, and screws

TYPICAL PHYSICAL PROPERTIES:

Density	7.94 g/cm^3 at room temperature
Thermal Conductivity	0.057 cal/cm^2/sec/cm/$^\circ$C at 600°C
Av. Coeff. of Thermal Exapnsion	17.0 μcm/cm/$^\circ$C at 600°C
Specific Heat	0.11 cal/cm^2 $^\circ$C (20–700°C)
Electrical Resistivity	91.0 microhm-cm at 30.6°C

TYPICAL MECHANICAL PROPERTIES:

F_{tu}, 1800°F (982°C) plus age*	145 ksi (102 kg/mm^2)
1650°F (899°C) plus age	157 ksi (110 kg/mm^2)
F_{ty}, 1800°F plus age	95 ksi (67 kg/mm^2)
1650°F plus age	102 ksi (72 kg/mm^2)
e(2 in or 4D), 1800°F plus age	24 percent
1650°F plus age	25 percent
E (tension)	29.1 x 10^3 ksi (20.5 x 10^3 kg/mm^2)

FABRICATION CHARACTERISTICS:

Weldability	More difficult than austenitic stainless steels; easiest of PH stainless steels (fusion and resistance methods)
Formability	Similar to austenitic steels, but slightly more resistant
Machinability	Same as for 300 series of stainless steels, but at slower rates

COMMENTS:

A superalloy, with high strength, good resistance to corrosion and oxidation, and low relaxation, for service at temperatures as high as 1300 $^\circ$F (704°C); also excellent properties at cryogenic temperatures.

* 1325°F (718°C)

SYMBOLS

a	One-half notch section dimension
A	Area of cross section; "A" basis for mechanical property values (MIL-HDBK-5A)
Å	Angstrom unit
AC	Air cool
AMS	Aerospace Material Specifications
Ann	Annealed
ASTM	American Society for Testing Methods
Av or Avg	Average
B	"B" basis for mechanical property values (MIL-HDBK-5A)
b	Subscript "bending"
bcc	Body centered cubic
BHN	Brinell hardness number
br	Subscript "bearing"
Btu	British thermal unit(s)
°C	Degree(s) Celsius
c	Subscript "compression"
CD	Cold drawn
CF	Cold finished
cm	Centimeter
c_p	Specific heat
CR	Cold rolled
CW	Cold worked
CVM	Consumable vacuum melted
D or Dia	Diameter
DPH	Diamond pyramid hardness
e	Elongation in percent
E	Modulus of elasticity, tension
E_c	Modulus of elasticity, compression
e/D	Ratio of edge distance to hole diameter
E_s	Secant modulus
E_t	Tangent modulus
eV	Electron volt(s)
°F	Degree(s) Fahrenheit
f	Subscript "fatigue"
F_{bru}	Bearing ultimate strength
F_{bry}	Bearing yield strength

fcc	Face centered cubic
FC	Furnace cool
F_{cy}	Compressive yield strength
F_{su}	Shear stress; shear strength
F_{tu}	Ultimate tensile strength
F_{ty}	0.2% tensile yield strength (unless otherwise indicated)
g	Gram
G	Modulus of rigidity
HAZ	Heat affected zone in weldments
hcp	Hexagonal close pack
hr	Hour(s)
HT	Heat treat
IACS	International annealed copper standard
in	Inch
ipm	Inches per minute
^{o}K	Degree(s) Kelvin
K	Stress intensity factor; thermal conductivity
K_c	Measure of fracture toughness (plane stress) at point of crack growth instability
kg	Kilogram
K_{Ic}	Plane strain fracture toughness value
ksi	Thousand pounds per square inch
K_t	Theoretical elastic stress concentration factor
L	Longitudinal
lb	Pound
LT	Long transverse (same as transverse)
M	Bending moment
m	Meter
M	Subscript "mean"
Max	Maximum
ml	Milliliter
MIL	Military
Min	Minimum
mm	Millimeter
N	Cycles to failure
NSR	Notch strength ratio
NTS	Notch tensile strength
OQ	Oil quench
ppm	Parts per million
pt	Point; part

r	Radius
RA	Reduction in area; Rockwell hardness A scale
RB	Rockwell hardness B scale
RC	Rockwell hardness C scale
rpm	Revolutions per minute
RT	Room temperature
SA	Solution anneal
sec	Second
S-N	S = stress; N = number of cycles
Spec	Specifications; specimen
ST	Solution treat; short transverse
STA	Solution treated and aged
T	Transverse
t	Thickness; time
Temp	Temperature
typ	Typical
Var	Variable
VHN	Vickers hardness number
W	Width
WQ	Water quench

CONVERSION FACTORS

To Convert	To	Multiply By
angstrom units	millimeters	1×10^{-7}
Btu/lb/°F	cal/g/°C	1
Btu/ft²/sec/°F-inch	cal/g/cm²/sec/°C-cm	1.2404
circular mil	square centimeters	$5.067\ 075 \times 10^{-6}$
cubic feet	cubic meters	0.028 317
cubic feet/minute	liters/second	0.4720
cubic inches	cubic centimeters	16.387 162
feet	meters	0.304 800 609
foot-pounds	kilogram-meters	0.138 255
gallons (U.S.)	liters	3.785 411 784
inches	millimeters	25.4
ksi (thousand pounds per square inch	kilograms/square millimeter	0.70307
microns	millimeters	0.001
mils	millimeters	0.0254
ounces (avoir.)	grams	28.349 527
ounces (U.S. fluid)	milliliters	29.5729
pounds (avoir.)	kilograms	0.453 592 37
pounds/foot	kilograms/meter	1.488 16
pounds/cubic foot	grams/cubic centimeter	0.016 018 463
square feet (U.S.)	square meters	0.092 903 41
square inches (U.S.)	square centimeters	6.451 625 8

Temperature in °C = (°F − 32) (5/9)

Temperature in °K = °C + 273.15

Chapter 1

GENERAL INFORMATION

1.1 Alloy A-286 is a precipitation-hardening, heat-treatable, austenitic stainless steel developed as an improvement on the German alloy "Tinidur." As a "superalloy" or "heat-resistant alloy," it has been designed for service at temperatures as high as 1300°F (704°C) for applications requiring high strength and good resistance to corrosion at operating temperatures, and for service at higher temperatures where applications are at lower stresses.

1.2 Hot-working characteristics resemble those of other stainless steels rather than other superalloys. Machinability of A-286 is similar to that of other austenitic steels, including "gumming," in the soft solution-treated condition. The alloy is welded readily by shielded-arc and inert-gas-arc techniques; however, it is recommended that the material be in an essentially stress-free solution-treated condition prior to welding.

1.3 Good resistance has been shown against all atmospheres encountered in jet engines and turbo supercharger service up to at least 1300°F (704°C). Excellent performance is shown in 20-percent salt spray corrosion tests. The high nickel content affords more resistance to dilute, cool sulfuric acid solutions than 18-8 stainless steels.

1.4 Typical areas of application include structures for jet engines and superchargers, turbine wheels and blades, frames, castings, and afterburner parts. Alloy A-286 is particularly attractive for applications as fasteners and springs for elevated-temperature service because of relatively low stress-relaxation or loss of load in operations.

1.5 Precautions. Intergranular corrosion may occur in the aged condition, and care must be used in pickling with HNO_3—HF solutions after aging. Resistance to corrosion is not good in strong, selective environments such as in HNO_3—HF mixtures and boiling 65 percent sulfuric acid.

Chapter 1 - References

1.1 American Iron and Steel Institute, "High-Temperature High-Strength Alloys," AISI, February 1963.

1.2 Alloy Digest, "Allegheny A-286" (Filing Code SS-4), Engineering Alloys Digest, Inc., New Jersey, December 1952.

1.3 ASTM STP-160, "A-286 Alloy," August 1954, p. 70.

1.4 Allegheny Ludlum Steel Corporation, "A-286," Product Bulletin.

1.5 Carpenter Technology Corporation, "Carpenter A-286," Technical Data, June 1970.

1.6 Univeral-Cyclops/Specialty Steel Division, "Unitemp A-286," HT-3020, 1971.

1.7 Superior Tube, "Super Alloy Tubing," Bulletin 71, June 1968.

1.8 J.G. Sessler and H.G. Weiss, Eds., "Aerospace Structural Metals Handbook," AFML TR 68-115, 1971 Edition, Vol. I.

1.9 DMIC Memorandum 245, "Current and Future Usage of Materials in Aircraft Gas Turbine Engines," February 1, 1970.

Chapter 2

PROCUREMENT INFORMATION

2.1 General

Alloy A-286 is available as billets, bars, forgings, sheet, plate, strip, shapes, and tubing (refs. 2.1 through 2.5).

2.11 Alternate designation. American Iron and Steel Institute, AISI 660.

2.2 Procurement Specifications

AMS specifications that apply specifically to A-286 are listed in table 2.2. There are no specific Military or ASTM specifications.

2.3 Major Producers of the Alloy (United States only) include:

Altemp A-286	Allegheny Ludlum Steel Corporation Oliver Building Pittsburgh, Pennsylvania
Carpenter A-286	Carpenter Technology Corporation 150 W. Bern Street Reading, Pennsylvania
A-286	Republic Steel Corporation Special Metals Division Massilon, Ohio
A-286	Superior Tube 1938 Germantown Avenue Norristown, Pennsylvania
Unitemp A-286	Universal-Cyclops Specialty Steel Division 650 Washington Road Pittsburgh, Pennsylvania

2.4 Available Forms, Sizes, and Conditions

See table 2.2 for information on available forms and conditions. Consult producers for details on available sizes and purchase information.

TABLE 2.2. — AMS Specifications for Various Forms of Alloy

Source	Ref. 2.6	
Alloy	A-286	
Spec. No.	Item	Condition
5525C	Sheet, strip, and plate	Sol HT
5731D	Bars, forgings, tubing, and rings	Cons elec melted, 1800° F(982° C) sol treated
5732C	Bars, forgings, tubing and rings	Cons elec melted, 1800° F(982° C) sol and prec treated
5734C	Bars, forgings, and tubing	Cons elec melted, 1650° F(899° C) sol HT
5735G	Bars, forgings, tubing, and rings	1800° F(982° C) sol and prec HT
5736F	Bars, forgings, tubing, and rings	1800° F(982° C) sol treated
5737E	Bars, forgings, and tubing	Cons elec melted, 1650° F(899° C) sol HT and prec HT
5804B	Welding wire	Cold drawn, as drawn
5805B	Welding wire	Vac melted, cold drawn, as drawn
7235A	Rivets	1650° F(899° C) sol and partial prec HT
7477B	Bolts and screws	Upset headed, HT, roll-threaded, sol and prec HT
7478G	Bolts and screws	HT, roll-threaded, sol and prec HT
7479C	Bolts and screws	HT, roll-threaded, 1650° F(899° C) HT
7481A	Studs	HT, roll-threaded
7490J	Rings, flash-welded	--

Note: Specifications as of May 1971.

Chapter 2 - References

2.1 Alloy Digest, "Allegheny A-286," (Filing Code SS-4), Engineering Alloys Digest, Inc., New Jersey, December 1952.

2.2 Allegheny Ludlum Steel Corp., "A-286," Product Bulletin.

2.3 Superior Tube, "Super Alloy Tubing," Bulletin 71, June 1968.

2.4 Carpenter Technology Corp., "Unitemp A-286," Technical Data, June 1970.

2.5 Universal-Cyclops Specialty Steel Div., "Unitemp A-286," HT-3020, 1971.

2.6 Aerospace Material Specifications, Society Automotive Engineers, Inc., New York; latest Index, May 1971.

Chapter 3

METALLURGY

3.1 Chemical Composition

3.11 Nominal chemical composition. Published values for "typical chemical composition" (refs. 3.2–3.13) have been averaged and rounded to provide the nominal chemical composition in percent listed below:

C	0.05	Mo	1.20
Mn	1.33	Ti	2.14
Si	0.55	B	0.0005
Cr	15.0	V	0.26
Ni	25.4	Al	0.21
Fe	Balance		

3.12 Chemical composition range. The ranges of element concentration in percent listed below have been derived from the highest and lowest values reported as typical chemical compositions or ranges (refs. 3.2–3.16):

C	0.05 - 0.08	Ni	24.0 - 27.0
Mn	1.00 - 2.00	Mo	1.0 - 1.75
Si	0.40 - 1.00	Ti	1.75 - 2.60
P	0.02 - 0.04	B	0.002- 0.015
S	0.01 - 0.02	V	0.10 - 0.50
Cr	13.5 - 16.0	Al	0.16 - 0.36
Fe	Balance		

3.13 Chemical composition limits. AMS specified composition limits for A-286 are given in table 3.13 according to the requirements for various forms.

3.14 Alloying elements. The principal alloying elements are nickel and chromium. Phase diagrams for the iron-chromium-nickel system at room and elevated temperatures are given in figure 3.14.

The nickel provides strenghtening, stabilizes the fcc matrix, forms γ' and inhibits formation of deleterious phases; it is present in sufficient quantity to favor the austenitic structure and to reduce the temperature at which austenite transforms to martensite so that the austenite is retained on cooling to room temperature and even to cryogenic temperatures. Chromium provides resistance to oxidation as well as solid-solution strengthening (refs. 3.8, 3.17).

Aluminum and titanium are the primary hardener elements. By suitable heat treatment, they precipitate intermetallic phases such as ordered fcc γ' [$Ni_3(Ti, Al)$] from the matrix to provide high proof-stress at elevated temperatures (refs. 3.4, 3.8, 3.18).

3.2 Strengthening Mechanisms

3.21 General. Optimum properties of A-286 are obtained by heat treating and aging (precipitation hardening). Thus, it is not necessary to work it in the temperature range of 1000° to 1500° F (538° to 816° C) to produce high yield strengths as is required for other high-temperature alloys. (However, cold working affects some properties after aging so that modified heat treatments may be required.) Solution treatment at 1800° F (982° C) provides optimum stress-rupture properties after aging; solution treatment at 1650° F (899° C) provides maximum room temperature yield strength or short-time properties. After solution treating, A-286 is soft (about 150–160 BHN) and is in its most ductile condition. Aging at 1300°–1400° F (704°–760° C) results in an increase of hardness to 260–340 BHN. The high strength of the alloy is developed during the aging treatment by the random formation of a fine precipitate of [$Ni_3(Ti, Al)$] in the austenitic matrix (Refs. 3.3, 3.5, 3.6, 3.9, 3.15, 3.19).

3.22 Precipitation Hardening. A great number of investigations have been made on the strengthening mechanisms and microstructure of iron-base superalloys such as A-286. In one of these studies (ref. 3.20), it was shown that (a) A small Al content (up to 1 percent) increases the amount of age hardening of a Ti-bearing steel, but further additions decrease the amount; (b) Increase of Ti content at any Al content increases age hardening; (c) The amount of aging in a Ni-Al-Ti steel is greater than can be obtained with the single addition of similar amounts of Al and Ti; (d) The optimum composition for a 25Ni-15Cr steel would contain 1 percent Al and 2.5 percent Ti. The precipitating phase for this composition was identified as $Ni_3(Al, Ti)$.

In a study of the mechanical properties of austenitic steels containing γ' precipitate [$Ni_3(Ti, Al)$], it was determined that a large increase in proof-stress occurs during aging as a result of particle growth at almost constant volume fraction of precipitate. Up to the peak proof-stress, dislocations are paired because of the high antiphase-domain boundary energy, and this accounts satisfactorily for the increasing proof-stress. The value of the antiphase domain boundary energy is higher at higher Ti/Al ratios. Misfits between 0 and 0.4 percent have no effect on yield strength. During an Orowan looping process, which bypasses large particles, a transition occurs from paired to single dislocations that reduces the fall in stress with increasing particle size. A back stress detectable at low strains arises from stable Orowan loops and causes work-hardening. More marked work-hardening associated with debris in the slip planes is shown by alloys with high Ti/Al ratios (e.g., A-286), apparently a result of bypassing of particles by cross-slip which gives rise to complex slip interactions (ref. 3.4).

Aging at about 700° C causes the formation of the desirable strengthening γ' phase [$Ni_3(Ti, Al)$]. However, aging at higher temperatures, for example 800° C, or overaging, can cause the formation of a cellular precipitate, hexagonal η Ni_3Ti. A large amount of the η phase is considered undesirable because it leads to low ductility, particularly creep ductility (refs. 3.8, 3.20). In overaged alloys, deformation has caused the loss of coherency between the γ' and the austenite; slip was observed primarily in the γ'-austenite regions, but fracture of the cellular colonies was observed at large deformations (ref. 3.21). On the other hand, cellular precipitation can be considered a fairly stable form of dispersion hardening and thus show resistance to overaging, which can be useful in maintaining high-strength levels after aging or during testing at elevated temperatures (ref. 3.20). It has been suggested that the η Ni_3Ti phase be used to advantage to control the microstructure and properties of superalloys (ref. 3.11).

3.23 Solid-Solution Strengthening. It has been shown that solid-solution hardening is slight with respect to room-temperature properties of A-286. However, the presence of certain elements in the alloy can promote the strengthening of properties at elevated temperatures. These elements, generally interstitial in nature, also alter the lattice parameter of the fcc matrix, and thus the degree of hardening produced by a precipitate can be affected by means of the magnitude of developed coherency strains. For example, boron retards formation of η and markedly improves stress-rupture properties. Molybdenum and chromium are also solid-solution strengtheners (refs. 3.8, 3.18, 3.20).

3.24 Heat Treatment. The strength of alloy A-286 is obtained by a solution heat treatment (annealing) followed by an aging (precipitation hardening) treatment. Recommended treatments are given in the following subsections (refs. 3.1, 3.6, 3.15, 3.19).

3.241 Solution treatment for optimum stress-rupture properties.
Bars and forgings: heat to 1800°F (982°C), hold 1 hr at heat, cool rapidly.
Sheet and strip: heat to 1800°F (982°C), hold for 1 hr per inch (25.4 mm) of thickness, cool rapidly.
Large sections are oil- or water-quenched from the solution temperature. Sheet and strip may be water quenched or fan cooled if distortion must be held to a minimum.

3.242 Solution treatment for optimum short-time tensile properties.
Heat to 1650°F (899°C), hold 1 to 2 hours at heat, cool rapidly.

3.243 Aging treatment.
Heat to 1300° to 1400°F (704° to 760°C), hold 12 to 16 hours at heat and cool rapidly. A temperature of 1325°F (718°C) is generally used.

3.244 The effect of age-hardening on the properties of A-286 sheet at cryogenic temperatures is illustrated in figure 3.244.

3.25 Cold Working. Alloy A-286 may also be strengthened by cold working prior to aging; for example, tensile strengths of 150 to about 220 ksi (105 to 155 kg/mm²) are developed by cold reducing in amounts up to 60 percent and then aging in the range 1200° to 1300° F (647° to 704° C). As a general rule, as the amount of cold work is increased, the aging temperature should be lowered for maximum hardness and short-time tensile strength. Cold working affects mechanical properties because of its influence on grain-size growth and the reaction kinetics of aging. The critical amount of cold work must exceed 1 to 6 percent to avoid the growth of abnormally large grains. As far as the rate of hardening is concerned, A-286 may be reduced as much as 90 percent before a softening treatment is required (refs. 3.6, 3.19). The effect of cold working on room-temperature tensile strength of A-286 compared with stainless steel Type 302 is shown in figure 3.25.

3.251 The effect of aging temperature and cold-reduction on the hardness of A-286 is illustrated in figure 3.251. The effect of cold reduction and aging temperature on the tensile properties of A-286 is presented in table 3.251.

3.252 A double-aging treatment, that is, aging temperatures higher than normal followed by a second aging cycle at temperatures lower than normal, is somtimes used to obtain uniformity of properties in parts that have been cold-worked nonuniformly. In these instances, for A-286 parts with varying amounts of cold work, double-aging at 1400° F (760° C) and 1300° F (704° C), respectively, provides more uniform short-time tensile properties, hardness, and creep rupture properties than the usual single aging treatment at 1325° F (718° C); structural stability of the part in service is also improved (ref. 3.19). An example of the effect of double aging is given in table 3.252.

3.26 Stress Relief. Heat-resistant alloys, such as A-286, cannot be stress-relieved because the intermediate temperatures result in aging. Hence, in order to restore ductility and reduce stresses in cold-formed parts and weldments, the alloy is heated rapidly to the annealing (solution-treating) temperature. In forgings, finishing temperature is usually above 1700° F (926° C) so that stress-relieving is not required for as-forged parts (ref. 3.19).

3.3 Critical Temperatures

Melting range, 1371°–1426° C (2500°–2600° F) (refs. 3.6, 3.9). Intermetallic precipitation reaction, 750° to 800° C (1382°–1472° F) (ref. 3.20).

3.4 Crystal Structure

Alloy A-286 has a face-centered-cubic (fcc) matrix (austenite) strengthened by gamma prime precipitation, with a tendency to form topologically close packed phases such as sigma, mu, Laves, and chi (refs. 3.8, 3.13). The properties of precipitated intermetallic phases are given in table 3.4.

3.5 Microstructure

General. The structure of the austenitic solid solution in A-286 is modified by most of the elements added for precipitation hardening, and there is some correlation of lattice parameter with atomic size of the substitutional element. The size effect is important to solid solution strengthening and affords control by deliberate mismatch of alloying elements over the coherency strains resulting from precipitation hardening. Aluminum and titanium are potent substitutional elements. There is a propensity for stacking faults in A-286, although dislocation content is low. Stacking fault energy is lowered by chromium, molybdenum, and titanium, and increased by nickel. The effects of stacking fault changes will be seen in the nucleation and growth of precipitates as well as in the resistance to deformation by the austenite (ref. 3.13).

3.51 Gamma Prime (γ') Phase. The importance of the γ' phase is unique because it is only a titanium transition phase, based on ordered fcc [$Ni_3(Ti, Al)$];the equilibrium phase is η (Ni_3Ti). The γ' is the major hardening phase in A-286, and is the most important intermetallic compound because of its natural morphology with small interparticle distance, preference for general precipitation and large volume percent. Other favorable factors include the high ductility of the phase compared with minor precipitates and the coherency with the austenitic matrix because of close lattice matching. It forms as spherical precipitates (see figure 3.51) that have a low surface energy (refs. 3.8, 3.13, 3.20, 3.21).

3.52 Eta (η) Phase. In the approach to equilibrium, the γ' transition phase is replaced by η phase, hexagonal Ni_3Ti (see figure 3.52). As a cellular precipitate, forming in the range of 750°–1800°F (399°–982°C), it is nucleated at grain boundaries and can be detrimental to notched stress-rupture strength. Precipitation may also occur as Windmanstatten intergranular η which reduces hardness, strength, and physical properties, but not ductility. The presence of boron and aluminum retards both modes of formation (refs. 3.8, 3.13, 3.18, 3.21).

3.53 Beta (β) Phase. For best mechanical properties, β phase [$Ni(Al, Ti)$] should be avoided. It precipitates in a few hours at 1100°–1500°F (593°–816°C), but rapidly overages to massive plates (see figure 3.53) with large spacing values because of lattice disregistry.

3.54 Laves Phase. Austenitic steels are embrittled by the Laves phase at room temperature, but there is little effect at elevated temperatures; for example, Laves phase was found in the grain boundaries of A-286 with no influence on properties at 1100°F (593°C). The phase is precipitated from 1200°–2000°F (649°–1093°C) in a morphology that varies from general intergranular precipitation to grain boundary forms. It has been shown that nickel-containing phases

(γ', η, G) in A-286 can deplete the matrix composition in nickel and pave the way for Laves phase precipitation (ref. 3.13).

3.55 Chi (χ) Phase. The χ phase appears in the temperature region of 1200° – 1750° F (649° – 954° C) with aging times longer than 10 hours; the unit cell structure is $(Fe_{27}Ni_8Cr_{13})(Mo_{6.5}Ti_{4.5})$. The massive, blocky morphology of the χ phase at grain boundaries is not expected to contribute to hardening (refs. 3.13, 3.23).

3.56 Sigma (σ) Phase. The σ phase is a most well-known phase in iron-based austenites. Formation of σ, after prolonged times at 900° – 1700° F (482° – 926° C), is minimized by nickel, promoted by chromium, and stabilized by silicon. The σ phase can cause embrittlement at room or elevated temperatures to an extent influenced by the amount and distribution of the phase. A continuous grain boundary σ can be detrimental, but blocky morphology in fine-grained austenite can increase creep ductility (ref. 3.13).

3.57 G Phase. A common elemental composition for the G-phase, based on work with A-286, involves nickel, titanium, and silicon. G phase may be found after solution treatment; if not, aging more than 100 hours at 1200° – 1550° F (649° – 843° C) is required for formation. The morphology is generally globular at grain boundaries (see figure 3.57). This phase has little effect on room-temperature impact energy or short-time tensile properties at 1200° F (649° C); however, microcracking has been found in A-286 at the G phase—grain boundary interfaces in stress-rupture at 1200° F (refs. 3.8, 3.13).

3.6 Metallographic Procedures

3.61 General. The techniques for preparing A-286 specimens for examination of structure by optical microscopy are essentially those used for other austenitic stainless steels. For example, specimens may be polished mechanically by grinding to an 80- or 120-grit finish on a grinding belt or wheel and then polishing with successively finer emery papers (ref. 3.24). Alternatively, specimens may be electropolished, which eliminates difficulties of distortion and the collection of chips or particles on the metal surface that might arise from mechanical polishing, but may lead to unsatisfactory relief effects when large particles are present (ref. 3.25). Etching of specimens may also be performed as for stainless steels, by immersion or by electrolytic techniques. Details of etchant solutions are provided in reference 3.26 and the Marshall Space Flight Center "Materials Data Handbook: Stainless Steel Type 301." The techniques and agents described in the following subsections are those that have been used for recent, specific examinations of A-286.

3.62 Optical Microscopy. In a study of cyclic-strain-induced oxidation of A-286 and similar alloys, a macroetch of concentrated aqua regia was used first to reveal grain boundaries. For subsequent microscopic examination to reveal localized oxidation, a microetchant was used that consisted of 10 parts nitric acid, 10 parts acetic acid, and 5 parts hydrochloric acid (ref. 3.27).

3.63 Electron Microscopy. Intergranular precipitation of intermetallic compounds was studied by electron microscopy and x-ray diffraction (ref. 3.23). Specimens for electron microscopy were mechanically polished and then etched in a freshly-mixed solution of 92 percent hydrochloric acid, 5 percent sulfuric acid, and 3 percent nitric acid. Parlodion replicas were chromium-shadowed in high vacuum at a glancing angle of 20 degrees.

For a study of the interaction between dislocations and intermetallic precipitates, tensile strip specimens were electropolished and then etched electrolytically in a 10 percent oxalic acid solution to reveal the structure of the steel (ref. 3.21). (The procedure for electrolytic etching with oxalic acid is given in reference 3.24.) A two-stage replication procedure was used for electron microscopic examination of slip markings at different stages during deformation. The procedure involved a formvar replica of the specimen shadowed by a gold-palladium alloy and subsequent preparation of a carbon replica from the shadowed formvar replica. For transmission electron microscopy, specimen strips were chemically thinned to about 0.005 inch (0.127 mm) thickness and then electropolished with a standard acetic acid—perchloric acid solution.

Tensile strip specimens and aged sheet were examined in a study of the strengthening mechanisms in γ'-precipitating alloys (ref. 3.4). The tensile specimens were chemically thinned to 0.5-mm slices. Foils were prepared by dishing in 20 percent sulfuric acid at 50V and finally polishing in 10 percent perchloric acid in methanol at 12V.

TABLE 3.13. — Variation in AMS Specifications for Composition Limits

Source	Ref. 3.1							
Alloy	A-286							
Spec. No.(a)	5525C 5736F		5731C, 5734D 5735G, 5737E		5804B		5805B	
Element (b)	min	max	min	max	min	max	min	max
Carbon	-	0.08	-	0.08	-	0.08	-	0.08
Manganese	-	2.00	-	2.00	-	2.00	-	2.00
Silicon	-	1.00	-	1.00	-	1.00	-	1.00
Phosphorus*	-	0.025	-	0.025	-	0.020	-	0.010
Sulfur*	-	0.025	-	0.025	-	0.015	-	0.010
Chromium	13.50	27.00	13.50	16.00	13.50	16.00	13.50	16.00
Nickel	24.00	27.00	24.00	27.00	24.00	27.00	24.00	27.00
Molybdenum	1.00	1.50	1.00	1.50	1.00	1.50	1.00	1.50
Titanium*	1.90	2.30	1.90	2.35	2.00	2.45	2.00	2.45
Boron	0.0030	0.010	0.0030	0.010	0.0030	0.010	0.0030	0.010
Vanadium	0.10	0.50	0.10	0.50	0.10	0.50	0.10	0.50
Aluminum	-	0.35	-	0.35	-	0.35	-	0.35
Oxygen*	-	-	-	-	-	-	-	0.005
Hydrogen*	-	-	-	-	-	-	-	0.0005

* Indicates element variations

(a) See table 2.1 for description of specifications.

(b) Specifications that apply to chemical analysis are:

AMS 2248, Chemical Check Analysis Limits, Wrought Heat and Corrosion R sistant Steels and Alloys.

ASTM E353, Chemical Analysis of Stainless, Heat Resisting, Maraging, and Other Similar Chromium Nickel-Iron Alloys.

TABLE 3.251. — Effect of Aging Temperature after Cold Reduction on Tensile Properties

Source		Ref. 3.11								
Alloy		A-286								
Pre-Aged Condition		Cold Worked 30%			Cold Worked 65%			Cold Worked 80%		
Heat Treatment	Test Direction	F_{tu} (a), ksi	F_{ty}, ksi	Elong, %	F_{tu}, ksi	F_{ty}, ksi	Elong, %	F_{tu}, ksi	F_{ty}, ksi	Elong, %
None	L	132	120	5	167	149	2.5	178	153	2.7
	T	133	121	7	180	157	2.5	204	177	3.5
1100°F (593°C)	L	-	-	-	221	212	3.	239	230	2.8
	T	-	-	-	-	-	-	263	250	3.8
1200°F (649°C)	L	183	169	9	217	204	3.8	224	202	3.
	T	-	-	-	232	220	6.	243	226	4.5
1300°F (704°C)	L	185	163	11	175	140	10.	172	136	9.
	T	181	154	10	184	157	10.	-	-	-

(a) 1 ksi = 0.70307 kg/mm². Note: Elongation in 2 in (1 in = 25.4 mm).

TABLE 3.252. — Effect of Double-Aging on Yield Strength

Source	Ref. 3.19
Alloy	A-286
Condition Prior to Aging	1650°F (899°C) for 2 hr, oil quenched
Aging Treatment	Yield Strength
1300°F (704°C) for 16 hr, air cooled	89.1 and 91.6 ksi (62.6 and 64.4 kg/mm²) for 2 heats
1300°F (704°C) for 2 hr, air cooled, plus 1200°F (649°C) for 16 hr	91.6 and 101 ksi (64.4 and 71.0 kg/mm²) for 2 heats

TABLE 3.41. — Properties of Precipitated Intermetallic Phases

Source	Ref. 3.13				
Alloy	A-286				
Phase	Crystal Structure	Lattice Constants, 3×10^{-7} mm a_0	c_0	Electron/ Atom Ratio	R_A/R_B (a)
γ', B_3A	$L1_2$ - fcc [$Ni_3(Ti, Al)$]	3.60		8.25	1.17
η, B_3A	DO_{24} - hex (Ni_3Ti)	5.11 - 5.12	8.30 - 8.32	8.25	1.17
β, BA	B_2 - bcc [Ni(Al, Ti)] or (NiAl)	2.91 - 2.72	-	6.5	0.87
Laves, B_2A	C_{14} - hex [$(Fe, Mn, Cr, Si)_2$-(Mo, Ti, Cb)]	4.75 - 4.83	7.69 - 7.77	<8	1.05 - 1.68
χ	A_{12} - cubic	8.91 - 8.94	-	6.3 - 7.6	1.03 - 1.15
σ	D_{8b} - tetragonal	-	-	5.6 - 7.6	-
G, $A_6B_{16}Si_7$	fcc	11.13 - 11.47	-	-	-

(a) Ratio of atomic radii of atoms.

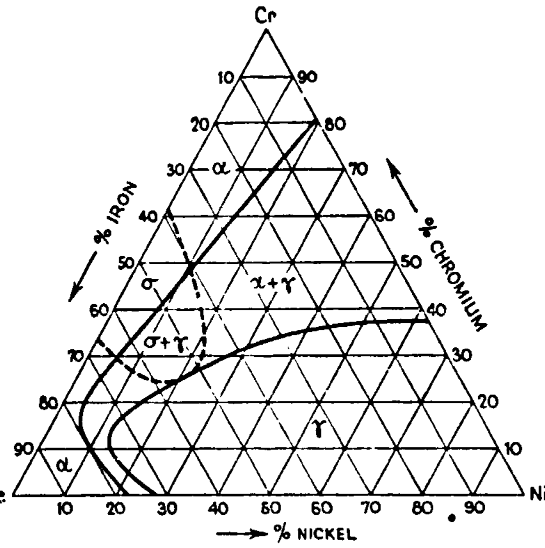

Room Temperature

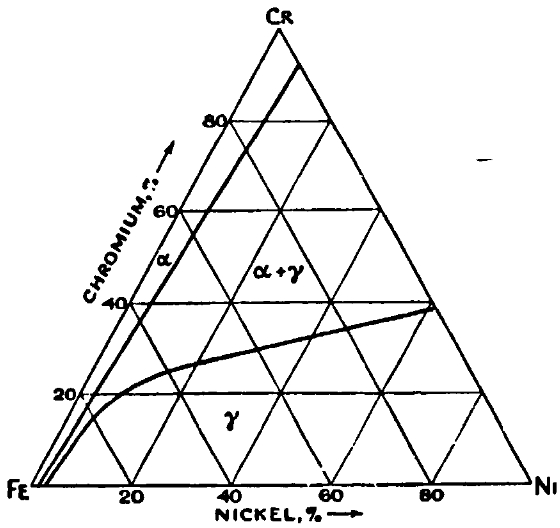

800°C

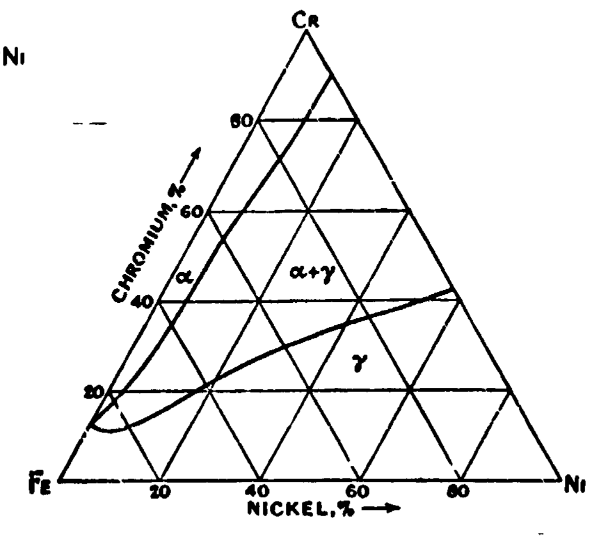

1000°C

FIGURE 3.14. – Phase diagrams for the iron-chromium-nickel system at room and elevated temperatures.

(Ref. 3.16)

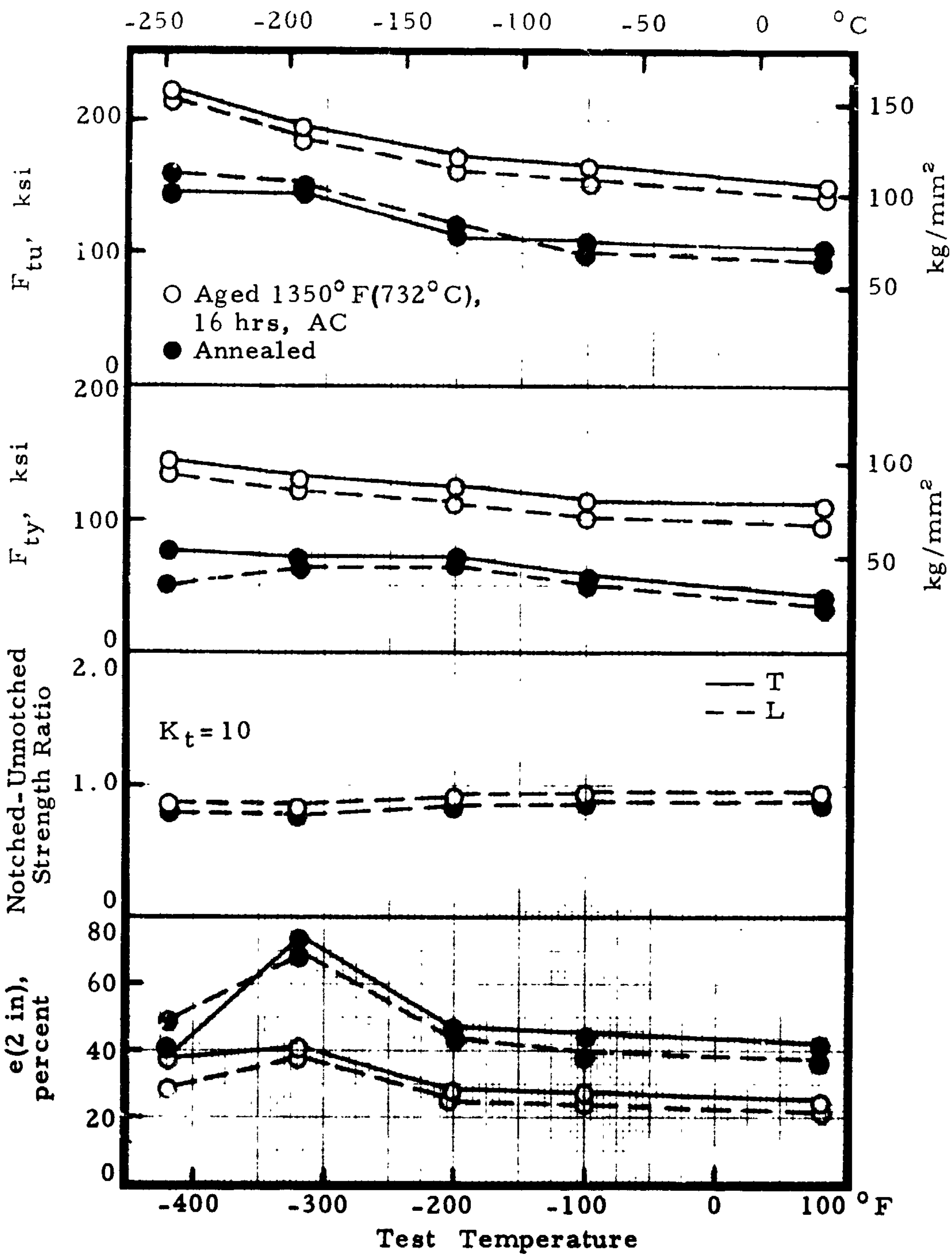

FIGURE 3.244. — Effect of age-hardening on properties of A-286 sheet at cryogenic temperatures· 0.095-inch (2.41-mm) thick.

(Ref. 7.12)

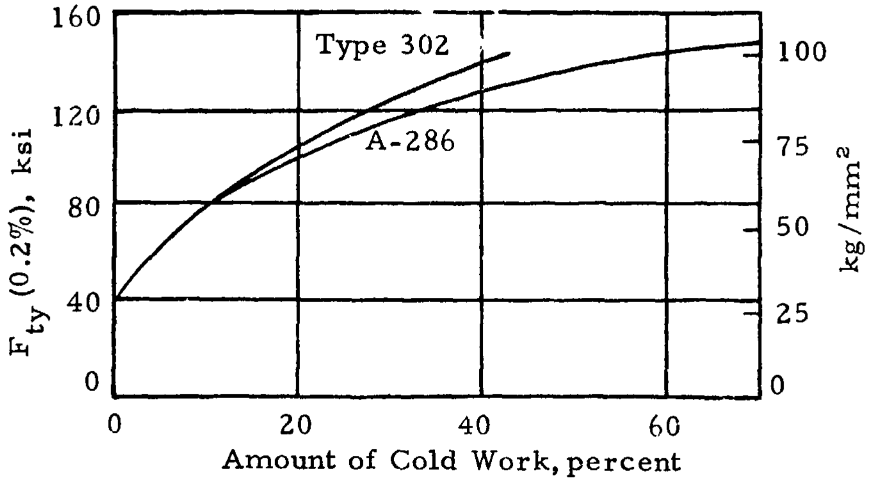

FIGURE 3.25. — Effect of cold-working on room temperature tensile strength of A-286 compared with stainless steel Type 302.
(Ref. 3.19)

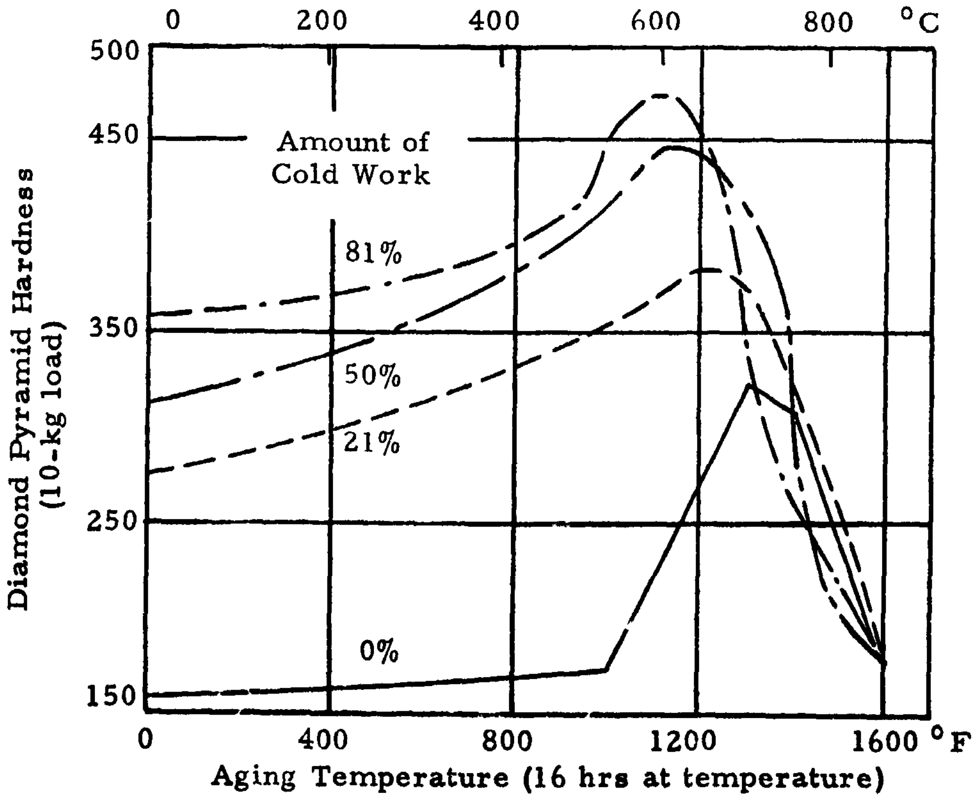

FIGURE 3.251. — Effect of cold reduction and aging temperature on hardness of A-286.
(Ref. 3.19)

FIGURE 3.51. — Fine precipitate of γ' [Ni_3(Al, Ti)] in experimental steel (15-Cr-25Ni-0.87Ni-2.28Ti), aged 50 hours at 800°C; 750X. (Ref. 3.20)

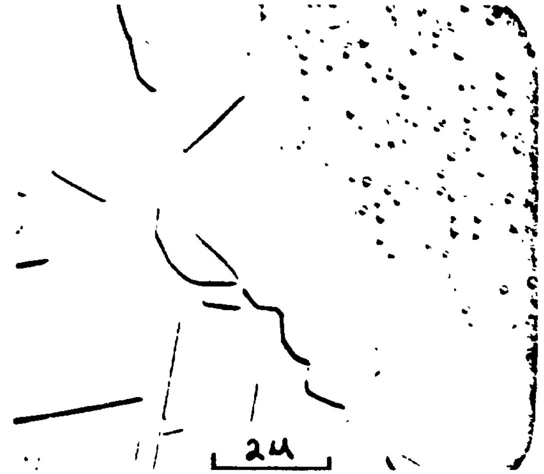

FIGURE 3.52. — Platelets of η [Ni_3Ti] in A-286 aged 1000 hours after solution treatment at 927°C for 4 hours. (Ref. 3.13)

FIGURE 3.53. — Massive plates of β [Ni(Ti, Al)] in experimental steel (15Cr-25Ni-2.95Al-2.75 Ti), aged 50 hours at 800°C; 750X. (Ref. 3.20)

FIGURE 3.57. — Globular G phase, spherical γ', and Widmanstatten platelets of η in Fe-16Cr-25Ni-Ti alloy; solution treated 4 hours at 927°C and aged 200 hours at 815°C. (Ref.3.13)

Chapter 3 - References

3.1 Aerospace Material Specifications, Society Automotive Engineers, Inc., New York; latest Index, May 1971.

3.2 ASTM STP-187, page 80.

3.3 ASTM STP-160, August 1954, p. 70.

3.4 D. Raynor and J.M. Silcock, "Strengthening Mechanisms in γ'-Precipitating Alloys," Metal Sci. J., 4, 121 (1970).

3.5 Allegheny Ludlum Steel Corp., "A-286," Product Literature.

3.6 Universal-Cyclops Specialty Steel Division, "Unitemp-A-286," HT3020, 1971.

3.7 1971 SAE Handbook, Society Automotive Engineers, Inc., New York.

3.8 C.P. Sullivan and M.J. Donachie, Jr., "Microstructures and Mechanical Properties of Iron-Base (-Containing) Superalloys," Metals Eng. Qtr., 11 (4), 1 (1971).

3.9 American Iron and Steel Institute, "High Temperature High Strength Alloys," February 1963.

3.10 R.H. Raring, et al., "Progress Report of NASA Special Committee on Material Research for Supersonic Transports," NASA TN D-1798, May 1963.

3.11 D.R. Muzyka, "Controlling Microstructures and Properties of Superalloys via Use of Precipitated Phases," Metals Eng. Qtr., 11 (4), 12 (1971).

3.12 G.P. Sabol and R. Stickler, "Microstructure of Nickel-Based Superalloys," phys. stat. solid., 35, 11 (1969).

3.13 R.F. Decker and S. Floreen, "Precipitation from Substitutional Iron-Base Austenitic and Martensitic Solid Solutions," in Precipitation from Iron-Base Alloys, Metallurg. Soc. Conf., Cleveland, 1963, Gordon & Breach, New York, 1965.

3.14 Carpenter Technology Corp., "Carpenter A-286," Technical Data, June 1970.

3.15 Superior Tube, "Super Alloy Tubing," Bulletin 71, June 1968.

3.16 J.H.G. Monypenny, Stainless Iron and Steel, Vol. 2, "Microstructures," Chapman & Hall, Ltd., London, 1954.

3.17 C.J. Slunder, A.F. Hoenie, and A.M. Hall, "Thermal and Mechanical Treatment for Precipitation-Hardening Stainless Steels," NASA SP-5089, 1968.

3.18 C.P. Sullivan and M.J. Donachie, Jr., "Some Effects of Microstructure on the Mechanical Properties of Nickel-Base Superalloys," Metal Eng. Qtr., 7 (1), 36 (1967).

3.19 Metals Handbook, 8th Ed., Vol. 2, "Heat Treating, Cleaning, and Finishing," American Society for Metals, Metals Park, Ohio, 1964.

3.20 K.J. Irvine, D.T. Llewellyn, and F.B. Pickering, "High-strength austenitic stainless steels," J.I.S.I., 199, 153 (1961).

3.21 F.G. Wilson and F.B. Pickering, "Some Aspects of the Deformation of an Age-Hardened Austenitic Stee.," J.I.S.I., 207, 490 (1969).

3.22 Marshall Space Flight Center, "Effects of Low Temperatures on Structural Metals," NASA SP-5012, December 1964.

3.23 H.J. Beattie, Jr., and W.C. Hagel, "Intergranular Precipitation of Intermetallic Compounds in Complex Austenitic Alloys," Trans. Metall. Soc. AIME, 221, 28 (1961).

3.24 ASTM Standards, A262-64T, Part 3, American Society for Testing and Materials, 1968.

3.25 J.M. Camp and C.B. Francis, "The Making, Shaping, and Treating of Steel," 6th Edition, United States Steel Co., 1951.

3.26 J.P. Vidosic, "Study of Phase Identifications in Steel and Aluminum Alloys," Georgia Institute of Technology, Final Project Report A641 for NASA, September 1963.

3.27 L.F. Coffin, Jr., Trans. ASM, 56, 339 (1963).

Chapter 4

PRODUCTION PRACTICES

4.1 General. The production of superalloy steels such as A-286 involves a two-stage refining process. The steel is first melted and refined in an electric arc furnace to produce an ingot for remelting. This ingot is made the consumable electrode in a remelt process conducte in vacuum to ensure a high-purity alloy that will have the desired qualities of high strength, resistance to temperature, and resistance to corrosion (ref. 4.1).

Production of mill products is similar to practices for other stainless steels.

4.2 Manufacture of Wrought Products

4.21 Air Melting. Alloy A-286 is first produced by the double-slag process (as for other stainless steels) that ensures a fully deoxidized or "killed" ingot for additional processing. Production of this air melt must be carefully controlled to ensure the highest possible quality in the final vacuum-melted product (refs. 4.1, 4.2).

4.22 Remelting. The demands of advancing aerospace technology for supe strong and super-resistant materials have been highly instrumental in encouraging the development of remelting processes that at least minimize the concentration of elements in alloy compositions that have deleterious effects on physical and mechanical properties (refs. 4.2, 4.3). For example, purity of the steel is one of many factors which determines the notch strength of a steel in a given alloy systen Also, the tolerance for embrittling factors is affected by changes in the alloying content. More specifically, it has been shown that the gas content of the consumable-electrode vacuum melt is far less tha that of the air melt, for example, 29 percent less hydrogen, 62 percent less oxygen, and 93 percent less nitrogen. Additionally, improvement in workability has resulted from improved microstructure and minimization of segregation (ref. 4.4).

In the remelt process, the ingot from the air melt is placed as the electrode in a vacuum-melting furnace. After the furnace is sealed off, it is evacuated and then current is applied to the electrode. As the electrode melts, oxygen, nitrogen, and hydrogen are removed from the melt because of the high vacuum (ref. 4.1). By 1956, consumable electrode - vacuum melted ingots were produced up to 26-inch (66-cm) diameter (ref. 4.4), and by 1969, up to 45-inch (144-cm) diameter (ref. 4.3).

A comparison of the transverse ductility of A-286 from an air-melte and a vacuum-melted heat is given in figure 4.221. A comparison of the fatigue strength of air-melted vs consumable electrode-vacuum melted A-286 is given in figure 4.222.

4.23 Rolled Products (ref. 4.5). Except for coils of thin strips or rods for subsequent wire fabrication, rolled products are usually produced in straight or flat sections. After solidification, cast ingots weighing up to 10,000 pounds (4,350 kg) are removed from the mold and heated in a furnace in a sulfur-free atmosphere. (Even small amounts of sulfur will cause the material to be hot short and, possibly, to crack during rolling at elevated temperatures.) Ingots may be forged before rolling, or may go directly to the blooming mill for rolling into rectangular slabs; the hot-working range is narrow, which necessitates frequent reheating during the operations of ingot breakdown. If the final product is to be bar stock, ingots are forged to squares. (Round shapes may also be forged in diameters of 3-1/2 inches to 6 inches (8.9 to 15.2 cm). After rolling or forging in the blooming mill, billets are surface-conditioned and the hot top end is removed. Usually, ultrasonic inspection is made at this time, particularly since it is difficult to heal defects in stainless steels during hot rolling.

The billets are hot rolled on 3-high mills down to 3/8 inch (9.5 mm) plate. Billets may be cross rolled to minimize directional variations. Frequent heating may be required as well as surface conditioning. At this time, the alloy is pickled and may be shot-blasted before further rolling. Rolling is generally performed on a 2-high mill for thicknesses of 0.045 to 3/8 inch (1.14 to 9.5 mm). The sheet may be finished hot or cold. Rolling to thinner sheet is usually done cold on a cluster mill. Typical fabrication schedules for bar involve hot rolling of the forged bars down to 2-1/4 inches (63.5 mm) on a 24-inch (61-cm) mill, followed by surface conditioning and reheating for rolling on a 10-inch (25.4-cm) mill down to 5/16 inch (0.79 cm) diameter rod. For wire production, rod is coiled at this stage by cold drawing into wire as small as 0.001 inch (0.025 mm) in diameter.

Hot rolled sheet and plate are generally annealed after rolling, and descaled by acid pickling or vapor blasting. Then, the alloy may be rolled, leveled, and sheared to length; sheet products may be stretch straightened and cut to size. Cold rolled products may be given a temper treatment for delivery in the cold-reduced and tempered condition (CRT). Mechanical properties depend on the amount of cold reduction and the tempering temperature. Bar products over 2-1/4 inches (63.5 mm) diameter generally are straightened, annealed or tempered, and ground to finished size. Bars of smaller diameter are straightened, ground, heat treated, descaled, and pickled prior to cooling. Most rolled products are shipped from the mill in the solution treated (annealed) condition.

4.24 Extrusions (refs. 4.5, 4.6). Tubing and structural shapes have been produced by the hot extrusion process. Extruded shapes such as tees and angles can be cold drawn to improve tolerances and achieve thinner gages. For example, tee sections with 0.062-inch (1.57 mm) webs have been extruded from A-286. Techniques for extrusion are similar to practices for stainless steel. By use of the Ugine-Sejournet glass-lubrication process, extrusions have been made at ratios up

97:1 for A-286. In this process, billets are transferred from the heating furnace to the charging table of the extrusion press. As a billet rolls into position before the container, it passes over a sheet of glass fiber or a layer of glass powder that fuses to the surface of the billet. Also, a glass-fiber pad is placed in front of the die face during extrusion. Billets are heated in either gas- or oil-fired furnaces by induction or by salt-bath heating; long induction times are required. Successful extruding of A-286 requires accurate temperature control, working within a narrow temperature range, minimized transfer time from furnace to extrusion press, and controlled speed of extrusion so that overheating does not result from the heat of deformation.

Products, where possible, are quenched after extrusion to remove any adhering glass. In some instances, air cooling is required if the extrusion cross-sectional area is large or if the alloy is sensitive to quench cracking. Detwisting on hydraulic torsional stretchers or straightening on roll straighteners is usually required for extrusion products.

4.3 Forging (refs. 4.5, 4.6)

4.31 Billets, ingots, and bars for forging generally are produced by practices used for conventional stainless steels. Requirements for forging billets are relatively small; thus, suppliers stock a few standard sizes and either cog or roll them to the sizes specified by the customer. Forging billets are usually supplied in the overaged condition, developed by holding solution-treated material at 1150° F (621° C) for several hours. Overaged material must be solution-treated prior to precipitation hardening. If billets are supplied in the solution-treated condition, they may be precipitation hardened directly after forging.

4.32 Wire, Rod, and Tube. Alloy A-286 is readily drawn into tube, rod, and wire. The tubing is used extensively for both hydraulic and deicing systems in aircraft. Rod and wire are used for fasteners and springs where resistance to corrosion is important.

4.4 Castings (ref. 4.8)

4.41 Alloy A-286 is cast in investment molds. For consistent properties at a higher level, particularly ductility, it must be cast under vacuum from certified vacuum-melted master heats. Alumina, magnesia, or zirconia crucibles are satisfactory after they have been cured by several wash heats. Alumina or zirconia facing material is preferable to a silica facing in investment molds, poured at a preheat of up to 1900° F (1038° C), because silica may react to form surface defects in the casting. The production cycle for casting a 12-pound (5.2-kg) charge is 6 minutes.

Alloy A-286 castings are solution annealed at 2000° F (1094° C) for 1-1/2 hours per inch (per 25.4 mm) of section thickness, followed by rapid cooling in air to room temperature.

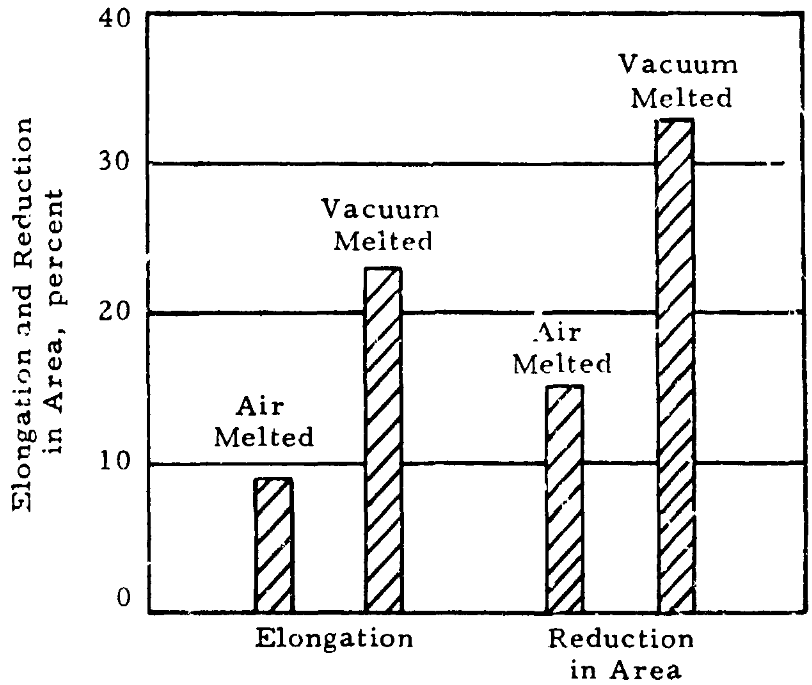

FIGURE 7.4221. — Transverse ductility of air-melted vs. consumable-electrode vacuum melted A-286.
(Ref 4.4)

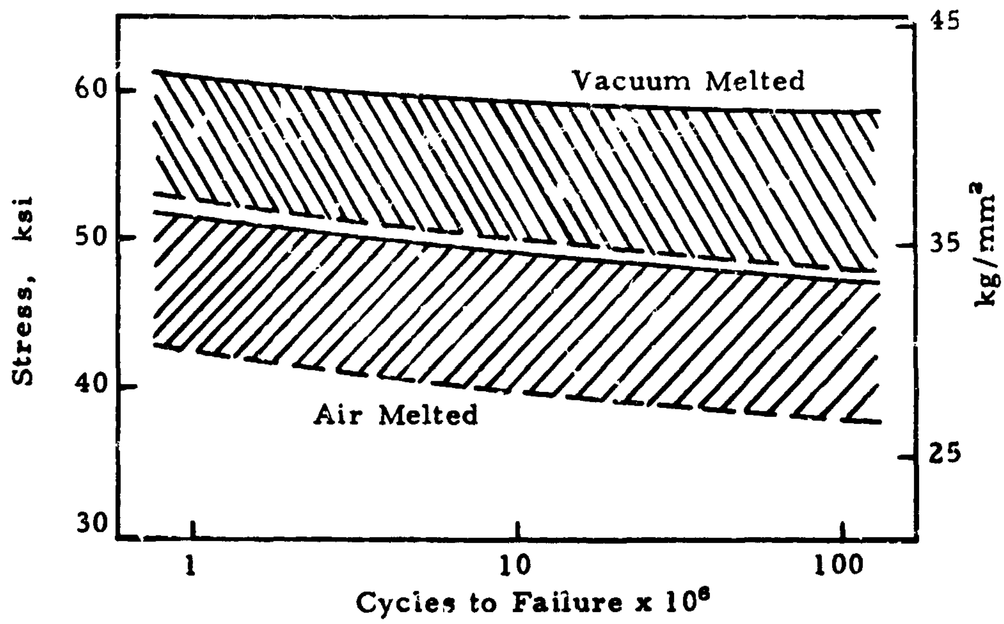

FIGURE 7.4222. — Fatigue strength at 1200°F (649°C) of air-melted and consumable-electrdoe vacuum-melted A-286.
(Ref. 4.4)

Chapter 4 - References

4.1 Republic Steel Corp./Special Metals Div., "Now and Tomorrow with High Performance Alloys," June 1969.

4.2 S.J. Matas, "Influence of Impurities and Related Effects on Strength and Toughness of High Strength Steels," paper presented at American Society for Metals, Golden Gate Metals Conference, February 13, 1964, San Francisco, California.

4.3 R. Schlatter, "Vacuum Melting of Specialty Steels," J. Metals, 22 (4), 33 (1970).

4.4 R.K. Pitler, E.E. Reynolds, and W.W. Dyrkacz, "Consumable Electrode Vacuum Remelting of High-Temperature Alloys," Conf. of Metall. Soc. of AIME on High Temperature Materials, Cleveland, Ohio, April 16-17, 1957, Ch. 25.

4.5 D.E. Strohecker, A.F. Gerds, and F.W. Boulger, "Deformation Processing of Precipitation-Hardening Stainless Steels," NASA SP-5088, 1968.

4.6 L.M. Christensen, "Development of Improved Methods, Processes, and Techniques for Producing Steel Extrusions," ML-TDR 64-231, July 1964.

4.7 A.M. Sabroff, et al., "A Manual on the Fundamentals of Forging Practice, AFML TDR 64-95 Suppl., December 1964.

4.8 J.G. Kura, V.D. Barth, and H.D. McIntire, "Shaping of Precipitation-Hardening Stainless Steels by Casting and Powder Metallurgy," NASA SP-5086, 1968.

Chapter 5

MANUFACTURING PRACTICES

5.1 General. Techniques for fabricating precipitation-hardenable (PH) stainless steels are not very much different from those used for other stainless steels. Alloy A-286 is slightly more resistant to deformation than the austenitic stainless steels during hot working. It is the most forgeable of heat-resisting alloys. In the solution-treated condition, it is somewhat stiffer than stainless steels such as Types 316 and 310; however, it can be satisfactorily cold drawn and formed. Machining can be performed with the same techniques and equipment as used for the 300 series of stainless steels, but at slower rates (refs. 5.1 through 5.5).

5.11 Blanks for secondary deformation processes may be produced by the cutting, preforming, or welding of material in the annealed or solution-treated condition to the desired shapes and sizes. Shearing is the most economical and most widely used method. Blanking, normally performed on a punch press to produce the desired shape in one operation, may be used for materials of less than 0.125-inch (3.175-mm) thickness; dies should be rigid and guide pins must be used. Low- or high-speed bands may be used for sawing. Slitting, hand-shearing, routing, and nibbling are also used. Thermal cutting is often more efficient for PH steel material thicker than 1/4 inch (6.35 mm). PH steel blanks must be deburred to minimize damage to forming tools and assure safety in handling. Deburring may be accomplished by draw filing or grinding on materials of less than 0.040 inch (1.016 mm) thick; for greater thicknesses, grinding wheels or machining operations (milling) are suggested (ref. 5.6). Surfaces should be free of imperfections, soluble substances (oil, grease), and contaminants, such as iron, that will reduce resistance to corrosion.

5.2 Forming

5.21 Alloy A-286 is normally cold worked in the annealed (solution-treated) condition. As annealed, Rockwell B hardness is 75–85 and formability is good. It is one of the most popular high-temperature alloys for cold heading applications. For this purpose, dead soft annealed wire is sometimes used, but more often the wire is given a slight cold draw to provide better shearability and resistance to flattening (ref. 5.1). Forming processes include:

Brake bending	**Tube forming**
Deep drawing	**Roll forming**
Spinning	**Roll bending**
Shear forming	**Dimpling**
Drop hammer forming	**Joggling**
Trapped-rubber forming	**Sizing**
Stretch forming	**Explosive forming .**

5.22 In brake forming, A-286 is more easily bent at room temperature than other PH steels such as 17-7 PH, PH 15-7 Mo, AM 350, and AM 355 (ref. 5.7); lowest springback among the aged alloys is shown by A-286 (ref. 5.8). In deep-drawing processes, A-286 can probably be formed at a higher speed than most PH steels (ref. 5.6), that is, greater than 10—20 feet per minute (3—6 m/min). Shear forming, generally used to reduce machining time on parts with shapes that cannot be made by conventional forming methods, has been used successfully for A-286 jet-engine shafts (ref. 5.9). The derivation of limits for drop-hammer-forming of A-286 are discussed in reference 5.7. From the standpoint of buckling in compression-flange forming (by trapped-rubber forming), A-286 has the best formability compared with other PH steels (ref. 5.10). Alloy A-286 can be stretched (stretch forming) more without splitting than other PH steels (ref. 5.7), but can withstand less stretching strain in tube forming (ref. 5.11). It is more easily formed by linear roll binding and joggling than other PH steels (ref. 5.12).

5.3 Forging

5.31 The narrow range of temperature permissible for forging A-286 is generally limited on the low side by a drop in forgeability due to carbide precipitation. For most PH alloys, this reaction starts at about 1750° F (954° C) (ref. 5.6). Alloy A-286 forged at a temperature of 2150° F (1177° C) displays low decarburization, low scale, fair grain size control, fair forgeability, and no thermal cracking (ref. 5.13). Temperatures recommended for A-286 forgings receiving given nominal amounts of reduction are as follows:

Maximum forging temperature	2150° F (1177° C)
Light reduction,up to 15 percent	1800° F (982° C)
Moderate reduction, 15—50 percent	2100° F (1149° C)
Severe reduction, >50 percent	2150° F (1177° C)
Variable reduction	2100° F (1177° C).

Heating in a reduced atmosphere should be avoided to prevent pick up of nitrogen or carbon; neutral or slightly oxidizing atmospheres are recommended for forging A-286 (refs. 5.1, 5.6). Subsequent scale can be removed by pickling in HF—HNO_3 mixture or by grit blasting (see Chapter 11). Lubrication practices are the same as for austenitic steels. Specific cooling procedures are rarely needed after forging for heat-resisting alloys; if forging temperatures are correctly maintained, the forgings can be cooled in still air and will be in suitable condition for heat treating (ref. 5.5).

5.4 Machining

5.41 Alloy A-286 is slower to machine than the 300 series of stainless steels, and exhibits the same gumminess and work-hardening characteristics so that rigid machine setups and sharp tools are required. To overcome the gumming condition, the alloy is often partially aged (1 hour at 1325° F, 718° C) or fully aged (16 hours at 1325° F), or overaged (several hours at 1500° F, 816°C) prior to machining. After overaging and machining, re-solution treating and aging are required to develop optimum properties (ref. 5.1).

Other suggestions for successful machining include the use of relatively low cutting speeds with recommended cutting fluids to reduce buildup, friction, and tool-chip temperatures. By using sharp tools of recommended geometries, work hardening is minimized. Also, tools should cut, not push, metal and they should never rub or dwell in the cut (ref. 5.14).

Machine tools for cutting A-286 need the following characteristics to insure rigid, vibration-free operation (ref. 5.14): (a) Dynamic balance of rotating elements; (b) True running spindle; (c) Snug bearings; (d) Rigid frames; (e) Wide speed/feed ranges; (f) Ample power to maintain speed; (g) Easy accessibility for maintenance. Milling machines and lathes also should have backlash elimination devices as well as snug, clean, correctly-lubricated gibs and slides. Typical parameters for machining A-286 are given in table 5.41. Extensive detail on machining practice is given in reference 5.14.

5.5 Electrochemical Machining

5.51 Most of the specific data and information on electrolyte composition and operating conditions for electrochemical machining (ECM) of A-286 are proprietary (ref. 5.14). However, some available data on representative operating conditions are summarized in table 5.51. As indicated in the table, good surface smoothness was obtained for cavity-sinking with a sodium nitrate electrolyte (ref. 5.16), and good cutting results with a sodium chloride—boric acid electrolyte (ref. 5.17). When the electrolytes for cutting contained either sulfuric or tartaric acid, or hydrochloric acid and tartaric acid, poorer cutting performance (maximum feed rate of 0.27 in/min (6.86 mm) was observed.

Data published on the effects of ECM on the properties of A-286 indicate that no intergranular corrrosion occurs, and fatigue strength is essentially identical to that of the parent metal (ref. 5.18). In a study of the susceptibility of various steels to hydrogen embrittlement as a result of ECM, an aqueous etchant was used that included 15 volume-percent HCl, 17 volume-percent HNO_3, and 31 volume-percent H_3PO_4. No evidence of hydrogen embrittlement was observed in subsequent constant-strain-rate bend tests (ref. 5.20).

TABLE 5.41. — Typical Machining Parameters

Source	Refs. 5.14, 5.15					
Alloy	A-286					
Operation	Cond. (a)	Tool (b) Grade	Fluid	Depth of Cut, in (c)	Speed, fpm (c)	Feed
Turning	ST	C-2	none	0.025	150	0.008 ipr
		T-5	none	0.25	40	0.010
	STA	C-2	none	0.187	80	0.013
		T-15	none	0.25	45	0.01
Face milling	ST	C-2	I	0.25	120	0.004 ipt
		T-15	I	0.25	55	0.003
	STA	C-2	I	0.25	120	0.004
		T-15	I	0.25	55	0.003
End milling	ST	C-2	I	0.050	100	0.0035 ipt
		T-15	I	0.050	40	0.0035
	STA	C-2	I	0.25	150	0.005
		T-15	I	0.25	40	0.0025
Slab milling	ST	C-2	II	0.25	140	0.006 ipt
		T-5	II	0.25	50	0.005
	STA	C-2	II	0.25	110	0.006
		T-15	II	0.25	50	0.005
Drilling	ST	T-15	-	-	10-20	0.0005 ipr, 1/8-in drill; 0.007 ipr, 1-in drill
	STA	-	-	-	10-20	0.001 ipr, 1/8-in drill; 0.010 ipr, 1-in drill
Tapping	STA	M-10	-	-	30	-
Broaching	ST, STA	T-15	-	-	9	chip load, 0.002 ipt
Surface grinding	ST	downfeed, rough, 0.001 ipp; table speed, 20 fpm; wheel speed, 6000 fpm downfeed, finish, 0.0005 ipp; table speed, 20 fpm; wheel speed, 3000 fpm				

(a) ST, 180-220 Bhn hardness; STA, 280-320 Bhn hardness.

(b) C-2, carbide tool; M- and T-, high speed steel; see reference 5.14 for tool geometries and alternatives

(c) 1 inch = 25.4 mm; 1 ft = 30.5 cm.

I, sulfurized oil

II, chlorinated oil

TABLE 5.51.— Representative Chemical Machining Conditions

Source	Refs. 5.14, 5.16, 5.17, 5.19		
Alloy	A-286		
Parameter	Cavity Sinking	Operation Cutting	Grinding
Electrolyte	$NaNO_3$, 5.0 lb/gal (600 g/l)	NaCl, 200-227 g/l H_3BO_3, 25 g/l	"Anocut #90" (a)
Temperature	100° F (38° C)	70° F (21° C)	-
Inlet pressure range	240/240 psi (0.17/0.17 kg/mm^2)	-	-
Flow rate	3.9 gal/min (14.8 l/min)	-	-
Current	741 A	-	80-130 A
Applied voltage	12.0	10-12	5
Feed rate	0.040 in/min (1.02 mm/min)	0.071 in/min (1.80 mm/min)	3.7 in/min (94 mm/min)
Depth (or length of cut)	0.510 inch (13.0 mm)	0.0 to 1.2 in 0.0 to 30.5 mm)	0.005 inch (0.127 mm)
Cathode wheel speed	-	7200 surf ft/min (2196 surf m/min)	-
Surface roughness	12 – 20 μin (av) (0.3–0.5 μm)	-	Satisfactory

(a) Anocut Engineering Company, Chicago, Illinois

Chapter 5 - References

5.1 Carpenter Technology Corporation, "Carpenter A-286," Technical Data, June 1970.

5.2 Univeral-Cyclops/Specialty Steel Div., "Unitemp A-286," HT3020, 1971.

5.3 Metals Handbook, Vol. 3, "Machining," American Society for Metals, Metals Park, Ohio, 8th Edition, 1967.

5.4 Metals Handbook, Vol. 4, "Forming," American Society for Metals, Metals Park, Ohio, 8th Edition, 1969.

5.5 Metals Handbook, Vol. 5, "Forging and Casting," American Society for Metals, Metals Park, Ohio, 8th Edition, 1970.

5.6 D.E. Strohecker, A.F. Gerds, and F.W. Boulger, "Deformation Processing of Precipitation-Hardening Stainless Steels," NASA SP-5088, 1968.

5.7 W.W. Wood, et al., "Final Re[illegible]t on Sheet Forming Technology," Vols. I and II, Report No. ASD [illegible]DR 6[illegible]-7-871, July 1963.

5.8 Allegheny Ludlum Steel Corp., "Tensile [illegible]rties of AM-350 Cold-Drawn Wire," Tech. Data Sheet 126-71659-350.

5.9 F. Jacobs, "Effects of Shear Forming Upon the Properties of Materials," Temco Aircraft Corp., ASD TR 62-380, August 1962.

5.10 J.M. Raymer et al., "Metastable Austenitic Forming of High Strength Pressure Vessels," AVCO Corp., ML TDR 64-174, July 1964.

5.11 W.W. Wood, et al., "Final Report on Advanced Theoretical Manufacturing Technology," Vols. I and II, AFML TR 64-411, June 1965.

5.12 W.W. Wood, et al., "Theoretical Formability," Vols. I and II, ASD TR 61-191, August 1961.

5.13 A.M. Sabroff, et al., "A Manual of the Fundamentals of Forging Practice," AFML TDR 64-95, Suppl., December 1964.

5.14 C.T. Olofson, J.A. Gurklis, and F.W. Boulger, "Machining and Grinding of Ultrahigh-Strength Steels and Stainless Steel Alloys," NASA SP-5084, 1968.

5.15 Metal Progress Databook: 1968, pp. 111-113.

5.16 J. Bayer, M.A. Cummings, and A.U. Jollis, "Final Report on Electrolytic Machining Development," AFML TDR 64-313, September 1964.

5.17 J.E. Clifford, D.E. Semons, and J. McCallum, "High-Temperature Alloy Cutting Program," AMC TR 59-7-617, January 18, 1959.

5.18 R.J. Favor and H.G. Popp, "Materials Property Data Compilation. Part I. Hastelloy X," 5th Qtr. Rept., Cont. AF 33(657)-8017, May 1961.

5.19 H.W. Jacobus, "Surface Effects of Electrolytic Machining," Report No. A243, Cont. AF 33(657)-11215, December 11, 1963.

5.20 R.L. Jones, "Susceptibility of Materials to Hydrogen Embrittlement from Chemical Milling Operations," Cnovair/General Dynamics, Report No. MRG-219, March 16, 1961.

Chapter 6

SPACE ENVIRONMENT EFFECTS

6.1 General. Stainless steels are used successfully in both structural and nonstructural applications for aerospace vehicles. In general, these alloys are relatively insensitive to degradation under typical space environment conditions.

6.2 The low pressure encountered in space is conducive to the loss of materials of construction by sublimation (or evaporation) because molecules which leave the surface of materials are not returned by collisions with ambient gas molecules. Thus, above altitudes of about 160 km, the mean free path of a molecule at ambient temperatures is so long in comparison with the size of the spacecraft that any molecule which leaves the surface will not return. Loss of material by sublimation in the vacuum of space is intuitively obvious, but the effect of very high vacuum on the rupture and fatigue properties of materials is unexpected; however, experiments have indicated that the density of the gas surrounding a material is an important parameter defining its behavior under stress. Apparently, the character of the gas layer adsorbed on materials influences certain mechanical properties. Thus, prolonged exposure of materials to a space environment will alter or remove adsorbed gas layers and some of the physical properties of the materials in space will be different than on earth.

The removal of material from a spacecraft structure will obviously lead to an overall weakening of members. The weakening of a member can be simply computed by knowledge of the mass-strength relationship. Where gross sublimation of a material is involved, tests made before and after exposure of specimens to a vacuum will furnish experimental values. Ideally, the tests should be performed in an atmosphere closely resembling the space environment; however, for practical evaluation of the effects of sublimation, the most important condition to be met is that a molecule leaving the surface of the test piece has a negligible chance of returning.

The rate of evaporation of an ideal, pure substance is given by Langmuir's equation:

$$E = \frac{P}{17.14}\sqrt{\frac{M}{T}}$$

where E is the rate in $g\text{-}sec^{-1}\text{-}cm^{-2}$ of exposed surface, M is the molecular weight of the material, P is the equilibrium vapor pressure in torr, and T is the absolute temperature, $^{\circ}K$.

Comparison of predictions from the above equation with experimental data indicate that the Langmuir equation is conservative; thus, the equation must be employed cautiously. Further, it is necessary to recognize that its use to predict vacuum volatility is limited by:

a. The vapor pressure, P, in the equation is the equilibrium pressure. In the space environment, molecules which leave the surface of the liquid or solid phase do not return, and thus equilibrium is not established.

b. The molecular weight of the evaporating molecules must be known; for most materials, this molecular weight is frequently different than assumed (association).

c. Oxide films or thin coatings may act as barriers to the escape of molecules.

d. In practice, most materials are complex mixtures (alloys or polymers) which defy simple treatment. The average assumed molecular weight of a system can not be used in the equation.

e. The process of evaporation for systems of practical interest is very different from the purely random process assigned to ideal systems. For example, evaporation from localized planes of high surface energy is much greater than from planes of low energy; this leads to uneven evaporation, and etching of the surface becomes evident.

As is evident from the above discussion, the Langmuir equation is limited to approximations of evaporation rates in a space environment; it is useful in that it assists in the selection of appropriate materials of construction for spacecraft. For example, the equation indicates that every substance has a rate of evaporation in free space as long as the absolute temperature is not zero. Thus, at a given temperature, say, 25°C, one should select materials which exhibit very low vapor pressures; obviously, the usual metals of construction (iron, copper, etc.) can qualify, but there is some question about the lighter metals such as cadmium, magnesium, aluminum, etc. Table 6.1 illustrates the estimated sublimation losses suffered by metals in a space environment over a moderate range of temperatures; it is anticipated that at lower temperatures, the rate of evaporation will be infinitesimal. It is evident that zinc does not appear to be a useful metal for the construction of spacecrafts or components which are exposed to the high vacuum of space. Pure magnesium metal barely qualifies for the construction of spacecrafts; however, the alloys of magnesium which are currently used show considerably lower losses because the surface presented to the space environment acts as a barrier for sublimation (oxide-chromate conversion coatings, etc.). Thin films of lead (as in soldered joints) may be weakened by prolonged exposure to the space environment. On the other hand, a thin coating of pure tin will act as an efficient barrier for sublimation of other materials. (Ref. 6.5).

6.3 The effects of nuclear and indigenous space radiation on the mechanical properties of A-286 are not expected to be very significant. The results of some studies of irradiation of the alloy are discussed in Chapter 9.

Sputtering of the surface by atomic or molecular particles can deteriorate surface finishes in a relatively short period. The sputtering process is associated with a minimum threshold energy value for atomic or molecular particles striking a material surface. Typical values which have been obtained for this threshold energy are 6, 11, and 12 eV for O, N_2, and O_2 particles, respectively, to remove one or more atoms from the materials' surface upon which they impinge (ref. 6.1). Loss of metal by this mechanism can vary over a wide range and the greatest loss may be expected during solar storms (ref. 6.1). However, loss of metal by sputtering has little structural significance, although it may seriously affect optical and emissive properties of the material surface.

The surface erosion of metals and alloys due to corpuscular radiation is probably insignificant, amounting to something of the order of 254 nanometers per year. Indigenous space radiation, however, will tend to accelerate the removal of surface films on A-286 which might result in the loss of lubricity and an increased propensity to "cold weld." The interaction of indigenous radiation with desorption gases might cause some spurious, transient electrical conditions if the alloy is used for electrical applications.

6.4 Micrometeoroids can produce surface erosion similar to sputtering but on a more macroscopic scale, and may also produce punctures. They vary widely in mass, composition, velocity, and flux; generalizations about rates of erosion and penetration, therefore, must be used with care. The predicted frequency of impact as a function of meteoroid mass is given in figure 6.1. Calculations of armor thickness required for meteoroid protection are given in reference 6.11.

TABLE 6.1. — Evaporation Rates in Vacuum of Typical Elements Used in Aerospace Alloys (a, b)

Source	Ref. 6.14				
Element	Evaporation Rate, g/cm^2/sec				
	−100° C	0° C	100° C	250° C	500°C
Aluminum	1.2×10^{-81}	1.1×10^{-48}	2.0×10^{-33}	1.7×10^{-21}	6.5×10^{-12}
Titanium	$<10^{-99}$	2.5×10^{-60}	4.1×10^{-42}	7.4×10^{-28}	2.0×10^{-16}
Iron	$<10^{-99}$	$6.8 \times 10^{-}$[illegible]4	[illegible]$.4 \times 10^{-44}$	4.9×10^{-29}	9.1×10^{-17}
Nickel	$<10^{-99}$	5.7×10^{-70}	1.3×10^{-48}	6.7×10^{-32}	1.7×10^{-18}
Copper	1.2×10^{-94}	1.4×10^{-56}	6.2×10^{-39}	4.0×10^{-25}	4.7×10^{-14}
Chromium	9.5×10^{-92}	1.0×10^{-54}	1.4×10^{-37}	3.8×10^{-24}	2.2×10^{-13}
Vanadium	$<10^{-99}$	1.9×10^{-87}	2.1×10^{-61}	5.0×10^{-41}	1.2×10^{-24}
Manganese	2.2×10^{-72}	1.1×10^{-42}	6.5×10^{-28}	3.8×10^{-18}	1.6×10^{-9}
Silicon	$<10^{-99}$	1.9×10^{-62}	3.6×10^{-43}	4.3×10^{-28}	5.5×10^{-16}
Magnesium	2.9×10^{-36}	5.3×10^{-20}	1.8×10^{-12}	1.3×10^{-6}	6.6×10^{-2}
Zinc	3.5×10^{-30}	5.1×10^{-15}	1.8×10^{-9}	2.3×10^{-4}	2.80

(a) The actual evaporation rate of each element in combination with others will be lower.

(b) The values may be in error by several orders of magnitude as they have been extrapolated from high-temperature data. The rates at low tempeatures will be considerably less than the values given in the table.

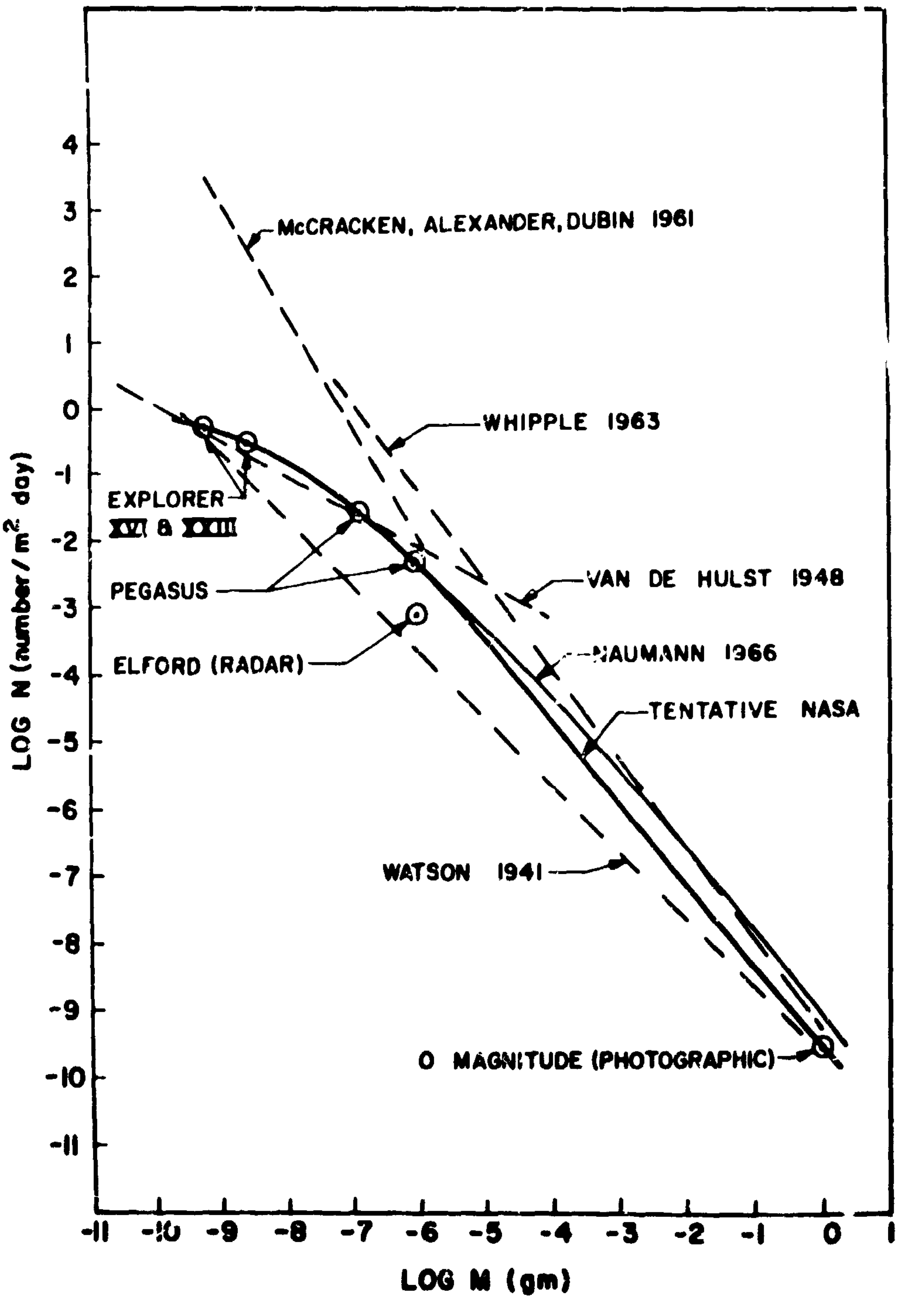

FIGURE 6.1. — Various estimates of meteoroid mass influx. (Ref. 6.3)

Chapter 6 - References

6.1 C.G. Goetzel, J.B. Rittenhouse and J.B. Singletary, Eds., Space Materials Handbook, Addison-Wesley Press, Palo Alto, California, 1965.

6.2 J.R. Redus, "Sputtering of a Vehicle Surface in a Space Environment," NASA TN D-1113, June 1962.

6.3 SAMPE, The Effects of the Space Environment on Materials, Western Periodicals Co., North Hollywood, California, 1967.

6.4 L.E. Kaechele and A.E. Olshaker, "Meteoroids - Implications for the Design of Space Structures," Aerospace Engineering, 19, May 1960.

6.5 R.F. Muraca, et al., "Design Data for Pressurized Gas Systems," NASA Contract NAS7-105, November 1963.

6.6 F.L. Whipple, "On Meteoroids and Penetration," J. Geophys. Res., 68, 4929 (1963).

6.7 H.C. van de Hulst, "Zodiacal Light in the Solar Corona," Astrophys. J., 105, 471 (1947).

6.8 F.G. Watson, Between the Planets, The Blakiston Co., Philadelphia; revised, Harvard University Press, Cambridge, Mass., 1956.

6.9 C.W. McCracken et al., "Direct Measurements of Interplanetary Dust Particles in the Vicinity of the Earth," Nature, 192, 441 (1961).

6.10 R.J Naumann, "The Near-Earth Meteoroid Environment," NASA TN D-3717, November 1966.

6.11 C.D. Miller, "Meteoroid Hazard Evaluation for Simple Structures with Various Orientations," NASA TN D-6056, October 1970.

6.12 K.S. Clifton and P.J. Naumann, "Pegasus Satellite Measurements of Meteoroid Penetration," NASA TM X-1316, 1966.

6.13 W.M. Alexander et al., "Zodiacal Dust: Measurement by Mariner IV," Science, 106, 1240 (1965).

6.14 S. Dushman, Vacuum Techniques, John Wiley & Sons, New York, 1949.

6.15 M. Kangilaski, "Radiation Effects Design Handbook: Sec. 7, Structural Alloys," NASA CR-1873, October 1971.

f

Chapter 7

STATIC MECHANICAL PROPERTIES

7.1 Specified Properties

7.11 NASA Specified Properties
7.12 AMS Specified Properties
7.121 AMS specified properties for various products, table 7.121.
7.13 Military Specified Properties
7.14 Federal Specified Properties
7.15 ASTM Specified Properties

7.2 Elastic Properties and Moduli

7.21 Poisson's ratio at various temperatures, figure 7.21.
7.22 Young's modulus of elasticity, E
7.221 Design value of E, 29.1×10^3 ksi (20.5×10^3 kg/mm^2) (ref. 7.4).
7.222 Values of E at room and elevated temperatures, see figure 7.21.
7.23 Compression modulus, E_c
7.231 Design value of E_c, 29.1×10^3ksi (20.5×10^3 kg/mm^2) (ref. 7.4).
7.24 Modulus of rigidity (shear modulus), G
7.241 Design value of G, 10.4×10^3 ksi (7.31×10^3 kg/mm^2) (ref. 7.4).
7.242 Values of G at room and elevated temperatures, see figure 7.21.
7.25 Tangent modulus
7.251 Tangent modulus in compression at various temperatures, figure 7.251.

7.3 Hardness (see also Chapter 3)

7.31 AMS specified hardness for various products, see table 7.121.
7.32 Typical hardness values (refs. 7.2, 7.5, 7.6):

ST 1800°F (982°C) + aging - Rc = 26–32
ST 1800°F (982°C) + aging - Rb = 92–95
ST 1650°F (899°C) + aging - Bhn = 302

7.4 Strength Properties (see also Chapters 3 and 12)

7.41 Tension
7.411 Design mechanical properties for STA sheet, strip, plate, bars, forgings, and mechanical tubing, table 7.4111.
7.412 Typical tensile properties of various products
7.4121 Tensile test data for vacuum-melt heats from two different parent melt heats, table 7.4121.
7.4122 Typical tensile properties at room temperature of various mill products, table 7.4122.
7.4123 Effect of cold reduction on tensile properties of aged bar and wire, figure 7.4123.
7.413 Stress-strain diagrams
7.4131 Stress-strain curves in tension for sheet at room and elevated temperatures, figure 7.4131.
7.4132 Stress-strain curves to failure for sheet at room and elevated temperatures, figure 7.4132.
7.4133 Typical stress-strain curves for sheet at room and cryogenic temperatures, figure 7.4133.

7.414 Effect of temperature on tensile properties

7.4141 Effect of temperature on ultimate tensile strength, figure 7.4141.

7.4142 Effect of temperature on tensile yield strength, figure 7.4142.

7.4143 Effect of elevated temperatures on tensile properties of bar stock, figure 7.4143.

7.4144 Effect of elevated temperatures on tensile properties of STA tubing, figure 7.4144.

7.4145 Effect of elevated temperatures on tensile properties of 15-percent cold drawn and aged wire, figure 7.4145.

7.4146 Effect of elevated temperatures on tensile properties of 40-percent cold drawn and aged wire, figure 7.4146.

7.4147 Effect of cryogenic temperatures on tensile properties of bar stock and cold-worked-and-aged bar, figure 7.4147.

7.4148 Effect of cryogenic temperatures on tensile properties of STA sheet, figure 7.4148.

7.42 Compression (see also table 7.411)

7.421 Stress-strain curves in compression for sheet at various temperatures, figure 7.421.

7.422 Effect of temperature on compressive yield strength, figure 7.422.

7.43 Bending

7.431 Annealed (1800°F, 982°C) sheet shall withstand, without cracking, bending at room temperature through the angle indicated below, around a diameter equal to the nominal thickness of the material with axis of bend parallel to the direction of rolling (ref. 7.15):

Nominal thickness, inch	Nominal thickness, mm	Angle, deg, min
to 0.249	6.32	180
0.249 - 0.749	6.32 - 19.0	90

7.44 Shear and torsion (see also table 7.411)

7.441 Effect of temperature on the ultimate shear strength, figure 7.441.

7.442 Effects of cryogenic temperature on double-shear strength of cold-drawn and aged bar, figure 7.442.

7.45 Bearing (see also table 7.411)

7.46 Fracture

7.461 Notch properties

7.4611 Effect of temperature on notch strength of cold-reduced and aged sheet, figure 7.4611.

7.462 Fracture toughness

7.4621 K_{IC} = 181 ksi$\sqrt{in}$ (641 kg/mm$^{3/2}$) for forging, cold worked and aged at 1250–1300°F (687°–704°C); specimen 3.0 in (76.2 mm) thick by 3.4 in (86.4 mm) wide, with crack length of 0.65 in (16.5 mm); (ref. 7.16).

TABLE 7.121. — AMS Specified Properties for Various Products

Source	Ref. 7.1						
Alloy	A-286						
Product	F_{tu}, min ksi	F_{tu}, min kg/mm[a]	F_{ty}, min ksi	F_{ty}, min kg/mm[a]	e(4D), min, %	Redn. Area, %	Hardness
Sheet, strip, and plate (air melt); 1800° F (982° C) ST							
0.001-0.0015 in (a)	105	73.8	-	-	10	-	-
>0.0015-0.002	105	73.8	-	-	12	-	-
>0.002-0.004	105	73.8	-	-	20	-	-
>0.004	105	73.8	-	-	25	-	-
1800° F (982° C) ST plus aging (b)							
0.001-0.0015 in	125	87.9	95	66.8	4	-	Rc,24-35
>0.0015-0.002	130	91.4	95	66.8	8	-	24 - 35
>0.002-0.004	135	94.9	95	66.8	10	-	24 - 35
>0.004	140	98.4	95	66.8	15	-	24 - 35
Bars, forgings, tubing, and rings (air melt); 1800° F (982° C) ST plus aging (b)	130	91.4	85	59.8	15	18	BHN, 248 - 351
Bars, forgings, and tubing (cons elec melt); 1650° F (899° C) ST plus aging (b)	140	83.4	95	66.8	12	15	BHN, 277 - 363
Bars, forgings, tubing, and rings (cons elec); 1800° F (982° C) ST plus aging (b)	130	91.4	85	59.8	15	20	BHN, 248 - 341

(a) 1 inch = 25.4 mm

(b) 1325° F (718° C) for 16 hr, AC.

TABLE 7.411. – Design Mechanical Properties for STA Material

Source	Ref. 7.4					
Alloy	A-286					
Form	Sheet, strip, and plate		Bars, forgings, and mechanical tubing			
	Thickness >0.004 in (>0.102 mm)		-------		Consumable electrode melted	
Basis	S		S		S	
F_{tu}, ksi (kg/mm^2)	140	(98.4)	130	(91.4)	140	(98.4)
F_{ty}, ksi	95	(66.8)	85	(59.8)	95	(66.8)
F_{cy}, ksi	95	(66.8)	85	(59.8)	95	(66.8)
F_{su}, ksi	91	(64.0)	85	(59.8)	91	(64.0)
F_{bru}, ksi						
(e/D = 1.5)	210	(147)	195	(137)	210	(148)
(e/D = 2.0)	266	(187)	247	(173)	266	(187)
F_{bry}, ksi						
(e/D = 1.5)	142	(99.8)	127	(89.3)	142	(99.8)
(e/D = 2.0)	171	(120)	153	(107)	171	(120)
e, percent	15	(a)	15	(b)	12	(b)

(a) Elongation in 2 inches (50.8 mm)

(b) Elongation in 4D.

TABLE 7.4121. —Averages for Tensile Test Data for Vacuum Melt Heats from Two Different Parent Melt Heats (a)

Source	Ref. 7.7	
Alloy	A-286, 1-3/4 x 3-1/2 in (4.4 x 8.9 cm) bar	
Parent Air Melt	"A," 1.9-2.3 Ti	"B," 1.9-2.3 Ti
Composition, %	Vacuum melts	Vacuum melts
Carbon	0.03	0.04
Manganese	1.19	1.29
Sulfur	0.005	0.007
Phosphorus	0.019	0.023
Silicon	0.78	0.59
Nickel	25.48	24.77
Chromium	14.28	15.02
Molybdenum	1.20	1.21
Vanadium	0.27	0.29
Titanium	2.23	2.22
Aluminum	0.22	0.22
Boron	0.009	0.008
Mechanical Properties		
1800°F (982°C), 1 hr, OQ, 1325°F (718°C), 16 hr, AC		
0.02% F_{ty}, ksi (kg/mm²)	90.7 (63.8)	97.5 (68.5)
0.2% F_{ty}, ksi	108.2 (76.1)	113.2 (79.6)
F_{tu}, ksi	153.9 (108.2)	162.1 (114.0)
Redn of Area, %	45	45
Elongation, %	22	24
1800°F (982°C), 1 hr, OQ, 1650°F (899°C), 2 hr, OQ, 1325°F (718°C), 16 hr, AC		
0.02% F_{ty}, ksi	89.7 (63.1)	99.2 (69.7)
0.2% F_{ty}, ksi	106.0 (74.5)	114.6 (80.6)
F_{tu}, ksi	153.7 (108.0)	161.4 (113.5)
Redn of Area, %	44	46
Elongation, %	22	23
1800°F (982°C), 1 hr, OQ, 1650°F (899°C), 2 hr, OQ, 1300°F (704°C), 16 hr, AC		
0.02% F_{ty}, ksi	87.7 (61.7)	97.0 (68.2)
0.2% F_{ty}, ksi	103.0 (72.4)	111.0 (78.0)
F_{tu}, ksi	154.5 (108.6)	162.5 (114.2)
Redn of Area, %	43	48
Elongation, %	23	24

(a) Chemical analyses and tensile properties were reported for each of 3 vacuum melt heats from each parent heat; additionally, results were given for top and bottom of bar. Because of the excellent agreement of values, averages are presented.

TABLE 7.4122. — Typical Tensile Properties at Room Temperature of Various Mill Products

Source	Refs. 7.2, 7.8, 7.9, 7.13					
Alloy	A-286					
Product/Treatment	F_{ty}, 0.2% offset ksi	kg/mm²	F_{tu} ksi	kg/mm²	Elong, %	Redn in Area, %
Extrusions						
1800° F (982° C), WQ -L	119.5	84.0	162.0	113.9	29.0	45.2
+ 1325° F (718° C), AC -T	105.0	73.8	130.7	91.9	27.3	51.0
1650° F (899° C), WQ -L	85.6	60.2	148.5	104.4	25.4	42.4
+ 1325° (718° C), AC -T	88.8	62.4	147.4	103.6	24.0	33.7
1750° F (954° C), WQ -L	85.0	59.8	150.0	105.4	26.0	37.0
+ 1300° F (704° C), AC -T	82.9	58.3	131.0	92.1	15.0	20.0
Bar Stock						
1800° F (982° C), OQ + 1325° F (718° C), AC	96.0	67.5	146.	102.6	24.5	41.
Vacuum Castings						
2000° F (1093° C), OQ + 1650° F (899° C) + 1325° F (718° C), AC	85.4	60.0	106.0	74.5	10.5	17.
Tubing						
Annealed	35-60	25-42	110.	77.	50-25	

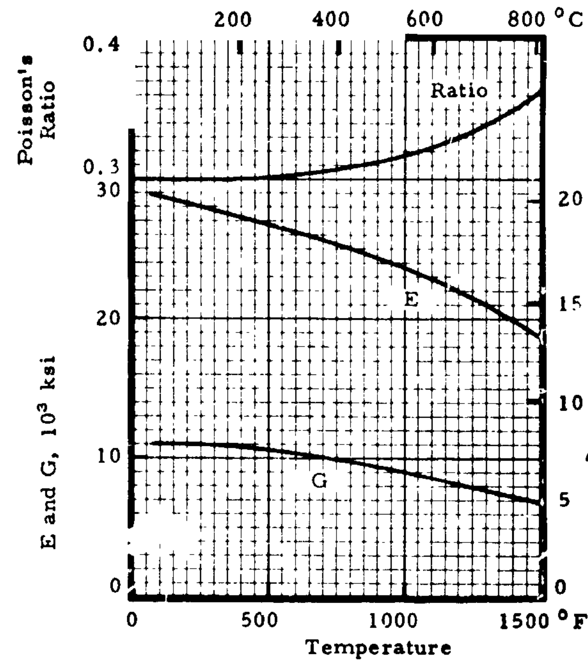

FIGURE 7.21. - Values of E, G, and Poisson's ratio for A-286 at room and elevated temperatures.
(Refs. 7.2, 7.3)

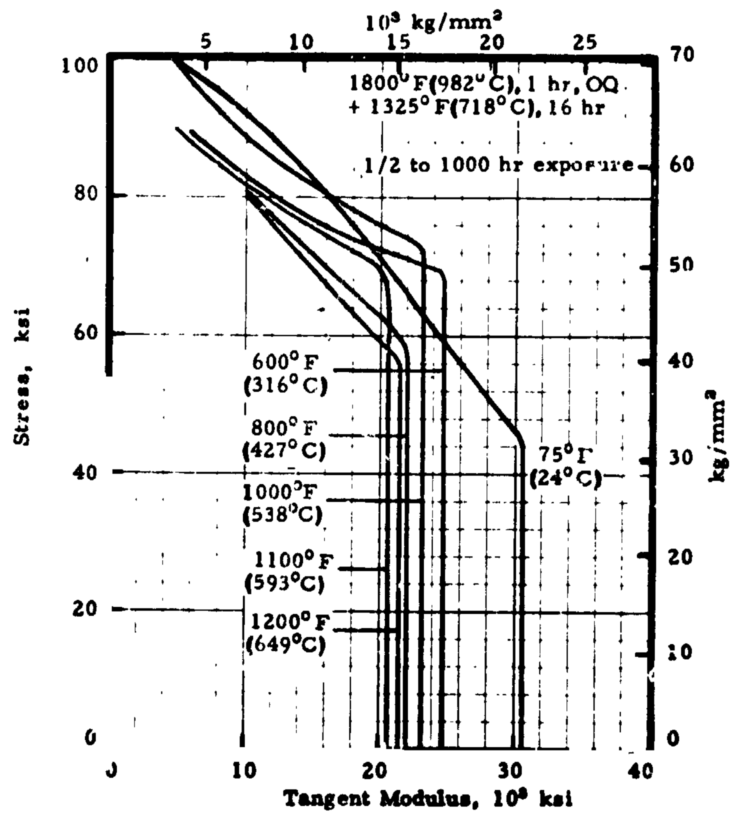

FIGURE 7.251. - Tangent modulus curves in compression for A-286 sheet at room and elevated temperatures; 0.062 in (1.58 mm).
(Refs. 7.10, 7.11)

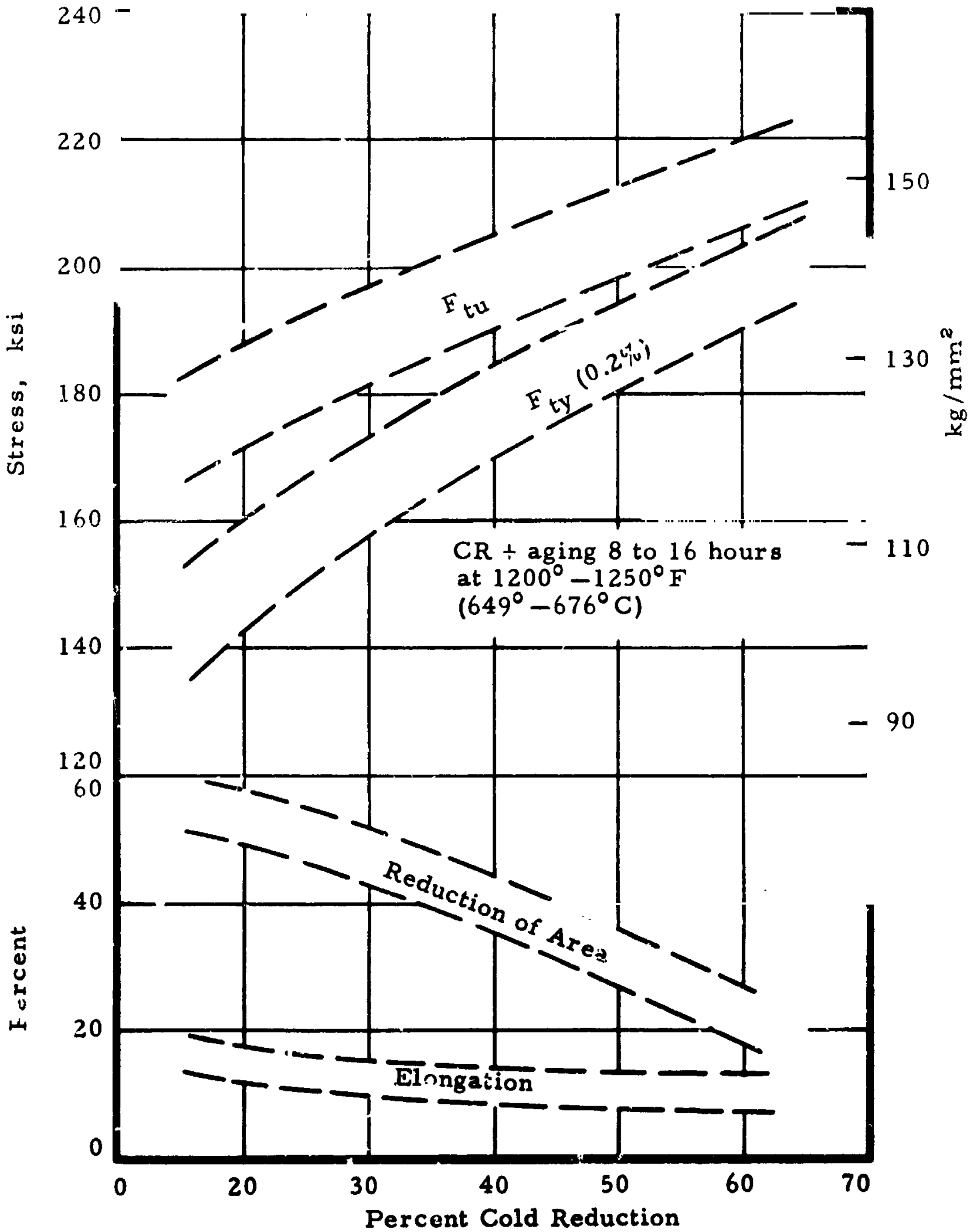

FIGURE 7.4123. – Effect of cold reduction on tensile properties of aged A-286 bar and wire.

(Ref. 7.2)

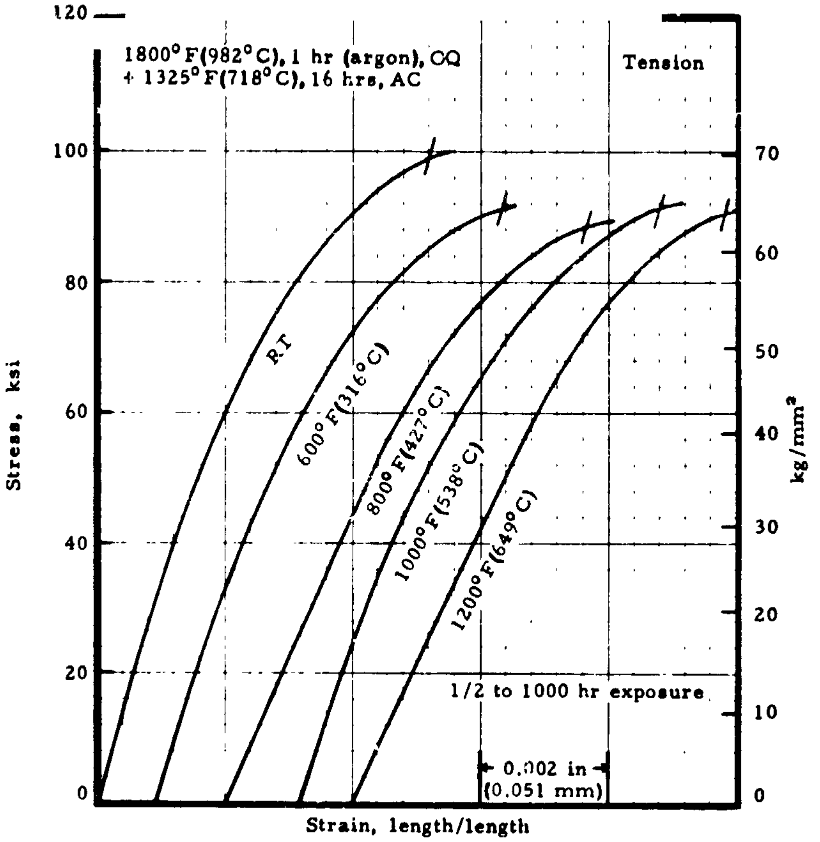

FIGURE 7.4131. — Stress-strain curves in tension for A-286 sheet at room and elevated temperatures; 0.062 in (1.57 mm). (Refs. 8.10, 7.11)

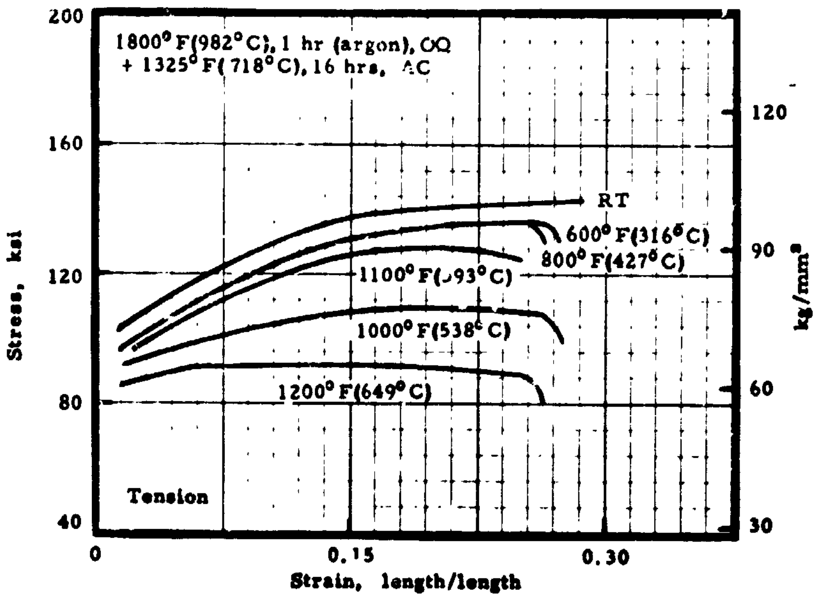

FIGURE 7.4132. — Stress strain curves to failure for A-286 sheet at room and elevated temperatures. (Refs. 7.10, 7.11)

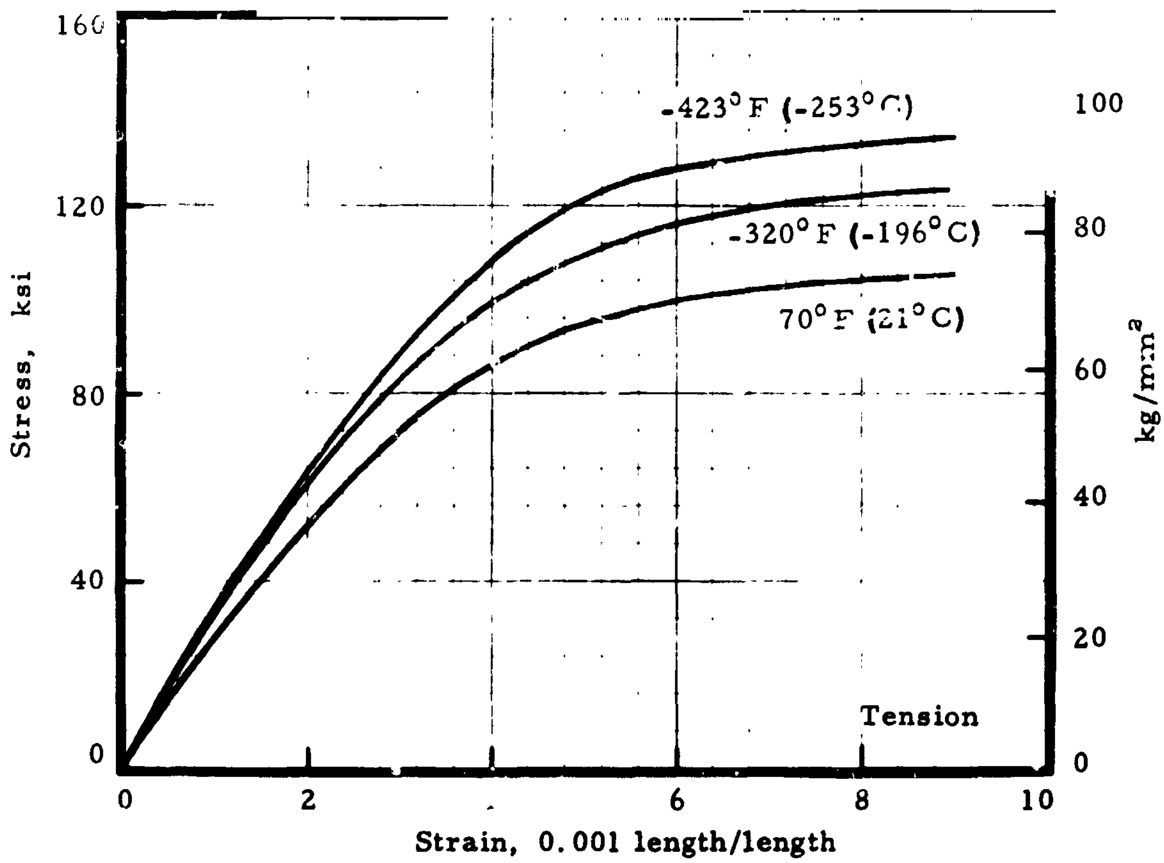

FIGURE 7.4133. -- Typical stress-strain curves for A-286 sheet at room and cryogenic temperatures; 0.050 in (1.27 mm). [1800° F (982° C), AC, 1325° F (718° C), 16 hrs]

(Ref. 7.17)

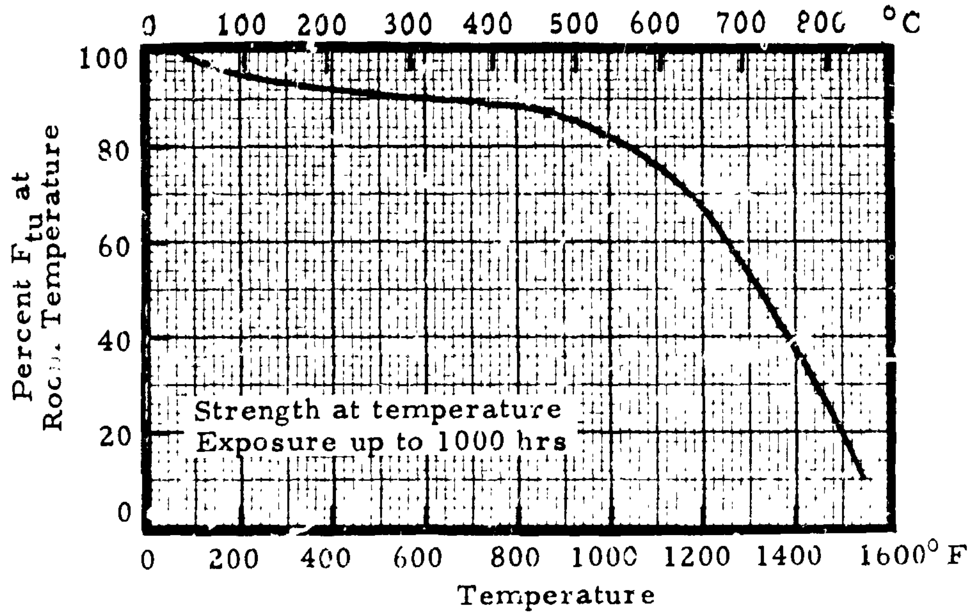

FIGURE 7.4141. – Effect of temperature on the ultimate tensile strength of A-286.
(Ref. 7.4)

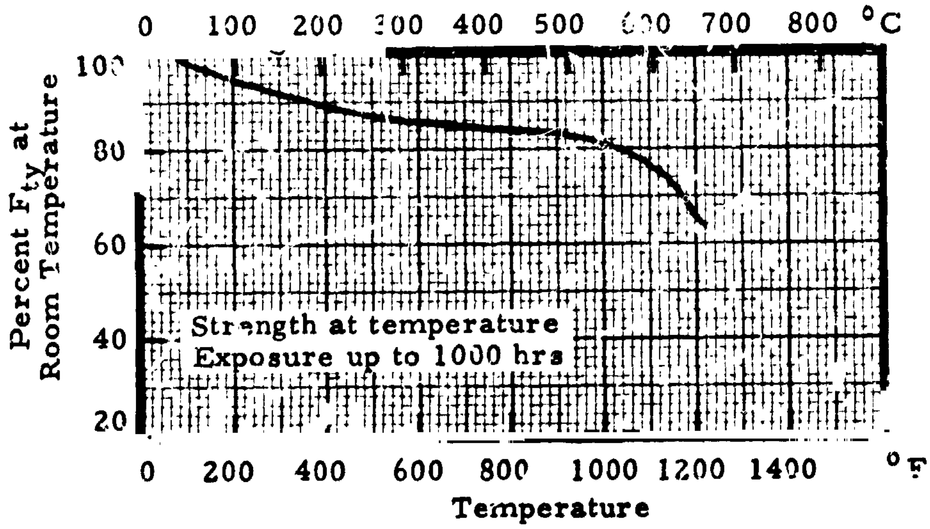

FIGURE 7.4142. – Effect of temperature on the tensile yield strength of A-286.
(Ref. 7.4)

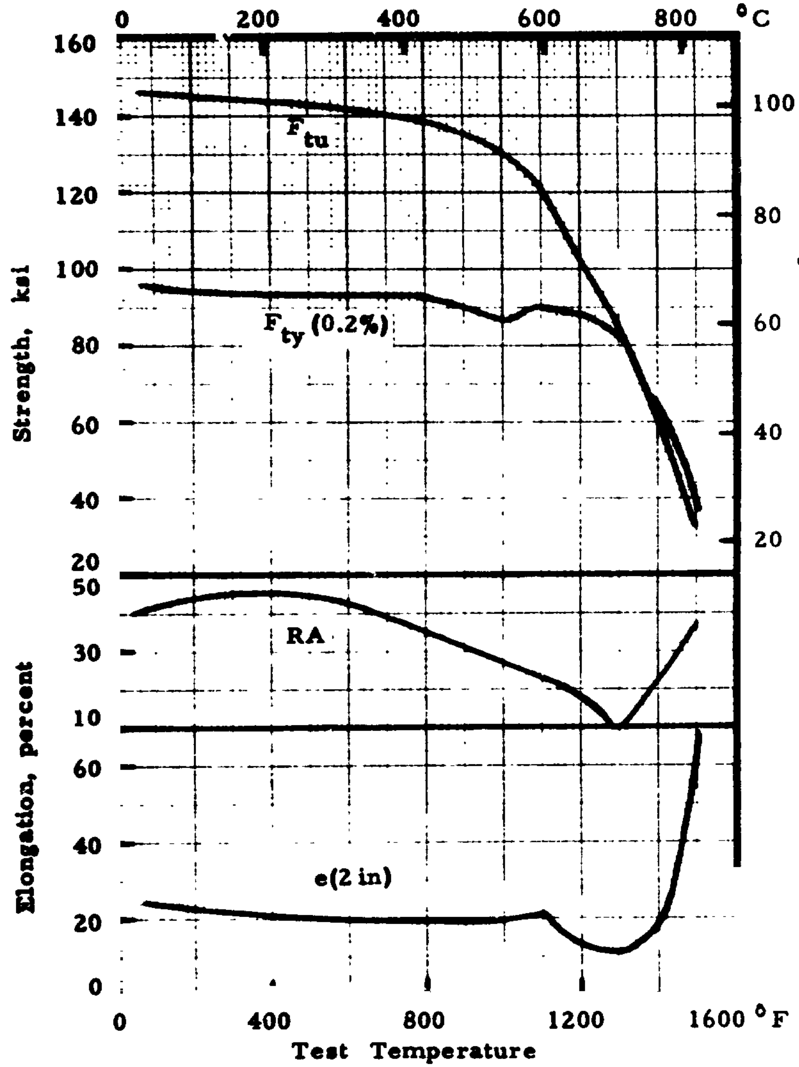

FIGURE 7.4143. – Effect of elevated temperatures on tensile properties of A-286 bar stock; 7/8-in (22.2-mm) diameter; 1088°F (982°C), 1 hr, OQ, + 1325°F (718°C), 16 hrs, AC. (Ref. 7.6)

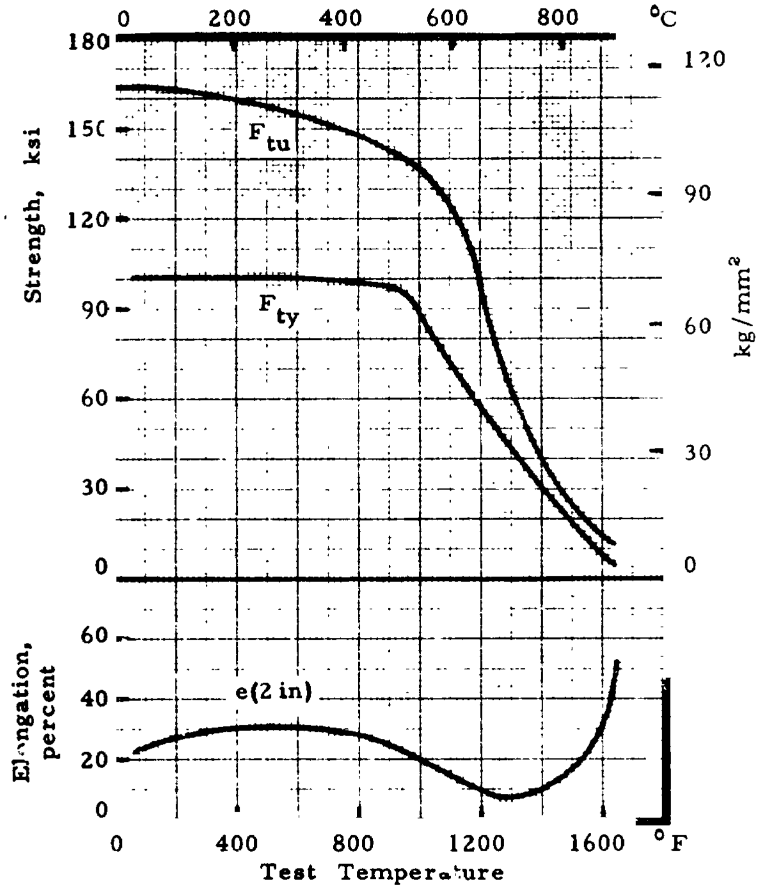

FIGURE 7.4144. – Effect of elevated temperatures on tensile properties of solution treated and aged A-286 tubing; 0.250-in (6.35-mm) O.D. by 0.028 (0.711-mm) wall or smaller. (Refs. 7.2, 7.13)

B

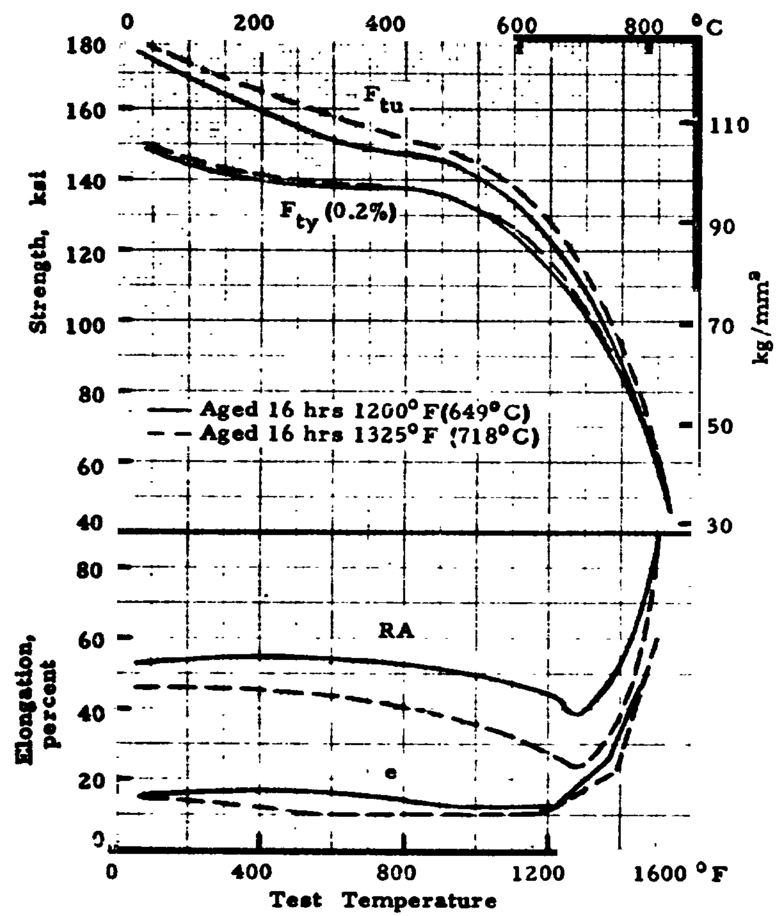

FIGURE 7.4145. — Effect of elevated temperatures on tensile properties of 15-percent cold-drawn and aged A-286 wire; 0.462-in (11.7-mm) diam. (Ref. 7.2)

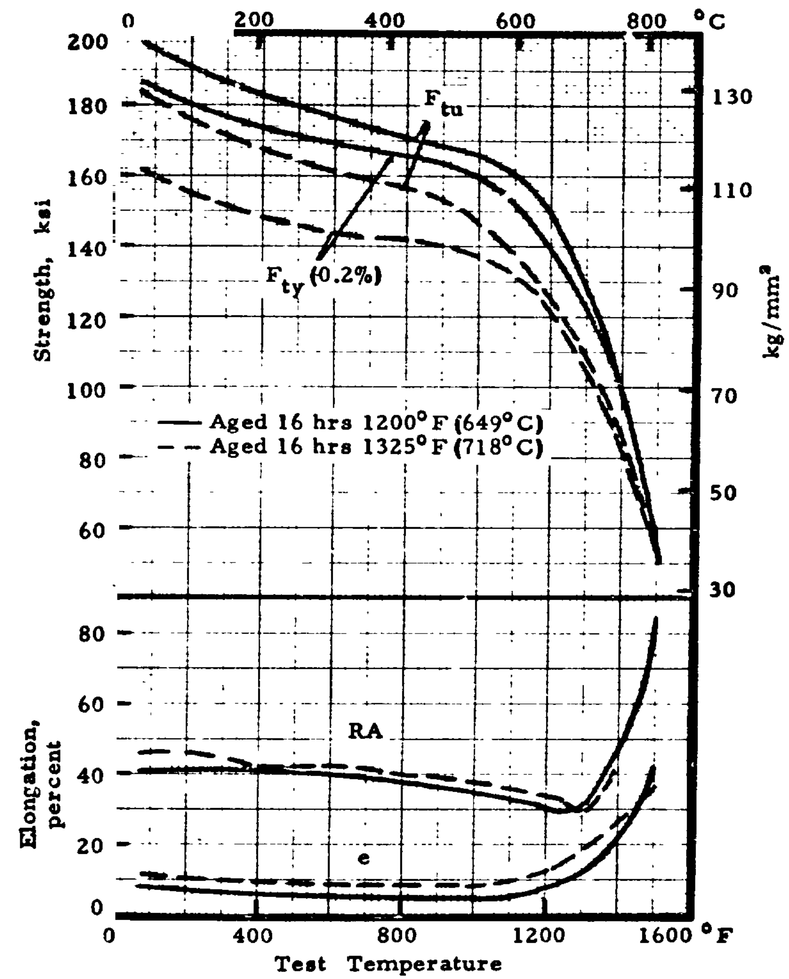

FIGURE 7.4146. — Effect of elevated temperatures on tensile properties of 40-percent cold-drawn and aged A-286 wire; 0.337-in (8.56-mm) diam. (Ref. 7.2)

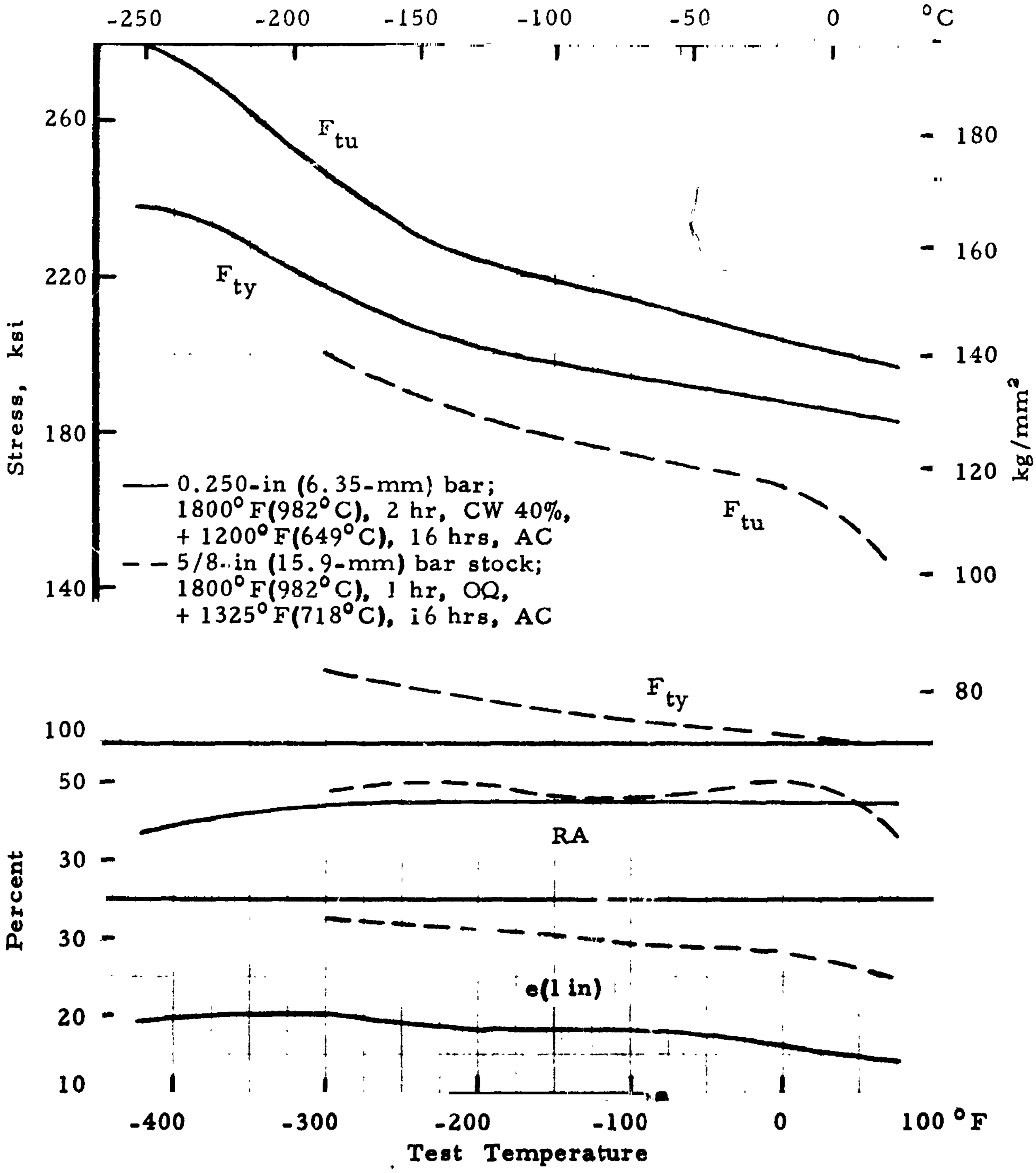

FIGURE 7.4147. — Effect of cryogenic temperature on tensile properties of A-286 bar stock and cold-worked-and-aged bar. **(Refs. 7.2, 7.14)**

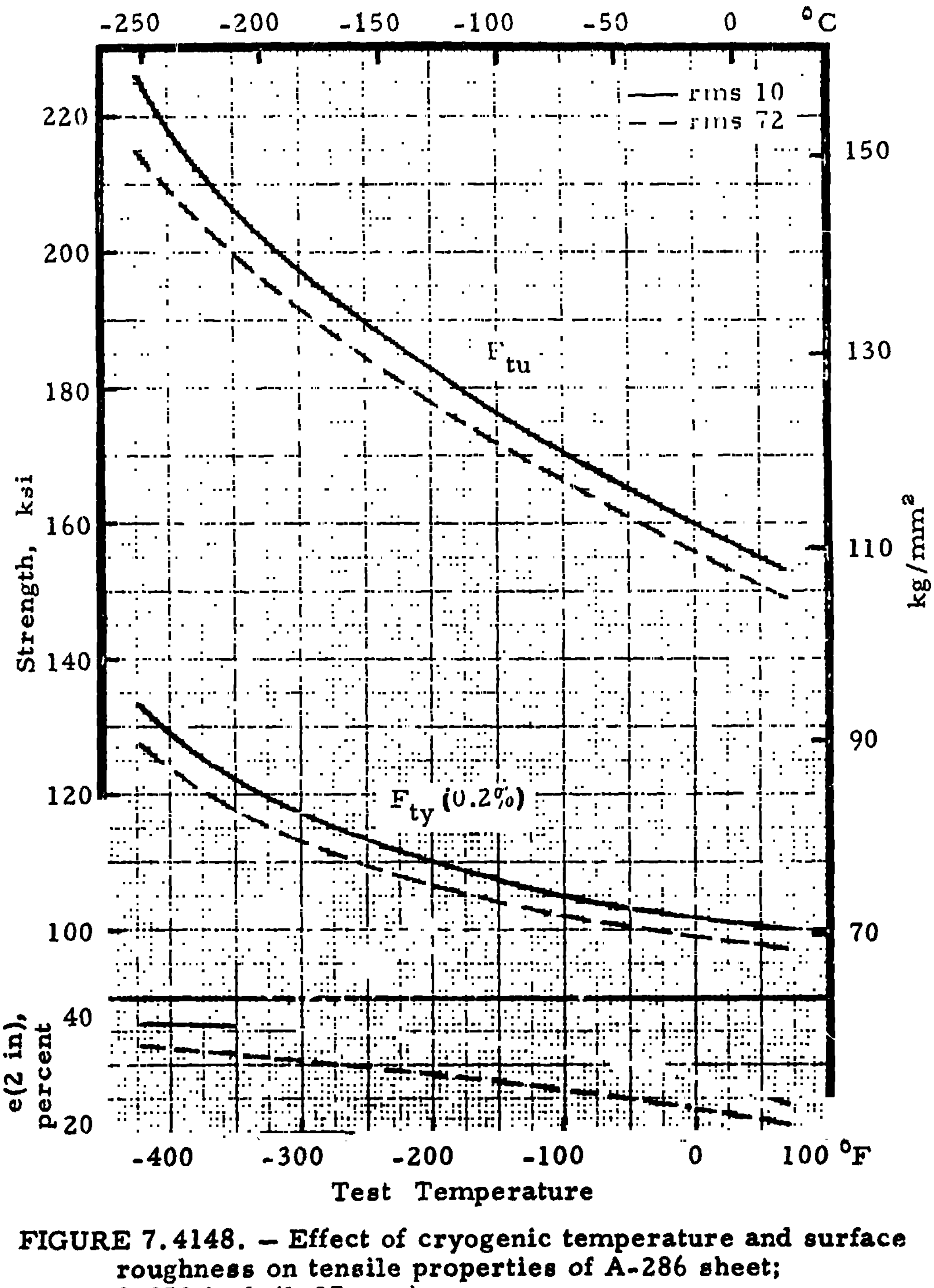

FIGURE 7.4148. – Effect of cryogenic temperature and surface roughness on tensile properties of A-286 sheet; 0.050 inch (1.27 mm).

(Ref. 7.17)

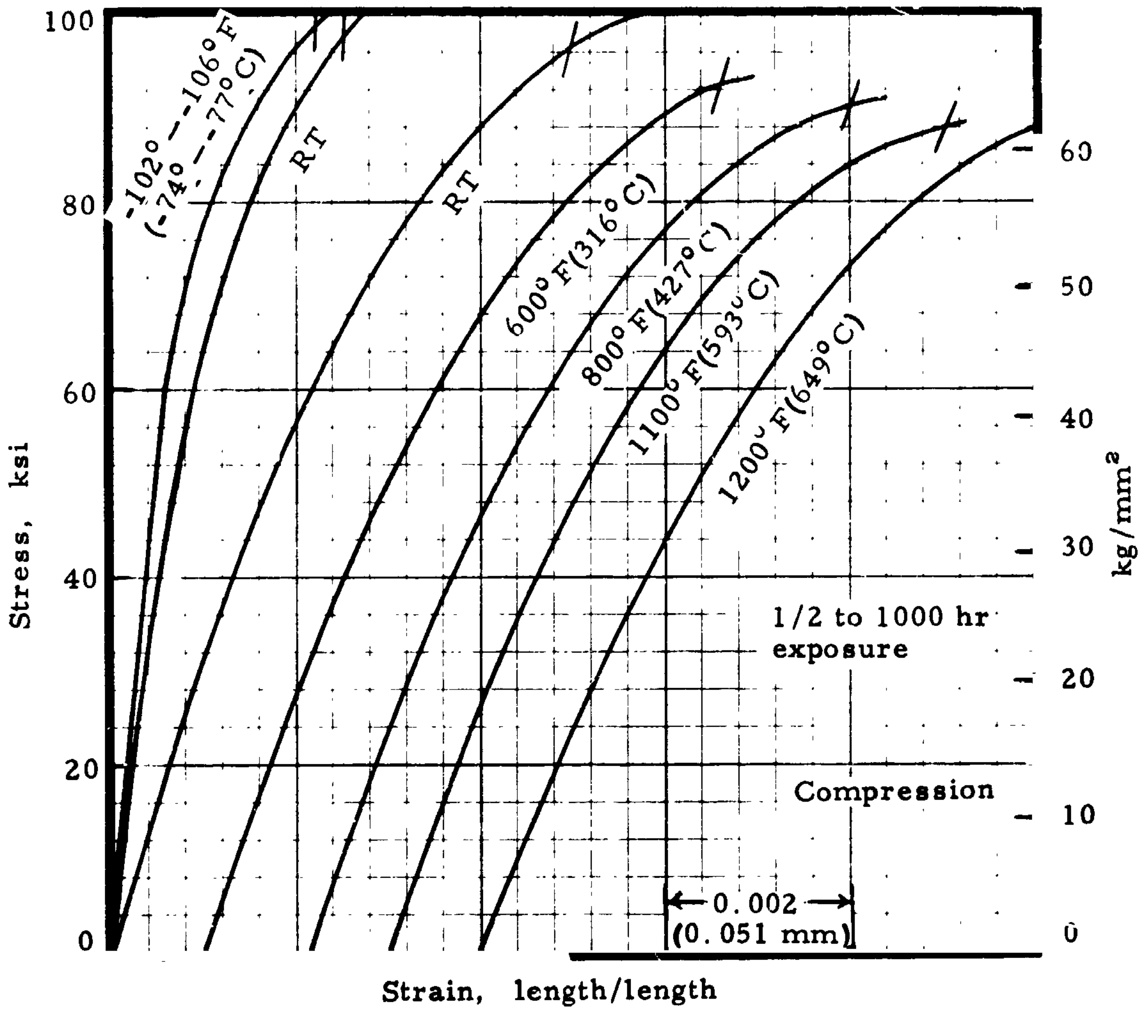

FIGURE 7.421. – Stress-strain curves in compression for A-286 sheet at various temperatures; 0.025-in (0.635-mm) thickness; 1800° F (982°C), 1 hr, OQ, plus 1325° F (718° C), 16 hrs. (Ref. 7.14)

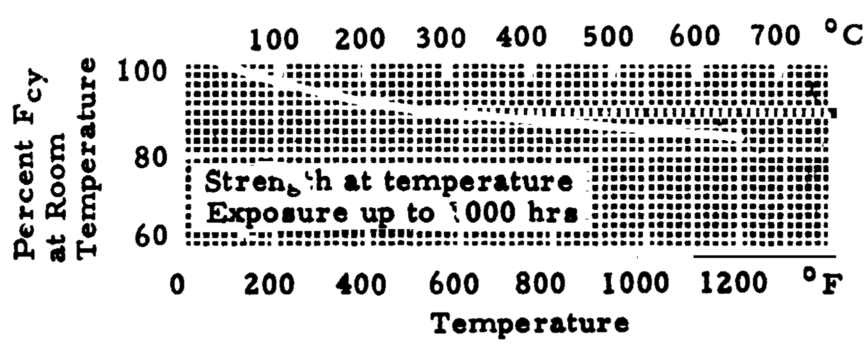

FIGURE 7.422. – Effect of temperature on compressive yield strength of A-286. (Ref. 7.4)

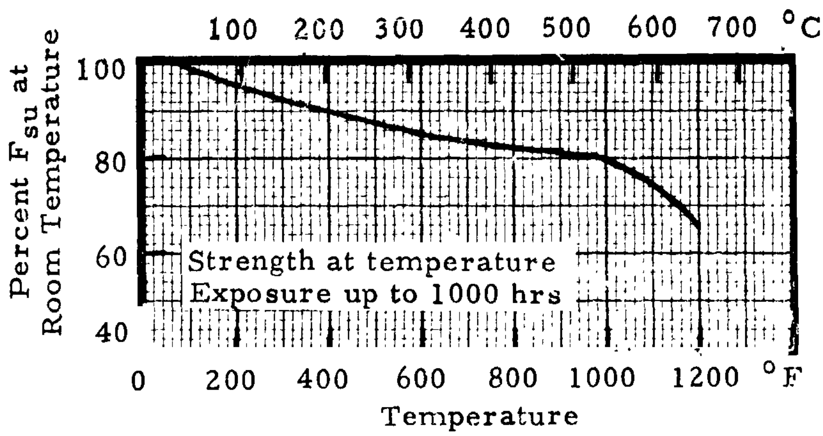

FIGURE 7.441. — Effect of temperature on the ultimate shear strength of A-286.
(Ref. 7.4)

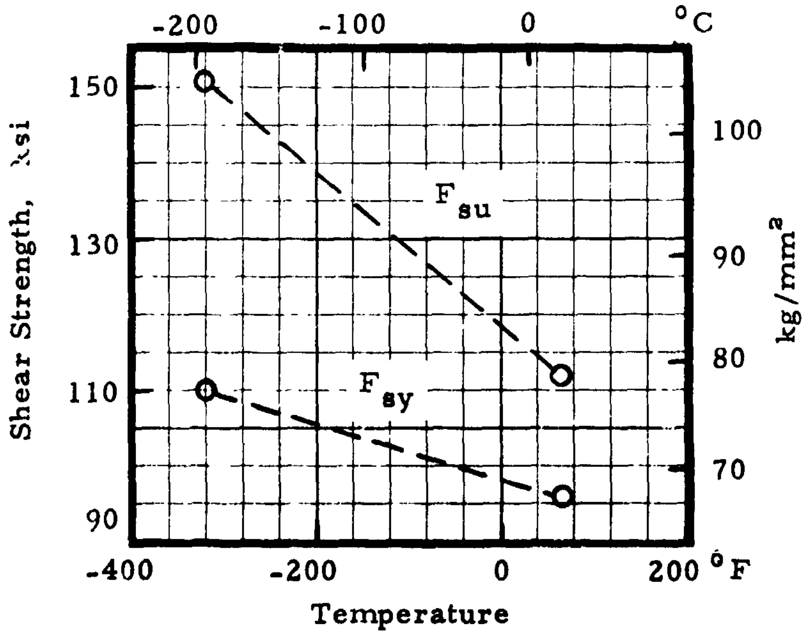

FIGURE 7.442. — Results of double-shear tests on 0.312-in (7.92-mm) bar; cold drawn and aged at 1200° F (649° C), 16 hrs.
(Ref. 7.14)

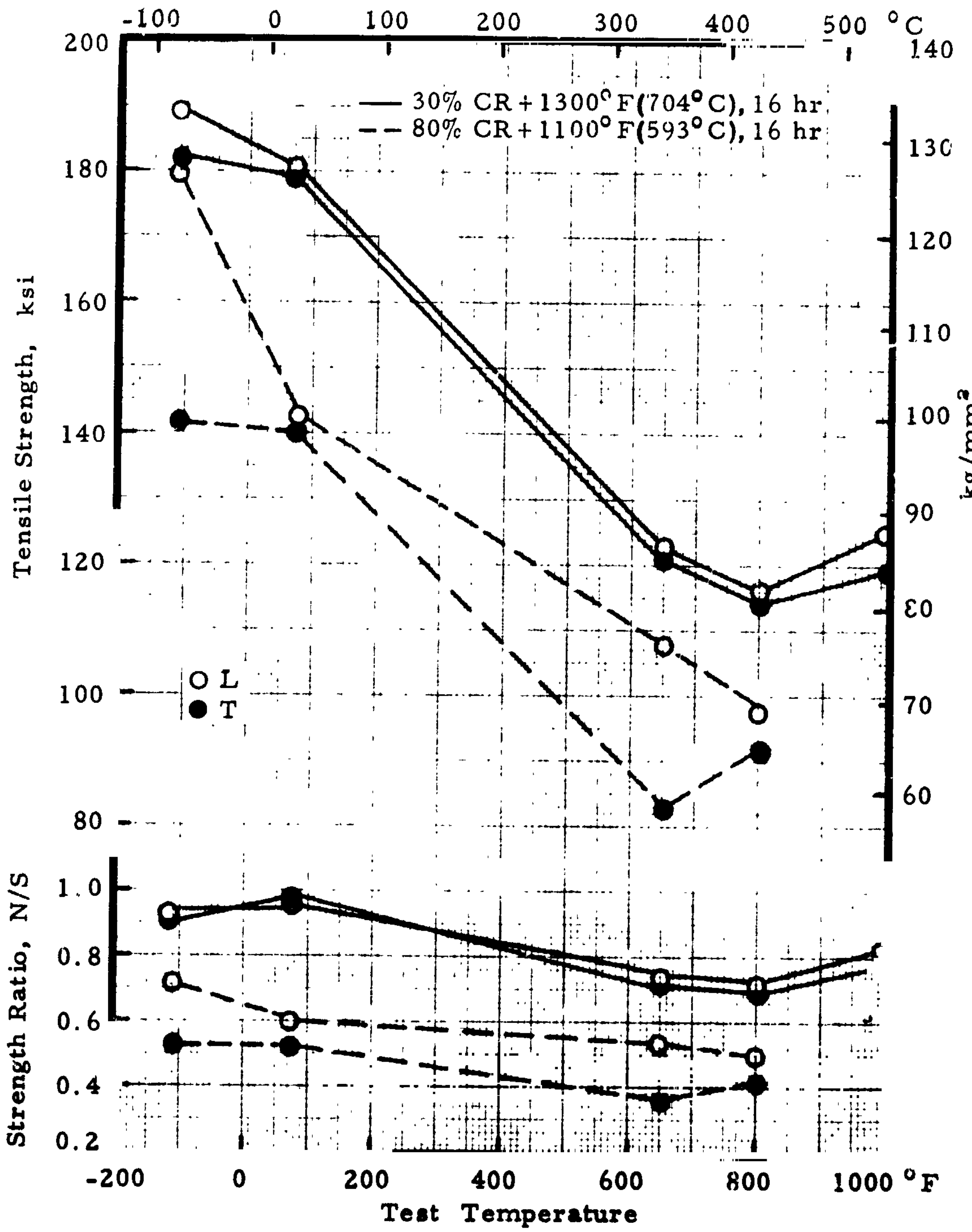

FIGURE 7.4611. — Effect of temperature on notch strength of cold reduced and aged A-286 sheet, 0.025 in (0.635 mm).

(Ref. 7.12)

Chapter 7 - References

7.1 AMS Material Specifications, Society Automotive Engineers, Inc., New York; latest Index, May 1971.

7.2 Universal Cyclops-Specialty Steel Division, "Unitemp A-286," HT 3020, 1971.

7.3 American Iron and Steel Institute, "High Temperature High-Strength Alloys," New York, February 1963.

7.4 Military Handbook 5-A, Dept. of Defense, FSC 1500, "Metallic Materials and Elements for Aerospace Vehicle Structures," February 1966; latest change order January 1970.

7.5 1971 SAE Handbook, Society Automotive Engineers, Inc., New York.

7.6 Superior Tube, "Super Alloy Tubing," Bulletin 71, June 1968.

7.7 Republic Steel/Special Metals Division, "Data on Some Republic Steel Consumable Electrode Vacuum Arc Remelt Steels," June 1969.

7.8 R.J. Fiorentino and A.M. Sabroff, "Availability and Mechanical Properties of High-Strength Steel Extrusions," DMIC Report 138, October 26, 1960.

7.9 Precision Metal Molding, 22, 57 (September 1964), "Vacuum-Melted Investment Casting Alloys."

7.10 J.R. Kattus, J.B. Preston, and H.L. Lessley, "Determination of Tensile, Compressive, Bearing, and Shear Properties at Elevated Temperatures," WADC TR 58-365, November 1958.

7.11 J.G. Sessler and V. Weiss, Eds., "Aerospace Structural Metals Handbook," AFML TR 68-115, 1971 Edition.

7.12 R.H. Raring, et al., "Progress Report of the NASA Special Committee on Materials Research for Supersonic Transports," NASA TN D-1798, May 1963.

7.13 Carpenter Technology Corporation, "Carpenter A-286," Technical Data, June 1970.

7.14 J.W. Montano, "An Evaluation of the Mechanical and Stress Corrosion Properties of Cold Worked A-286 Alloy," NASA TM X-64569, February 12, 1971.

7.15 AMS Specification 5525C, as revised 11-1-68.

7.16 K.E. Fritz and D.R. deForest, "High Strength Turbo Generator Retaining Ring Forgings of an Age-Hardenable Austenitic Alloy," J. Materials, 3 (2), 629 (1968).

7.17 E.H. Schmidt, "Fatigue Properties of Sheet, Bar, and Cast Metallic Materials for Cryogenic Applications," Rocketdyne Engineering Report R-7564 under Contract NAS8-18734, 30 August 1968; see also NASA Tech Brief 70-10199.

Chapter 8

DYNAMIC AND TIME DEPENDENT PROPERTIES

8.1 General. Alloy A-286 has excellent dynamic and time-dependent properties at elevated temperatures; for example, the relatively low stress-relaxation makes it particularly attractive for high-temperature bolt and spring applications (ref. 8.1). Additionally, experience has shown that for good design, A-286 has suffered practically no failures at cryogenic temperatures. On the basis of similar strength level and grain size, it has better fatigue strength than K-Monel (ref. 8.2).

8.2 Specified Properties

8.21 AMS spe ified stress-rupture requirements, table 8.21.

8.3 Impact Strength

8.31 V-Notch Charpy impact data for bar stock at cryogenic temperatures, figure 8.31.

8.32 V-Notch Charpy impact data for bar stock at elevated temperatures, figure 8.32.

8.4 Creep

8.41 Creep and creep rupture data

8.411 Creep strength of A-286 bar at elevated temperatures, figure 8.411.

8.412 Stress to rupture at elevated temperatures of tubing, figure 4.12.

8.413 Stress rupture properties for annealed and aged A-286 at elevated temperatures, figure 8.413.

8.42 Linear parameter master curves

8.421 Parameter plot of typical stress-rupture life for bar, figure 8.421.

8.43 Stress relaxation data

8.431 Relaxation of A-286 helical compression springs at constant deflection, figure 8.431.

8.432 Relaxation of springs with various stresses at 1000°F (538°C), table 8.432.

8.433 Producers' design data for bolts at elevated temperatures, table 8.433.

8.5 Stability (see also Chapter 7)

8.51 Effect of exposure on tensile properties of cold rolled and aged sheet, table 8.51.

8.52 Effect of exposure on notch strength of cold rolled and aged sheet, tabl3 8.52.

8.53 Effect of exposure and test temperature on shear strength of sheet and bar, figure 8.53.

8.54 Effect of exposure and test temperature on bearing properties of sheet, figure 8.54.

8.6 Fatigue

8.61 Reversed-bending flexural fatigue data for A-286 sheet at room and cryogenic temperatures, figure 8.61.

TABLE 8.21. — AMS Specified Stress Rupture Requirements

Source	Ref. 8.5								
Alloy	A-286								
AMS Spec No.	Product	Condition	Specimen	Exposure Temp °F	Exposure Temp °C	Exposure Axial Load or Stress, ksi	Exposure Axial Load or Stress, kg/mm^2	Rupture Life, min hrs	Elongation after Rupture
5734E 5734C	Bars, forgings, and tubing	Cons elec melted, 1650° F (899° C) ST plus HT (a)	Combination smooth and notched	1200	649	65	46	23	≥ 5% (4D), ≥ 48 hrs; ≥ 3% (4D) < 48 hrs
5735G 5736F	Bars, forgings, tubing, and rings	1800° F (982° C) ST plus HT (a)	Combination smooth and notched	1200	649	65	46	23	≥ 5% (4D) ≥ 48 hrs; ≥ 3% (4D) < 48 hrs
5731D 5732C	Bars, forgings, tubing, and rings	cons elec melted, 1800° F (982° C) ST plus HT (a)	Combination smooth and notched	1200	649	70	49	23	≥ 5% (4D), ≥ 48 hrs; ≥ 3% (4D), < 48 hrs
5525C	Sheet, strip, and plate	1800° F (982° C) ST plus HT (a) ≤ 0.005 in (b) 0.005-0.007 0.007-0.009 0.009-0.012 0.012-0.015 0.015-0.020 >0.020	Tensile	1200	649	62.5	44	 none 6 10 14 16 20 24	

(a) 1325° F (718° C), 16 hrs, AC (b) 1 inch = 25.4 mm

TABLE 8.432. – Relaxation of Springs with Various Stresses at 1000°F (538°C) (a)

Source		Ref. 8.11					
Alloy		A-286					
Temper		15% RA					
Stress		Relaxation, % Load Loss					
ksi	kg/mm²	5 hr	10 hr	20 hr	50 hr	100 hr	140 hr
10	7	5.0	5.0	5.0	5.0	5.0	5.0
20	14	5.0	5.1	5.5	5.5	6.0	6.0
40	28	5.8	6.3	6.4	6.8	7.5	7.5
60	42	4.7	5.5	6.0	6.4	7.2	7.5
80	56	6.0	6.8	8.2	9.0	10.0	10.0

TABLE 8.433. – Producers' Design Data for Bolts at Elevated Temperatures

Source		Ref. 8.12				
Alloy		A-286				
Temperature		Initial Tensile Stress		Min Relaxed Stress		Design Life, hours
°F	°C	ksi	kg/mm²	(a), ksi	kg/mm²	
700	371	40	28	40	28	-
850	455	90	63	-	-	35,000
1000	538	70	49	-	-	10,000
1000	538	30	21	-	-	10,000
1200	649	40	28	26	18	-
1350	732	20	14	-	-	10,000
1400	760	40	28	10	7	-

(a) Minimum relaxed stress after 1000 hours.

TABLE 8.51. — Effect of Exposure on Tensile Properties of Cold Rolled and Aged Sheet

Source	Ref. 8.13												
Alloy	A-286												
Thickness	0.025 in (0.635 mm)												
Cond.	Prior Exposure				Test Temperature		F_{tu}, ksi (kg/mm²)		F_{ty}, ksi (kg/mm²)		Elong, %		
	Temperature °F	Temperature °C	Stress, ksi (kg/mm²)	Time, hr	°F	°C	L	T	L	T	L	T	
30% CR + Age (a)	None		-	-	-110	-79	202 (142)	195 (137)	169 (119)	166 (117)	14	15	
	None		-	-	RT		185 (130	181 (127)	163 (115)	154 (108)	11	10	
	650	343	40 (28)	1000	RT		181 (127)	182 (128)	162 (114)	157 (110)	9	11	
	1000	538	40 (28)	1000	RT		190 (134)	185 (130)	168 (113)	162 (114)	12	11	
	None		-	-	650	343	166 (117)	167 (117)	151 (106)	147 (103)	6	6	
	650	343	40 (28)	1000	650	343	167 (117)	166 (117)	158 (111)	151 (106)	6	7	
	None		-	-	800	427	162 (114)	163 (115)	145 (102)	146 (103)	5	5	
	None		-	-	1000	538	153 (108)	152 (107)	138 (97)	136 (96)	4.5	4.8	
	1000	538	40 (28)	1000	1000	538	156 (110)	157 (110)	141 (99)	142 (100)	5.0	4.8	
80% CR + Age (b)	None		-	-	-110	-79	253 (178)	275 (193)	243 (171)	262 (184)	2.0	3.8	
	None		-	-	RT		239 (168)	263 (185)	230 (162)	250 (176)	2.8	3.8	
	650	343	40 (28)	1000	RT		238 (167)	264 (186)	229 (161)	- -	2.5	3.3	
	None		-	-	650	343	204 (143)	230 (162)	192 (135)	216 (152)	1.5	2.5	
	650	343	40 (28)	1000	650	343	207 (146)	200 (141)	197 (139)	- -	2.0	1.0	
	None		-	-	800	427	195 (137)	220 (155)	188 (132)	206 (145)	0.8	3.0	

(a) 1300°F (704°C), 16 hr.

(b) 1100°F (593°C), 16 hr.

TABLE 8.52. -- Effect of Exposure on Notch Strength of Cold Rolled and Aged Sheet

Source	Ref. 8.13									
Alloy	A-286									
Thickness	0.025 in (0.635 mm)									
Condition	Prior Exposure				Test		Sharp-Edge Notches			
	Temperature °F	Temperature °C	Stress, ksi (kg/mm²)	Time, hr	Temperature °F	Temperature °C	F_{tu}, ksi (kg/mm²) L	F_{tu}, ksi (kg/mm²) T	Ratio, N/S L	Ratio, N/S T
30% CR + Age (a)	None		-	-	-110	-79	189 (133)	182 (128)	0.94	0.93
	None		-	-	RT		180 (127)	180 (127)	0.97	0.99
	650	343	40 (28)	1000	RT		179 (126)	174 (122)	0.99	0.96
	1000	538	40 (28)	1000	RT		114 (80)	(b)	0.60	-
	None		-	-	650	343	123 (96)	121 (85)	0.74	0.72
	650	343	40 (28)	1000	650	343	143 (101)	123 (86)	0.86	0.74
	None		-	-	800	427	116 (82)	115 (81)	0.72	0.71
	None		-	-	1000	538	125 (88)	119 (84)	0.82	0.78
	1000	538	40 (28)	1000	1000	538	134 (94)	108 (76)	0.86	0.69
80% CR + Age (c)	None		-	-	-110	-79	180 (127)	142 (99)	0.71	0.52
	None		-	-	RT		143 (101)	140 (98)	0.60	0.53
	650	343	40 (28)	1000	RT		130 (91)	126 (89)	0.55	0.48
	None		-	-	650	343	108 (76)	83 (58)	0.53	0.36
	650	343	40 (28)	1000	650	343	112 (79)	123 (86)	0.54	0.61
	None		-	-	800	427	98 (69)	92 (65)	0.50	0.42

(a) 1300°F (704°C), 16 hrs.

(b) Failed during exposure.

(c) 1100°F (593°C), 16 hrs.

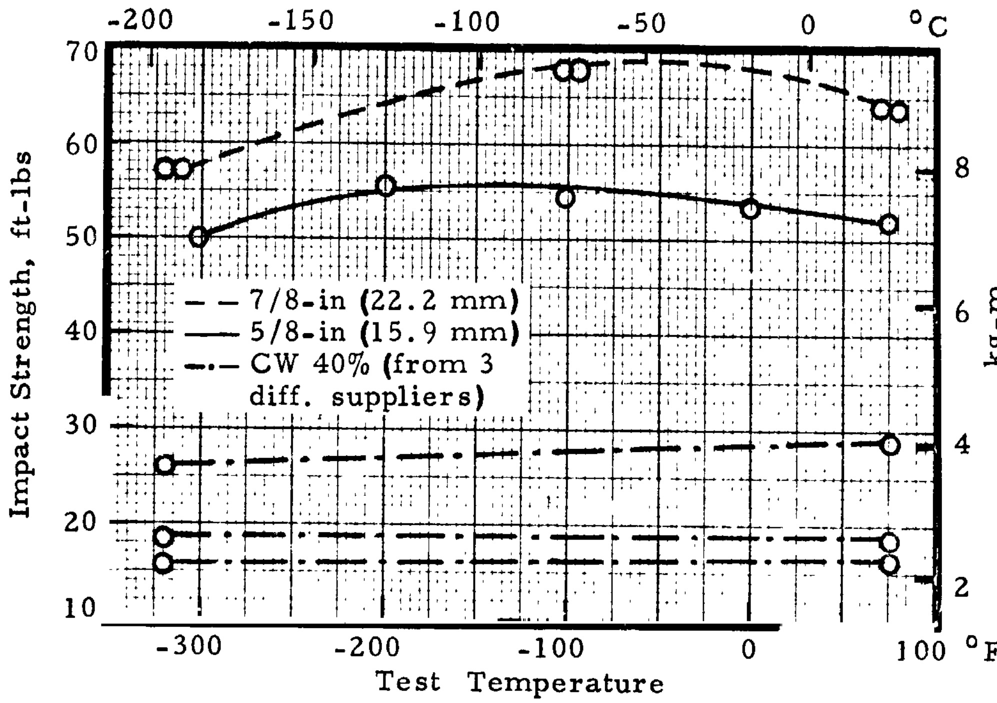

FIGURE 8.31. – V-Notch Charpy impact data at cryogenic temperatures for A-286 bar stock.
[5/8-in and 7/8-in: ST 1800° F(982° C), 1 hr, OQ + 1325° F(718° C), 16 hrs, AC.
CW 40%: aged 1200° F(649° C), 16 hrs, AC]
(Refs. 8.1, 8.4, 8.6 8.7)

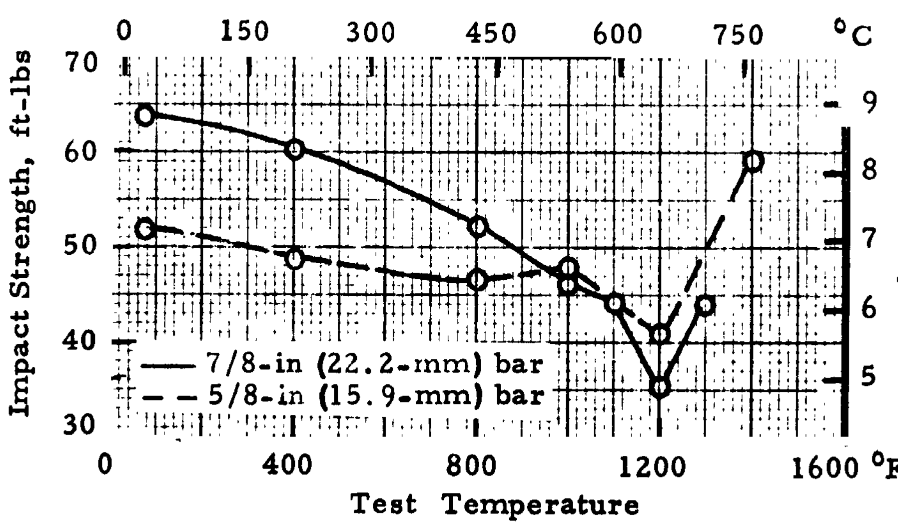

FIGURE 8.32. – V-Notch Charpy impact data at elevated temperatures for A-286 bar stock.
(Refs. 8.1, 8.4)

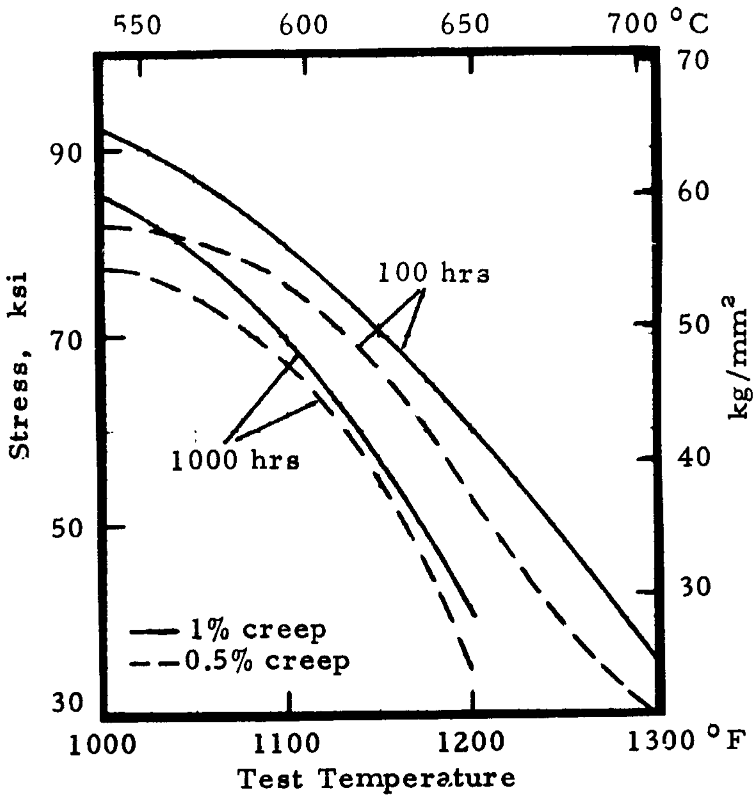

FIGURE 8.411. – Creep strength of A-286 bar at elevated temperatures. (Refs. 8.1, 8.3)

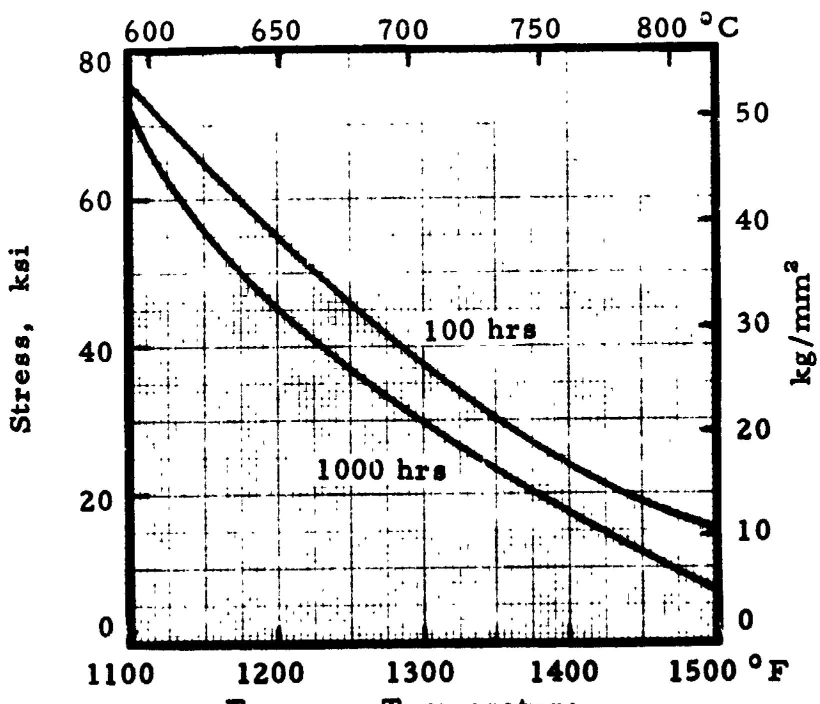

FIGURE 8.412. – Stress to rupture at elevated temperatures of A-286 tubing; 0.250 in (6.35 mm) O.D. by 0.028 in (0.711 mm) wall. (Ref. 8.8)

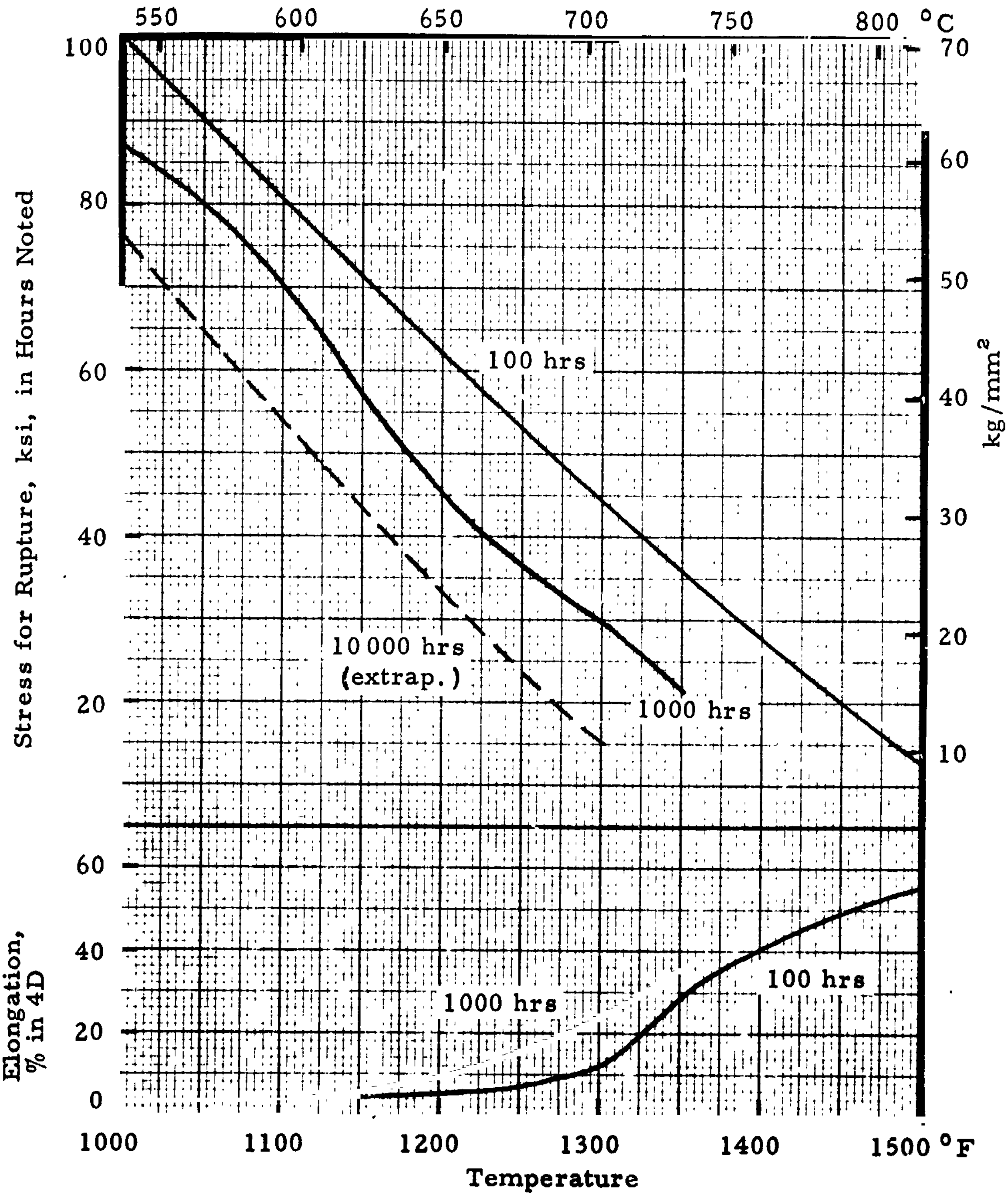

FIGURE 8.413. — Stress rupture properties of annealed and aged A-286 at elevated temperatures.

(Refs. 8.1, 8.9)

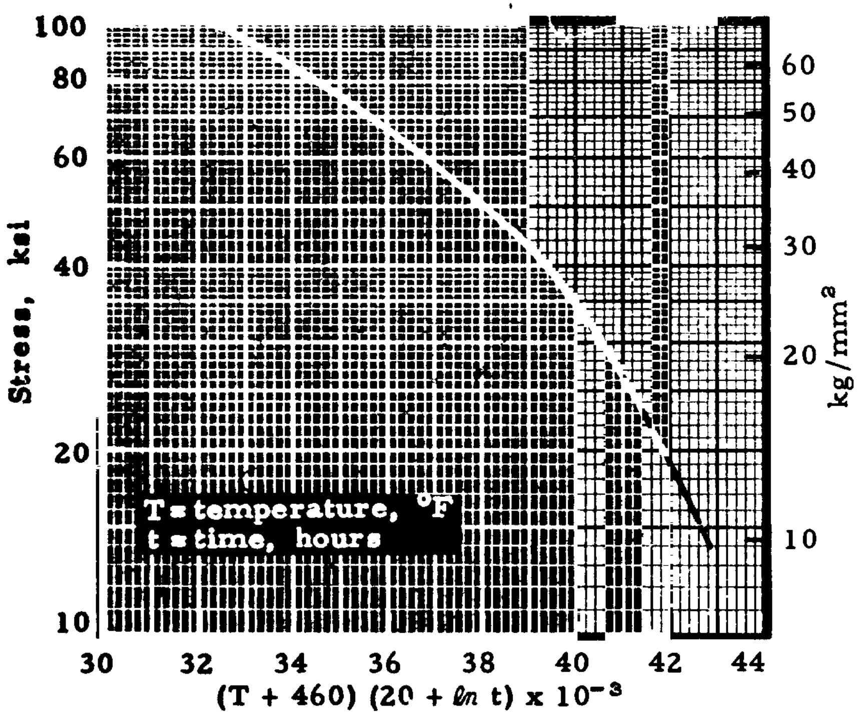

FIGURE 8.421. — Parameter plot of typical stress-rupture life for A-286 bar; 1800°F (982°C), 1 hr, OQ, 1325°F (718°C), 16 hrs, AC.

(Ref. 8.1)

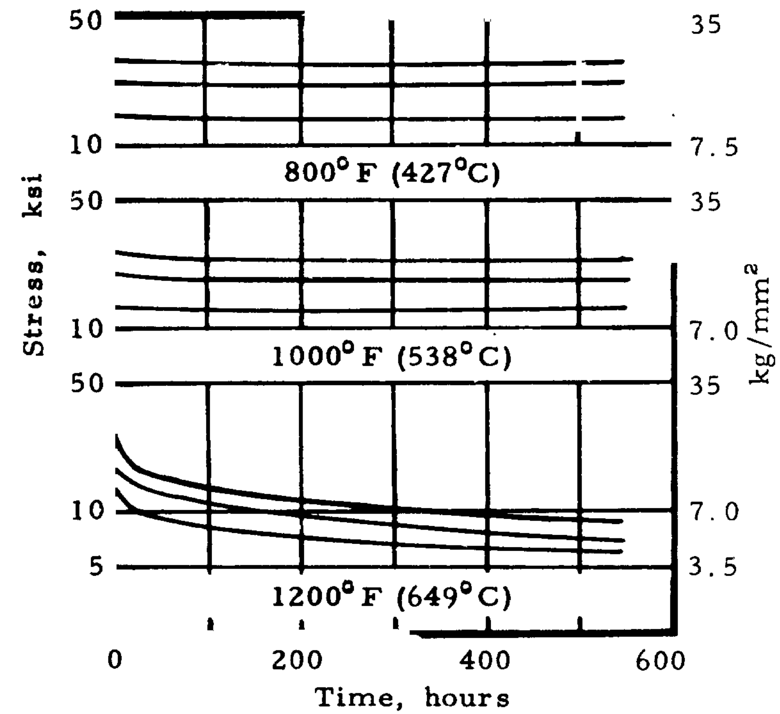

FIGURE 8.431. — Relaxation of A-286 helical compression spring at constant deflection; type "A," 0.063 in (1.60 mm). [Solution-treated, coiled, aged 1400°F (760°C), 16 to 20 hrs]

(Ref. 8.10)

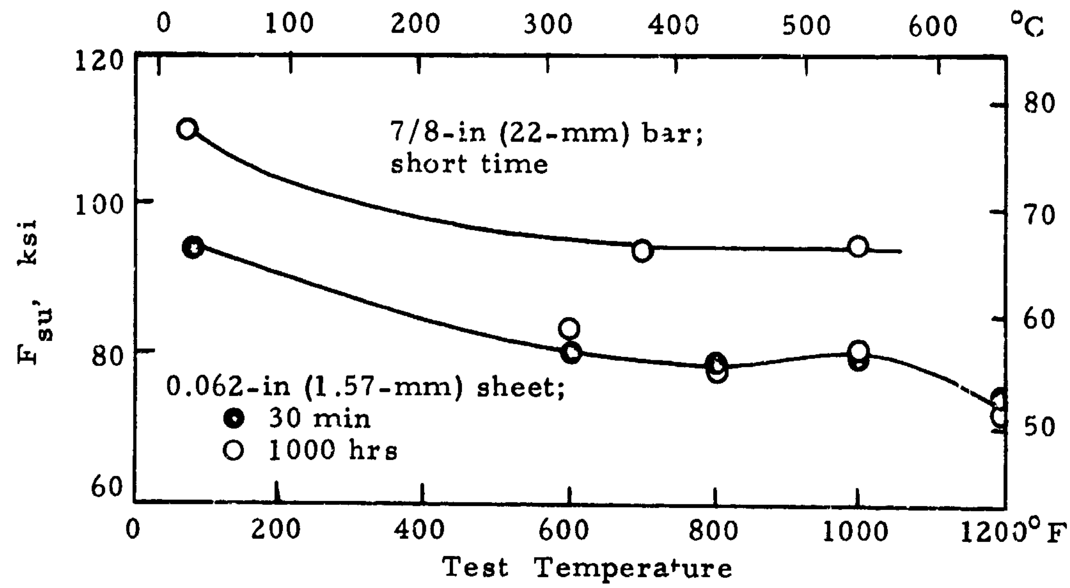

FIGURE 8.53. – Effect of exposure and test temperature on shear strength of A-286 sheet and bar. [1800°F (982°C), 1 hr, OQ, 1325°F (718°C), AC] (Refs. 8.14, 8.15)

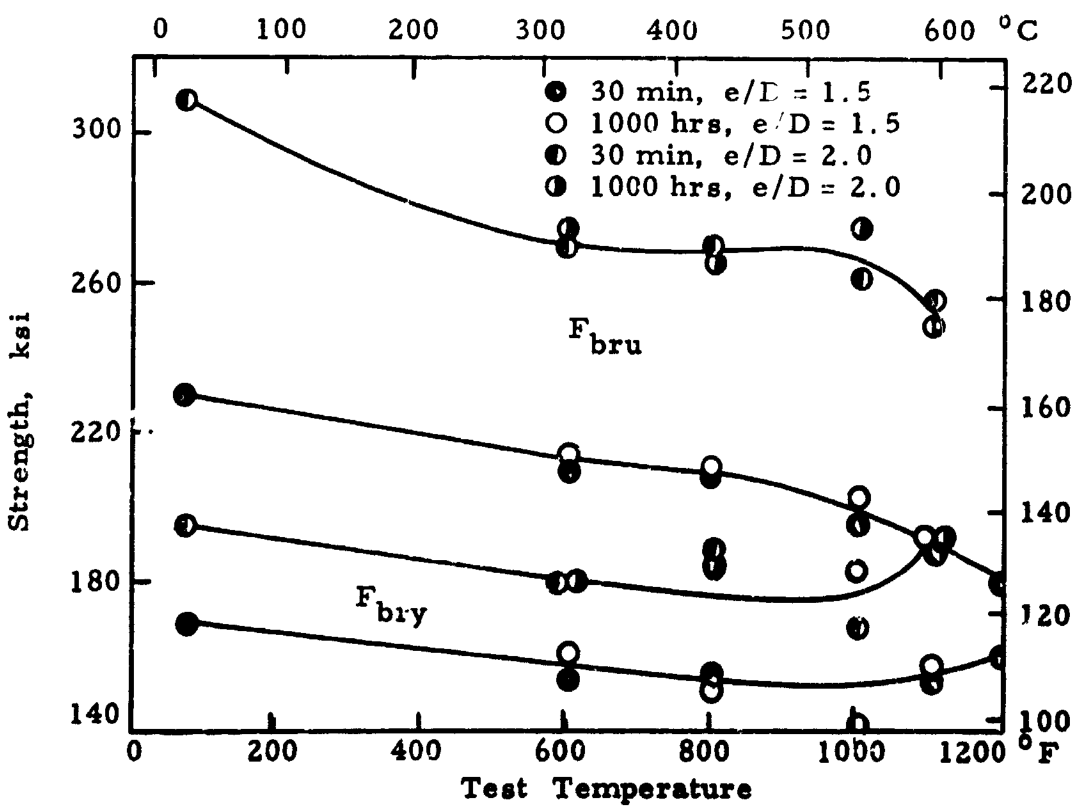

FIGURE 8.54. – Effect of exposure and test temperature on bearing properties of A-286 sheet, 0.062 in (1.57 mm). [1800°F (982°C), 1 hr, OQ, 1325°F (718°C), 16 hrs] (Refs. 8.14, 8.15)

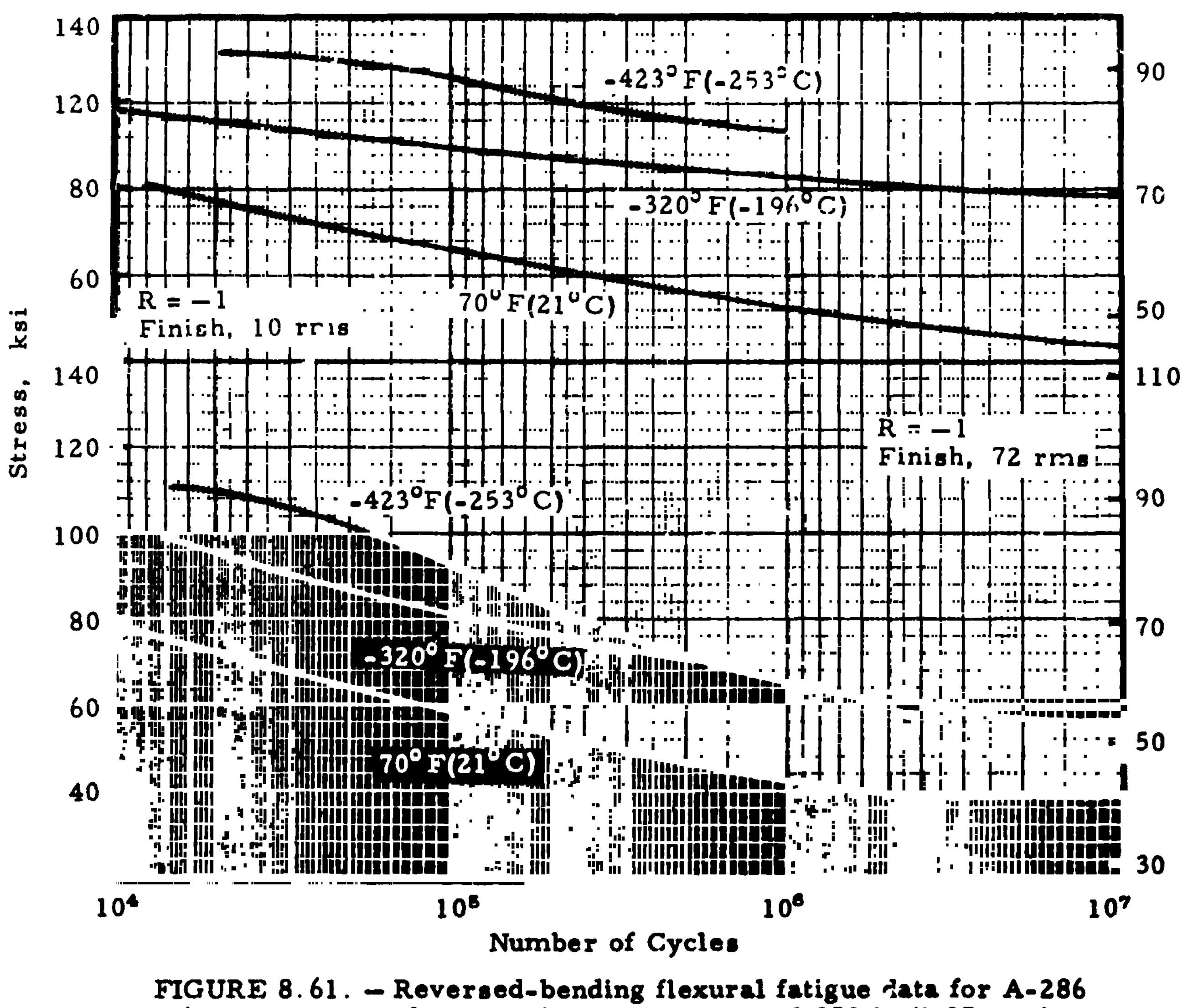

FIGURE 8.61. — Reversed-bending flexural fatigue data for A-286 sheet at room and cryogenic temperatures; 0.050 in (1.27 mm). [1800° F(982° C), aged 1325° F(718° C), 16 hrs]

(Ref. 8.2)

Chapter 8 - References

8.1 Universal-Cyclops Specialty Steel Division, "Unitemp A-286," HT 3020, 1971.

8.2 E.H. Schmidt, "Fatigue Properties of Sheet, Bar, and Cast Metallic Materials for Cryogenic Applications," Rocketdyne Report R-7564 under Contract NAS8-18734, 30 August 1968; see also NASA Tech Brief 70-10199.

8.3 Carpenter Technology Corporation, "Carpenter A-286," Technical Data, June 1970.

8.4 American Iron and Steel Institute, "High Temperature High-Strength Alloys," New York, February 1963.

8.5 AMS Material Specifications, Society of Automotive Engineers, Inc., New York; latest Index, May 1971.

8.6 Allegheny Ludlum Steel Corporation, "A-286," Product Data.

8.7 J.W. Montano, "An Evaluation of the Mechanical and Stress Corrosion Properties of Cold Worked A-286 Alloy," NASA TM X-64569, February 12, 1971.

8.8 Superior Tube, "Super Alloy Tubing," June 1968.

8.9 ASTM STP-160, "A-286," August 1954, p. 70.

8.10 R.G. Matters and R.E. Lochen, "Materials for Helical Compression Springs for Use at Constant Deflection from 600 to 1400 F," ASTM Proc., 56, 672 (1956).

8.11 J.W. Besemer and V.A. Stanton, "Springs for Use at High Temperature," Metal Progress, April 1965, p. 84.

8.12 Metals Handbook, 8th Edition, Vol 1, "Properties and Selection of Materials," American Society for Metals, Metals Park, Ohio, 1961.

8.13 R.H. Raring, et al., "Progress Report of the NASA Special Committee on Material Research for Supersonic Transports," NASA TN D-1798, May 1963.

8.14 J.R. Kattus, J.B. Preston, and H.L. Lessley, "Determination of Tensile, Compressive, Bearing, and Shear Properties at Elevated Temperatures," WADC TR 58-365, November 1958.

8.15 J.S. Sessler and V. Weiss, Eds., "Aerospace Structural Metals Handbook," AFML TR 68-115, 1971 Edition.

Chapter 9

PHYSICAL PROPERTIES

9.1 Density, ρ (at room temperature)

0.286 lb/in^3 (7.94 g/cm^3) (refs. 9.1 through 9.5)

9.2 Thermal Properties

9.21 Thermal conductivity, K, figure 9.21.
9.22 Thermal coefficient of expansion, α, see figure 9.21.
9.23 Specific heat,
0.11 Btu/in^2 ^{0}F (70^o – 1300^o F)
0.11 cal/cm ^{o}C (20 – 700^o C) (refs. 9.1, 9.2)
9.24 Thermal diffusivity

9.3 Electrical Properties

9.31 Electrical resistivity, table 9.31.

9.4 Magnetic Properties

9.41 The alloy remains essentially nonmagnetic, even after cold working (ref. 9.1).
9.42 Permeability (H=200 oersteds):

Solution treated,	1.010 (ref. 9.2)
Solution treated and aged,	1.007/1.003 (refs. 9.2, 9.1)
Cold worked and aged to Rc 40 min,	1.015/1.020 (ref. 9.1).

9.5 Nuclear Properties

9.51 The maximum hardening of austenitic steels by irradiation occurs at about 300^o C, and causes increases in room temperature yield and ultimate strength, accompanied by reductions in ductility. Annealing at 500^o to 600^o C can remove these changes in tensile properties. A drastic reduction of ductility takes place at elevated temperatures and cannot be removed by annealing to 1350^o C. The effect of irradiation on creep has not been firmly established, but there is general agreement that elongation at failure is reduced (ref. 9.8).
9.52 Effect of irradiation and testing at -257^o C on tensile properties of A-286, table 9.52.

9.6 Other Physical Properties

9.61 Emissivity
9.62 Damping capacity

TABLE 9.31. — Electrical Resistivity

Source		Refs. 9.1, 9.2	
Alloy		A-286	
Temperature °F	°C	Microhms-in	Microhms-cm
87	30.5	35.8	91.0
1000	538	45.5	115.6
1200	649	46.8	118.8
1350	732	47.3	120.1
1500	816	48.2	122.4

TABLE 9.52. — Effect of Irradiation at -257°C on Tensile Properties of Alloy Tested at -257°C

Source	Refs. 9.6, 9.7				
Alloy	A-286				
Specimen	F_{ty}, ksi (kg/mm²)	F_{tu}, ksi (kg/mm²)	Notched F_{tu}, ksi (kg/mm²)	Elong, %	Redn in Area, %
Unirrad.	135.9 (95.5)	223.6 (157.2)	185.8 (130.5)	37.5	31.0
Irrad. (a)	137.0 (96.3)	219.7 (154.5)	188.6 (132.6)	30.4	32.2
Unirrad. (b)	149.6 (105.2)	235. (165.2)	216.4 (152.1)	34.5	46.5
Irrad. (c)	152. (106.9)	229. (245.7)	245.7 (172.7)	33.5	16.
Unirrad. (b)	156.8 (110.2)	238.2 (167.4)	255. (179.3)	31.8	42.2
Irrad. (c)	165.7 (116.5)	238. (167.3)	239. (168.0)	31.0	39.7

(a) 5.0×10^{16} n/cm²

(b) Two different heats

(c) 1.0×10^{17} n/cm²

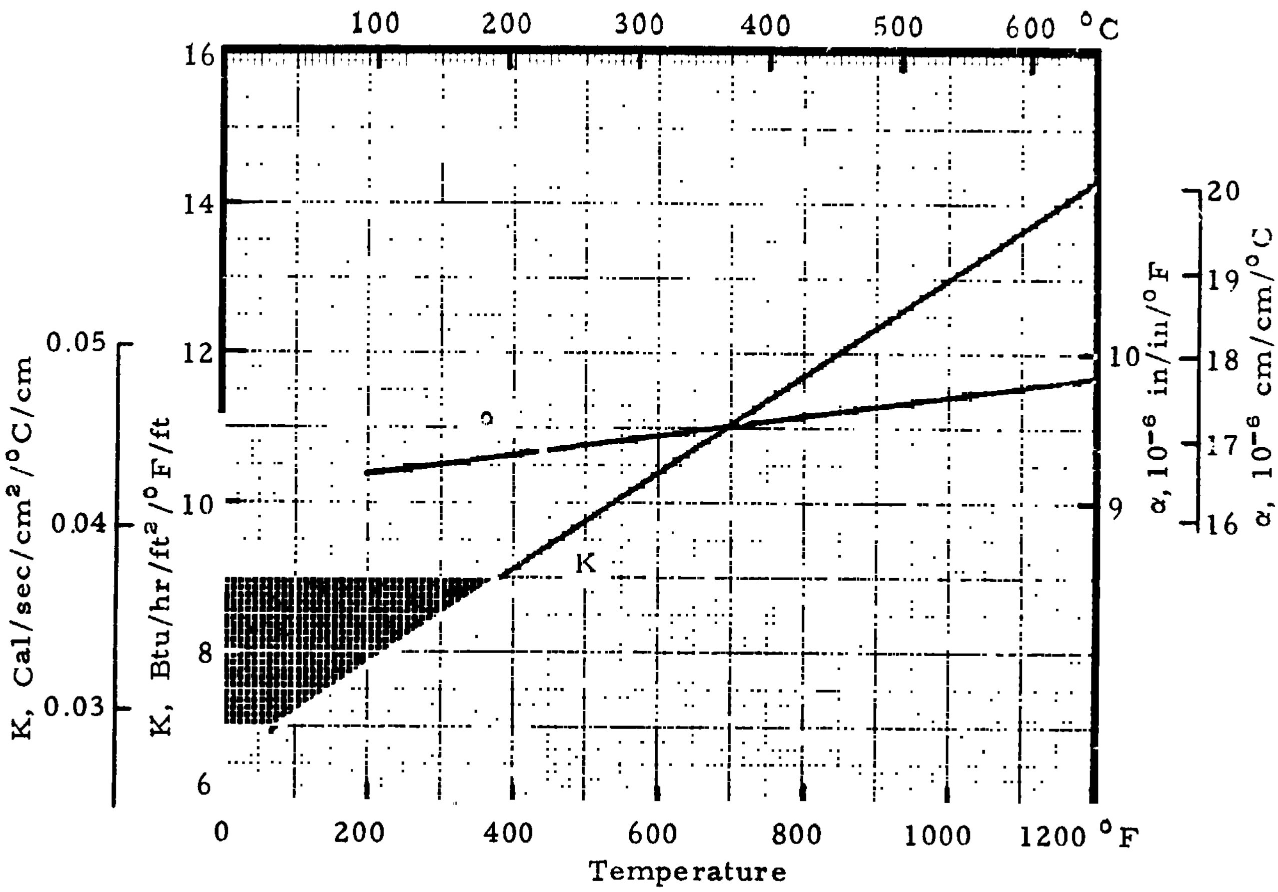

FIGURE 9.21. — Effect of temperature on the physical properties of A-286.

(Ref. 9.5)

Chapter 9 - References

9.1 Universal-Cyclops/Specialty Steel Div., "Unitemp A-286," HT 3020, 1971.

9.2 Allegheny Ludlum Steel Corp., "A-286," Product Literature.

9.3 American Iron and Steel Institute, "High Temperature High Strength Alloys," February 1963.

9.4 1971 SAE Handbook, Society Automotive Engineers, New York.

9.5 Military Handbook-5A, Dept. of Defense, FSC 1500, "Metallic Materials and Elements for Aerospace Vehicle Structures," February 1966; latest change order, January 1970.

9.6 J.J. Lombardo, C.E. Dixon, and J.A. Bagley, "Cryogenic Radiation Effects on NERVA Structural Materials," paper presented at 69th Ann. Mtg. ASTM, Atlantic City, New Jersey, June 27-July 1, 1966.

9.7 C.A. Schwanbeck, "Effect of Nuclear Radiation on Materials at Cryogenic Temperatures," NASA CR-54881, January 1965.

9.8 M. Kangilaski, 'Radiation Effects Design Handbook: Section 7. Structural Alloys," NASA CR-1873, October 1971.

Chapter 10

CORROSION RESISTANCE AND PROTECTION

10.1 General. In common with other stainless steels, A-286 tends to be passive by virtue of an oxygen-containing surface film. It shows good resistance to all atmospheres encountered in jet engine and turbo supercharger service up to at least 1300° F (704° C), and has shown excellent performance in 20-percent salt spray tests. Because of the high nickel content, A-286 is more resistant than 18-8 stainless steels to cool, dilute sulfuric acid solutions (ref. 10.1).

10.2 Corrosion in Water. The resistance of stainless steels to corrosion in water at high temperatures is generally excellent. However, case hardening of the steels by nitriding or malcomizing (see Chapter 11) can decrease initial corrosion resistance to the extent that usefulness is limited in water at 500° C. The rate of corrosion in supercritical water varies with test temperature. As shown in figure 10.2, A-286 is resistant to attack at 800° F (427° C) and 5000 psi (3.5 kg/mm^2); appreciably higher rates of corrosion are observed at 1000° and 1350° F (538° and 732° C) (ref. 10.2).

10.3 Oxidizing Environments. The resistance of A-286 to attack is not good in strong, selective oxidizing environments such as nitric—hydrofluoric acid and boiling 65-percent nitric acid. Intergranular corrosion may occur in the aged condition, and care must be used when pickling with nitric—hydrofluoric acid mixtures after aging (ref. 10.1).

Alloy A-286 is adequately resistant to oxidation without special coatings for service to temperatures up to about 1300° F (704° C). It does not compare favorably with stainless steel Types 309 and 310 above about 1500° F (816°C) (ref. 10.1).

Highly localized regions of surface oxidation have been observed in A-286 that is subjected to cyclic plastic strain at elevated temperatures of 950° to 1150°F (510° to 621° C). Apparently, there is localized and reversed grain boundary deformation that leads to repeated rupture of the protective oxide film, and also accelerated oxidation in the region of deformation. These regions become the nuclei for initiating fatigue cracks (ref. 10.3).

10.4 Propellant Environments. Alloy A-286 has been found compatible with the following propellants for long-term applications (ref. 10.4):

Condition	Propellant	Test Temperature
Rust-free	Aerozine-50,	55°-60°F (10°-16°C)
-	Hydrazine ,	<100° F (<38° C)
-	Unsymmetrical dimethylhydrazine,	<140° F (<60° C)
Annealed	Nitrogen tetroxide (<0.5% H_2O) ,	55°-60°F (10°-16°C)

10.5 Hydrogen Embrittlement. The austenitic stainless steels are not greatly affected by atomic hydrogen absorbed during descaling or electroplating processes (ref. 10.5). To investigate the mechanical aspects of hydrogen-induced failure in solution-treated and aged A-286, fracture toughness tests were conducted on precracked bead specimens loaded in 3-point bending. Hydrogen test environments were molecular hydrogen at a pressure of 680 torr and an atomic-molecular hydrogen mixture at a molecular hydrogen pressure of 8×10^{-3} torr; comparative runs were made in a vacuum environment. The fatigue cracks in A-286 would not propagate under the bending mode of loading in any of the environments; there were no failures (ref. 10.6).

10.6 Protective Measures. As pointed out earlier, surface treatment of A-286 for resistance to corrosion is rarely required. However, surface treatments used for improvement of other characteristics are discussed in chapter 11, along with available information on the effect that such treatments may have on resistance to corrosion.

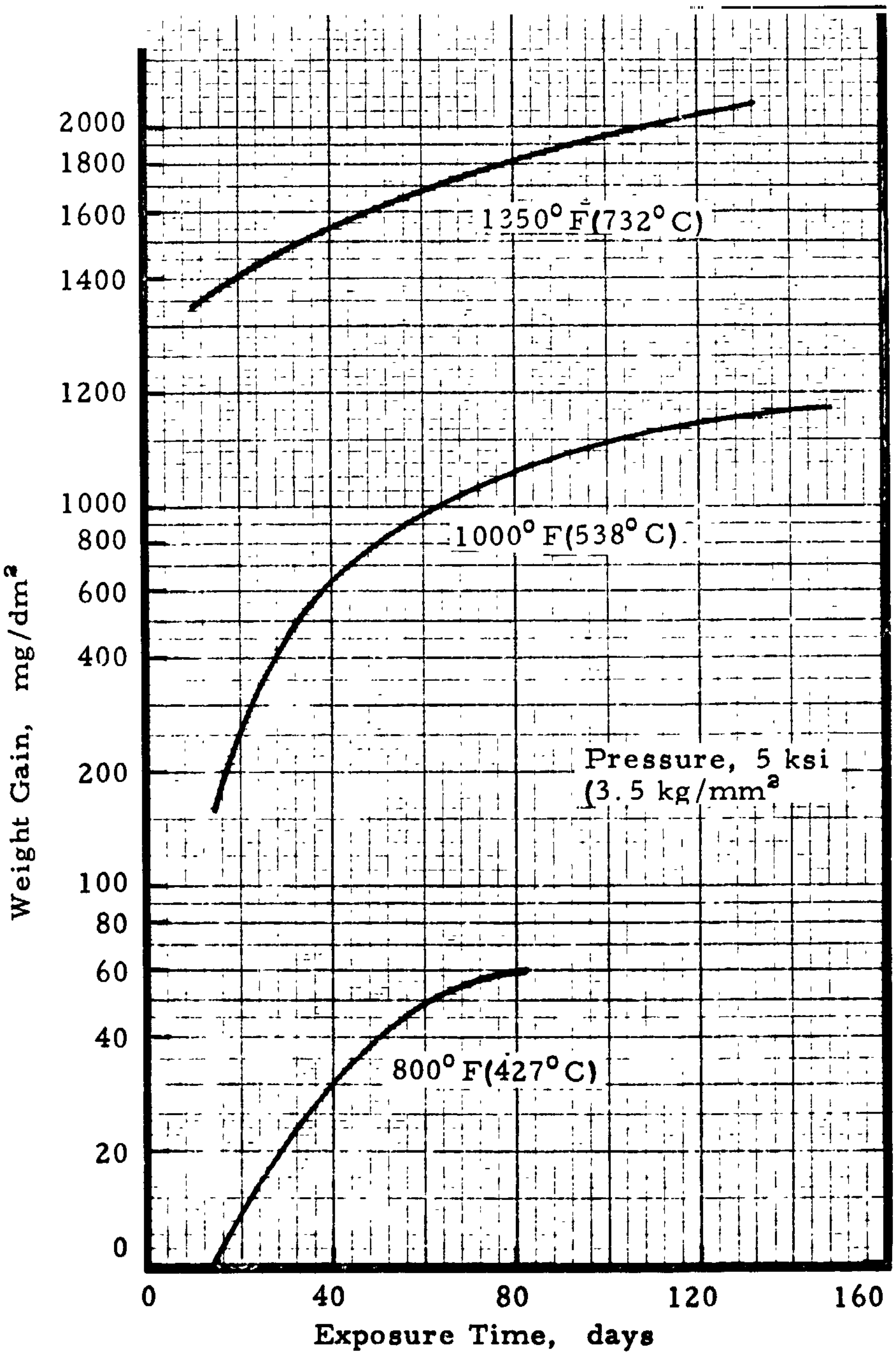

FIGURE 10.2. — Corrosion of A-286 in degassed supercritical water.

(Ref. 10.2)

Chapter 10 - References

10.1 Universal-Cyclops/Specialty Steel Division, "Unitemp A-286," HT 3020, 1971.

10.2 Karl F. Smith, "Stainless Steels," in C.R. Tipton, Jr., Ed., Reactor Handbook, Vol 1, Interscience Publishers, New York, 1960.

10.3 L. F. Coffin, Jr., "Cyclic-Strain-Induced Oxidation of High-Temperature Alloys," Trans. ASM, 56, 339 (1963).

10.4 K.D. May, "Advanced Valve Technology," NASA SP-5019, February 1965.

10.5 Battelle Memorial Institute, "Surface Treatments for Precipitation Hardening Stainless Steels," NASA SP-5090, 1968.

10.6 H.G. Nelson, "The Kinetic and Mechanical Aspects of Hydrogen-Induced Failure in Metals," NASA TN D-6691, April 1972.

Chapter 11

SURFACE TREATMENTS

11.1 General. The surface of alloy A-286 may be treated chemically, mechanically, or electrochemically to remove scale developed during heat treatment or to improve resistance to wear, resistance to stress-corrosion cracking, fatigue life, etc. In general, the end-use of heat-resisting alloys does not require that they have a polished finish.

11.2 Scale Removal. Scale formed during heat treatment may be removed mechanically by shot or grit blasting, tumbling, vapor honing, etc., or may be removed chemically by acid pickling solutions. The mechanical methods are generally employed as a supplement to chemical methods. In this instance, a final sand blasting will produce an attractive finish; however, it is mandatory that sand be used rather than steel grit to avoid surface contamination by metallic particles. On the other hand, mechanical methods are often preferred because of the possibility of intergranular corrosion resulting from strong pickling acids or prolonged pickling times (refs. 11.1, 11.2). The most widely used chemical procedures consist essentially of scale-conditioning in an oxidizing caustic bath followed by immersion in a pickling bath. Several examples of chemical procedures are summarized in table 11.2.

11.3 Mechanical Treatments. Mechanical treatments such as burnishing, explosive hardening, planishing, or peening are not generally used for components made of A-286. However, such treatments may occasionally be used to advantage (ref. 11.5). For example, it has been shown that shock loading does increase the hardness of A-286 and may effect economic savings by reducing aging time (refs. 11.5, 11.7). The peening of welds in A-286 sheet has produced a marked increase in fatigue strength compared with as-welded joints (ref. 11.8). A compendium of information on shot peening for improved fatigue properties and resistance to corrosion of high-strength alloys has recently become available (ref. 11.6).

11.4 Coatings. Precipitation-hardening stainless steels are not carburized intentionally because the process is detrimental to corrosion resistance and other properties. In order to avoid the effects of carburizing (i.e., carbon absorption), A-286, for example, is usually heat treated in an air atmosphere rather than in so-called neutral atmospheres which contain the products of fuel combustion (ref. 11.5).

All stainless steels, because of their chromium content, can be case-hardened by nitriding. Diffusion of nitrogen into the material is aided by the chromium content which facilitates the formation of a stable case with high hardness. This hardness increases wear resistance, develops antigalling properties, and improves fatigue resistance (ref. 11.5). On the other hand, nitriding detracts from resistance to corrosion because nitrogen, introduced by nitriding, combines with available chromium in the surface layers to form chromium nitride, which is not as protective as chromium oxide.

A proprietary nitriding process known as "Malcomizing" has been used for case-hardening of A-286 . The process requires temperatures of 920° to 1050° F (493° to 565° C) and times of 6 to 8 hours. It is recommended that A-286 be solution annealed and refrigerated prior to Malcomizing. Case depth after Malcomizing is 0.00335-0.005 in (0.0089-0.013 cm) and surface hardness is DPH 650—850 (ref. 11.9).

Torch-fusion techniques for hard-surfacing of A-286 have been used successfully for aircraft arresting-gear hookpoints (ref. 11.5).

11.5 Electroplated Coatings. In general, it is not necessary to electroplate A-286 for the usual reasons of improving corrosion resistance or other properties (ref. 11.5). However, in order to prevent tearing and scoring of extruded shapes, A-286 has been electroplated with an 0.04-inch (1.02 mm) layer of nickel prior to hot extrusion with standard glass lubricants (ref. 11.10).

Although the alloy is difficult to braze, it can be brazed readily if coated with nickel or iron (ref. 11.11). Additionally, stress-corrosion cracking may be prevented by electrodeposited Ni-Cd (ref. 11.12) on parts which cannot be stress relieved adequately.

After descaling or other surface preparations such as wiring, jigging, machining, and final cleaning, A-286 can be activated for electroplating by immersion, cathodic, or anodic treatments (ref. 11.5). After activation, the work is transferred to the plating bath as quickly as possible.

TABLE 11.2. — Examples of Chemical Descaling Procedures

Source	Refs. 11.1, 11.2, 11.3, 11.4			
Alloy	A-286			
Operation	Bath Composition	Temperature °F	°C	Time, min
(Ref. 11.2)				
Descale	NaOH with oxidizing additives	950	510	25-30
Quench	Water	Ambient		2-1/2
Neutralization	18% H_2SO_4 + 5% HCl	170-180	76-82	5
Rinse	Water	Ambient		2
Acid treatment	25% HNO_3 + 5% HF	Ambient		5-10
Rinse	Water	Ambient		1
(Ref. 11.1)				
Descale	Molten caustic	-	-	-
Quench	Water	-	-	-
Neutralization	12–15% H_2SO_4	140-160	60-71	15
Rinse	Water	-	-	-
Acid treatment	12–15% HNO_3 + 1–2% HF	110	43	10
Rinse	Hot water	-	-	-
(Ref. 11.3)				
Descale	Oxidizing salt	900	482	-
Quench	Water	-	-	-
Neutralization	20% H_2SO_4	-	-	5
Rinse	Water	-	-	-
Acid treatment	35–40% HNO_3 + 4% HF	-	-	20
Rinse	Water	-	-	-
(Ref. 11.4)				
Descale	1.5–2% NaH	700-730	371-388	5-20
Quench	Water	Ambient		1/4-1/2
Neutralization	2–10% H_2SO_4	70-140	21-60	1-3
Acid treatment	2–4% HF + 20% HNO_3	130-140	55-60	5-15
Rinse	Water	Ambient		1/4-1/2
High-pressure spray wash	Water, 100 psi (0.07 kg/mm^2)	Ambient		(a)

(a) Governed by part configuration; 1 min for parts with accessible surfaces.

Chapter 11 - References

11.1 Universal Cyclops /Specialty Steel Division, "Unitemp A-286," HT 3020, 1971.

11.2 Metals Handbook, 8th Ed., Vol. 5, "Forging and Casting," American Society for Metlas, Metals Park, Ohio, 1970.

11.3 L.J. Hull, "Techniques for Welding and Fabrication of the A-286 High Temperature Alloy," Welding Design and Fabrication, 34 (10), 58 (1961).

11.4 Metals Handbook, 8th Ed., Vol.2, "Heat Treating, Cleaning, and Finishing," American Society for Metals, Metals Park, Ohio, 1964.

11.5 Battelle Memorial Institute, "Surface Treatments of Precipitation Hardening Stainless Steels," NASA SP-5090, 1968.

11.6 Metals and Ceramics Information Center, "Shot Peening for Improved Fatigue Properties and Stress-Corrosion Resistance," December 1971 (AD 735-409).

11.7 B.G. Koepke, R.P. Jewett, and W.T. Chandler, "Strengthening Iron-Base Alloys by Shock Waves," ML TDR 64-282, 1964.

11.8 C.R. Smith and D.H. Love, "Development of Elevated Temperature Sheet Spot-Welded and Seam-Welded Joints," ASD TR 61-67, 1961.

11.9 Lindberg Steel Treating Co., "Malcomizing for Improved Properties in Stainless Steels."

11.10 L.M. Christensen, "Development of Methods, Processes, and Techniques for Producing Steel Extrusions," ML TDR 64-231, July 1964.

11.11 E.D. Huschke and G.S. Hopkin, III, "High-Temperature Vacuum Brazing of Jet Engine Materials," Welding J., Res. Suppl., 34 (5), 2335 (1958).

11.12 L.E. Gatzek, "Corrosion Control of Missiles in Long-Term Silo Environments," paper 916A, SAE Aeron. and Space Eng. and Mfg. Mtg., Los Angeles, Calif., Oct. 5-9, 1964.

Chapter 12

JOINING TECHNIQUES

12.1 General. Alloy A-286 is the most weldable steel in the group of precipitation-hardening austenitic stainless steels (ref. 12.1). It can be joined satisfactorily by fusion welding, resistance welding, and brazing (ref. 12.3). Welding processes are similar to those used for welding austenitic stainless steels (e.g., ref. 12.1). Specifications for A-286 welding wire, flash welded rings, bolts and screws, and rivets are listed in Chapter 2, table 2.1.

12.2 Welding. It is important that welding conditions be carefully controlled to avoid cracking in the weld or adjacent to the weld in the heat affected zone. This is especially true when large sections are being welded under restraint. Alloy A-286 passes through an area of low ductility upon cooling; if restraint conditions are severe, the cooling stresses may be relieved by cracking rather than deforming. It is good practice to solution treat after welding and then age harden. Heating to the solution temperature of 1650° F or 1800° F (899° or 982° C) should be accomplished as rapidly as possible (ref. 12.3).

The production of satisfactory joints is also dependent upon the proper selection of joining methods, proper joint design, and proper cleaning of material prior to making the joint (ref. 12.4). Details of weldment evaluation methods are given in reference 12.5

Contamination during joining or treating processes of either base or weld metal by dirt, grease, crayon marks, etc. can seriously affect resistance to corrosion. Carbon pickup can also affect heat-treatment response, and sulfur pickup can affect mechanical properties. Dirt and films of oil and grease can be removed by washing or degreasing operations; soaps can be removed with hot water. A hot alkaline wash followed by a hot water rinse is required for soluble oils, tallows, and fats (ref. 12.4). Removal of scale is discussed in chapter 11.

12.21 Fusion Welding. Fusion welding of A-286 is generally performed by the gas tungsten-arc process (TIG), but shielded metal arc and gas metal-arc (MIG) processes have also been used satisfactorily (refs. 12.1, 12.3, 12.4). Welding precautions are similar to those required for nickel-base alloys, such as careful control of gas current, arc length, speed of welding, filler metals, backing materials, and condition of equipment (ref. 12.6), with additional precautions inherent in the welding of superalloys: Stress-relief prior to welding is required for parts that have been worked or deformed; welded parts must be rapidly heated and cooled through the aging range to avoid embrittling carbide precipitations in the grain boundaries (see also section 12.2); as far as possible, fusion welds are designed in low stress areas because a matrix-strengthened filler metal is generally used, yielding between 80- to 90-percent joint efficiency (ref. 12.7). Tooling components for welding must be nonmetallic or nonmagnetic, and the tooling should not contaminate the base metal (ref. 12.4).

12.211 Tungsten Inert-Gas (TIG) Process. In thin sections under conditions of low restraint, hot-cracking tendencies are minimized with the TIG process. The weldability of A-286 is improved by keeping heat input to a minimum and using small, light stringer beads. Whenever multiple passes are required, it is usually necessary to use one of the dissimilar filler metals (ref. 12.1).

Alloy A-286 filler metal is usually used for TIG welding of light-gage material. In the instances where weld joint geometry is complex, a dissimilar filler metal is used, such as Inconel 92 which will also respond to the age-hardening treatment. Hastelloy W may also be used, but it does not age-harden. Other austenitic stainless steels may be used, such as Type 310, where resistance to corrosion is more desirable than high strength (ref. 12.1).

12.212 Electron Beam Welding. Electron beam welding has been used successfully to join A-286 to dissimilar metals, for example, a turbine wheel consisting of an A-286 turbine disc and a ring of Udimet-500 blades (ref. 12.4).

12.213 Mechanical Properties of Fusion Welds

12.2131 Tensile properties of TIG welds at room and elevated temperatures, table 12.2131.

12.2132 Tensile properties of MIG welds at room temperature, table 12.2132.

12.2133 Tensile properties of TIG welds in A-286 sheet at cryogenic temperatures, figure 12.2133.

12.22 Resistance Welding. Sheet products and bar of small cross section can be welded satisfactorily by spot, overlap spot, or seam welding. Flash, upset, or projection welding are used to a lesser degree. Alloy A-286 is generally resistance welded in the solution-treated condition, then aged or re-solution treated and aged after welding (refs. 12.3, 12.4, 12.7).

12.221 Spot and Seam Welding. Precipitation-hardening stainless steels have been welded successfully with conventional resistance spot-welding equipment. Because of the higher currents and electrode forces required for thicker sheet and the harder alloys, such as A-286, the larger press-type machines are more suitable. Factors to be considered are the same as for other steels: Joint overlap must be sufficient to contain the weld; weld locations must be accessible to the equipment to be used; forging pressure will be inadequate to provide proper contact of part of it is used to form the parts; sufficient spot spacing must be used so that current is not reduced at the desired location because of shunting through previously made welds (ref. 12.4). "Coring" or incipient melting is a feature that has been observed in spot welding A-286, which may resemble small cracks in the plane of the sheet extending from the edge of the weld nugget toward the unaffected base metal. Central cracking has also been observed. It is suggested that increases in electrode force and in weld time will reduce the likelihood of internal cracking (refs. 12.4, 12.12).

Little information is available directly on seam welding of A-286. However, studies have shown that the most common cause of porosity and internal cracks is incorrect weld spacing; successive weld nuggets must not be too close. Cracking can be reduced also by slower welding speeds and longer weld and cool times. Continuous seam welding eliminates cracking (refs. 12.4, 12.12).

12.222 Flash Welding. Flash welding is better adaptable to the high-strength heat-treatable alloys than arc, spot, or seam welding in two respects: (1) Molten metal is not retained in the joint; thus, cast structures that might be preferentially corroded are not present. (2) The hot metal in the joint is upset; this upsetting operation may improve the ductility of the heat affected zone. Other advantages include weight saving because there is no need for overlapping welding, flanges, bolting, or riveting. With suitable design, machining costs can be reduced. Machine capacity (especially transformer capacity) for welding A-286 does not differ greatly from that required for other steels; however, the upset-pressure capacity must be higher.

Flash welding conditions of greatest importance are flashing current, time and speed, and upset pressure and distance. In general, high flashing speeds and short flashing times are used when it is desirable to minimize weld contamination. Flash welds that have mechanical properties approaching those of the base metal are regularly produced in conventional machines, with joint efficiencies commonly better than 95 percent (ref. 12.4).

12.223 Mechanical Properties of Resistance Welds

12.2231 Operating conditions and resulting shear strengths for spot welds, table 12.2231.

12.2232 Effect of shot-peening on fatigue resistance of 4-spot welded joints in STA sheet, figure 12.2232.

12.2233 Tensile properties of flash butt-welds at room temperature, table 12.2233.

12.3 Brazing. Alloy A-286 can be brazed in vacuum or in atmospheres of pure dry hydrogen or argon. Mechanical properties of brazed joints are somewhat impaired because of the brazing time—temperature cycle, but may be improved by solution treating and aging after brazing (ref. 12.3).

As with any other welding procedure, surfaces must be clean and free of contaminants. Because of the aluminum and titanium content in A-286, brazing in controlled atmospheres is necessary to prevent the formation of refractory oxides of these metals on the alloy surface. Formation of the oxides may also be circumvented by copper or nickel plating of the alloy surface prior to brazing (ref. 12.4).

12.31 Comparison of the stress-rupture life at 1200° F (649° C) of A-286 base alloy and nickel-plated alloy with that of brazed welds is shown in figure 12.31.

12.32 Tensile properties of butt-brazed welds at room and elevated temperatures are plotted in figure 12.32.

12.33 It has been shown that the tensile strengths of braze-coated A-286, tested at 1200° F (649° C), are reduced more than 25 percent when a braze containing boron (e.g., AMS 4775) is used (ref. 12.14). (See also figure 12.32.) Additionally, ductility, as measured by elongation, may be reduced to zero. Consequently, brazing operations for the production of cooled turbine blades were examined carefully (ref. 12.18). It was found that even in an atmosphere of hydrogen with a dewpoint of -110° F (-79° C) and at temperatures to 2300° F (1260° C), deleterious oxide formation could not be prevented. Hence, electroplating of the base metal was used to promote wetting of the base metal by the braze alloys. A minimum thickness of 0.0002 inch (0.00508 mm) nickel plate was found to be satisfactory for successful brazing. The effect of nickel plate thickness on the stress-rupture life of A-286 brazed welds tested at 1200° F (649°C) is indicated in figure 12.33. It was also observed that a brazing alloy of Ni-Cr-Si was less harmful to the stress-rupture life of A-286 than one of Ni-Cr-Si-B.

12.4 <u>Fastening</u>. Successful fastening of the high-strength heat-resisting A-286 requires, of course, fasteners of at least equivalent properties, generally A-286 itself. The excellent tensile and stress properties of A-286 wire and bolts have been illustrated in Chapters 7 and 8. The tensile properties of A-286 rivets are generously recorded in MIL-HDBK-5A (ref. 12.16) for use with other high-strength corrosion-resistant alloys.

12.41 The shear strength of A-286 rivets compared with those of high-strength aluminum and nickel alloys is illustrated in figure 12.41.

12.42 The tensile strengths of A-286 rivets in A-286 sheet are summarized in table 12.42.

TABLE 12.2131. — Tensile Properties of TIG Welds (Manual) at Room and Elevated Temperatures

Source	Ref. 12.8								
Alloy	A-286								
Post-Weld Treatment	1310° F (710° C), 16 hrs, AC								
Sheet (a)	Temp. °F	°C	Fty (0.2%), ksi	kg/mm²	Ftu ksi	kg/mm²	Elongation (2 in), %	Redn in Area, %	Fracture Location
Base metal (0.032-in, 0.813-mm)	600	316	100.9	76.6	140.1	98.5	17	26	-
	1200	649	95.8	67.4	116.0	81.6	9	14	-
Across-the-weld	RT		100.3	72.4	150.6	105.9	13	16	weld
	RT		100.9	76.6	149.6	105.2	13	14	weld
	RT		99.3	69.8	148.6	104.5	12	14	weld
	1200	649	92.0	64.7	101.3	71.2	2	5	weld
	1200	649	92.6	65.1	107.0	75.2	4	6	weld
	1200	649	90.1	63.3	102.2	71.9	2	8	weld
Base metal (0.062-in, 1.58-mm)	1200	649	89.7	63.1	112.9	79.4	12	15.5	-
Across-the-weld	RT		98.0	68.9	138.8	97.6	13	21	weld
	RT		101.3	71.2	142.2	100.0	16	26	weld
	RT		99.8	70.2	141.9	99.8	15	24	weld
	1200	649	86.7	70.0	108.5	76.3	7	17	weld
	1200	649	85.8	60.3	101.0	71.0	4	10	weld
	1200	649	86.1	60.5	98.3	69.1	3	11	weld

(a) Condition of sheet prior to welding not reported.
No filler wire used.
No edge preparation used.

TABLE 12.2132. — Tensile Properties of MIG Welds at Room Temperature

Source	Ref. 12.8						
Alloy	A-286						
Condition	1650° F (899° C), 1 hr, OQ						
Form	1-1/2 x 1/2 in (38.1 x 12.7 mm) bar						
Post-Weld Treatment	F_{ty} (0.2%) ksi	F_{ty} (0.2%) kg/mm²	F_{tu} ksi	F_{tu} kg/mm²	Elongation (2 in), %	Redn in Area, %	Fracture Location
Base metal	100.6	70.7	148.2	104.1	25.5	46.7	-
Across-the-weld (a)							
1325° F (718° C), 16 hr, AC	105.1	73.9	139.8	98.3	13.0	35.4	HAZ
1325° F (718° C), 16 hr, AC + 1200° F (649° C), 20 hr, AC	109.3	76.8	139.8	98.3	11.0	42.1	weld
1650° F (899° C), 1 hr, OQ + 1325° F (718° C), 16 hr, AC +1200° F (649° C), 20 hr, AC	105.5	74.2	141.0	99.1	11.0	32.2	weld
1800° F (982° C), 1 hr, OQ + 1325° F (718° C), 16 hr, AC	93.0	65.4	128.9	90.6	17.0	43.4	weld
1800° F (982° C), 1 hr, OQ, + 1325° F (718° C), 16 hr, AC + 1200° F (649° C), 20 hr, AC	107.2	75.4	145.1	102.1	15.0	35.6	weld

(a) **Aircomatic process with pure argon gas cover.** 1/16 in (1.59 mm) A-286 filler wire. **Double-V groove design;** 80° total machined angle. **Welding speed, 12 in/min** (30.5 cm/min); 1 pass per side; 320-375 amperes; **reversed DC polarity;** 26.5-30.0 volts.

TABLE 12.2231. — Operating Conditions and Resulting Shear Strengths for Spot Welds

Source	Ref. 12.9										
Alloy	A-286 (a)										
Thickness	Tip face diameter, in	Tip face diameter, mm	Electrode force, lb	Electrode force, kg	Weld time, cycles	Weld current, amp	Nugget diameter, in	Nugget diameter, mm	Av shear strength lb	Av shear strength kg	Tension/shear ratio, %
0.036/0.036 in (0.91 mm)	3/16	4.76	950	431	15	4800	0.128	3.25	1090	494	61.2
			800	408	10	5200	0.145	3.68	1200	544	69.3
			1000	454	7.5	6100	0.100	2.54	920	417	44.3
0.064/0.064 in (1.63 mm)	1/4	6.35	1500	680	30	6900	0.255	6.47	2770	1256	78.8
			1700	771	20	7500	0.245	6.22	2580	1170	76.0
			1700	771	15	7900	0.245	6.22	2640	1198	76.7

Preweld condition: fully soft. Post-weld treatment: none.

TABLE 12.2232. — Tensile Properties of Flash Butt-Welds at Room Temperature

Source	Ref. 12.8						
Alloy	A-286						
Form/Condition	3/4-in (19-cm) bar; 1650°F (899°C), 1 hr, OQ						
Post-Weld Treatment	F_{ty} (0.2%) ksi	F_{ty} (0.2%) kg/mm²	F_{tu} ksi	F_{tu} kg/mm²	Elongation (2 in), %	Redn in Area, %	Fracture Location
Base metal	100.6	70.7	148.2	104.2	25.5	46.7	-
As-welded (a)	83.7	58.8	103.9	73.[illegible]	7.0	67.2	weld
950°F (510°C), 16 hr, AC	86.1	60.5	108.8	76.5	7.5	48.3	weld
1325°F (718°C), 16 hr, AC	98.5	69.3	147.3	103.6	22.0	40.6	weld

(a) Flashing burn-off, 0.5 in (12.7 mm); starting voltage, 450V; flashing voltage, 400V; **upset force,** 22.7–25.9 ksi (15.6–18.2 kg/mm²).

TABLE 12.42. – Ultimate and Yield Strengths of Protruding Head Solid Rivets in Sheet

Source		Ref. 12.16																	
Alloy		A-286																	
Rivet material		A-286 (NAS 1198)																	
Sheet material		A-286, solution-treated and aged																	
Test temperature		Room temperature						1200° F (649° C), stabilized 15 min						1200° F(649° C), rapid heating in 20 sec, tested in 15 sec					
Rivet diameter, in (mm)		1/8 (3.18)		5/32 (3.97)		3/16 (4.76)		1/8 (3.18)		5/32 (3.97)		3/16 (4.76)		1/8 (3.18)		5/32 (3.97)		3/16 (4.76)	
Sheet thickness		Ultimate strength																	
Inch	mm	lb	kg	lb	kg	lb	kg	lb	kg	lb	kg	lb	kg	lb	kg	lb	kg	lb	kg
0.020	0.508	478	217																
0.025	0.635	590	268	740	336			331	150					470	213				
0.032	0.813	745	338	932	423	1132	513	426	193	626	284			587	266	726	329		
0.040	1.02	923	328	1152	523	1397	634	560	254	801	363	962	436	752	341	930	422	1117	507
0.050	1.27	1023	464	1428	648	1677	761	682	309	1002	455	1204	546	783	355	1164	528	1397	634
0.063	1.60	1131	513	1578	716	1821	826			1044	474	1505	683			1198	543	1729	784
0.071	1.80	1170	531	1660	753	1909	866					1507	684						
0.080	2.03			1752	795	2008	911												
0.090	2.29			1790	812	2118	961												
0.100	2.54					2229	1011												
0.125	3.18					2504	1136												
0.160	4.06					2580	1170												
Rivet shear strength		1170	531	1790	812	2580	1170	682	309	1044	474	1507	684	783	355	1198	543	1729	784
		Yield strength																	
0.020	0.508	447	203					300	136					300	136				
0.025	0.635	613	278	695	315			374	170	464	210			374	170	464	210		
0.032	0.813	809	367	983	446	974	442	598	271	593	269	713	323	478	217	593	269	712	323
0.040	1.02	867	393	1243	564	1167	529	682	289	925	420	890	404	598	271	740	336	889	403
0.050	1.27	938	425	1331	604	1407	638			1044	474	1112	504	474	339	924	419	1110	503
0.063	1.60	1031	468	1447	656	1649	748					1400	635	783	355	1164	528	1398	634
0.071	1.80	1089	494	1518	689	1723	782					1507	684			1198	543	1552	704
0.080	2.03	1153	523	1597	724	1806	819											1563	709
0.090	2.29	1170	531	1686	765	1898	861											1575	714
0.100	2.54			1775	805	1990	903											1587	720
0.125	3.18			1790	812	2221	1007											1618	734
0.160	4.06					2543	1154											1661	753

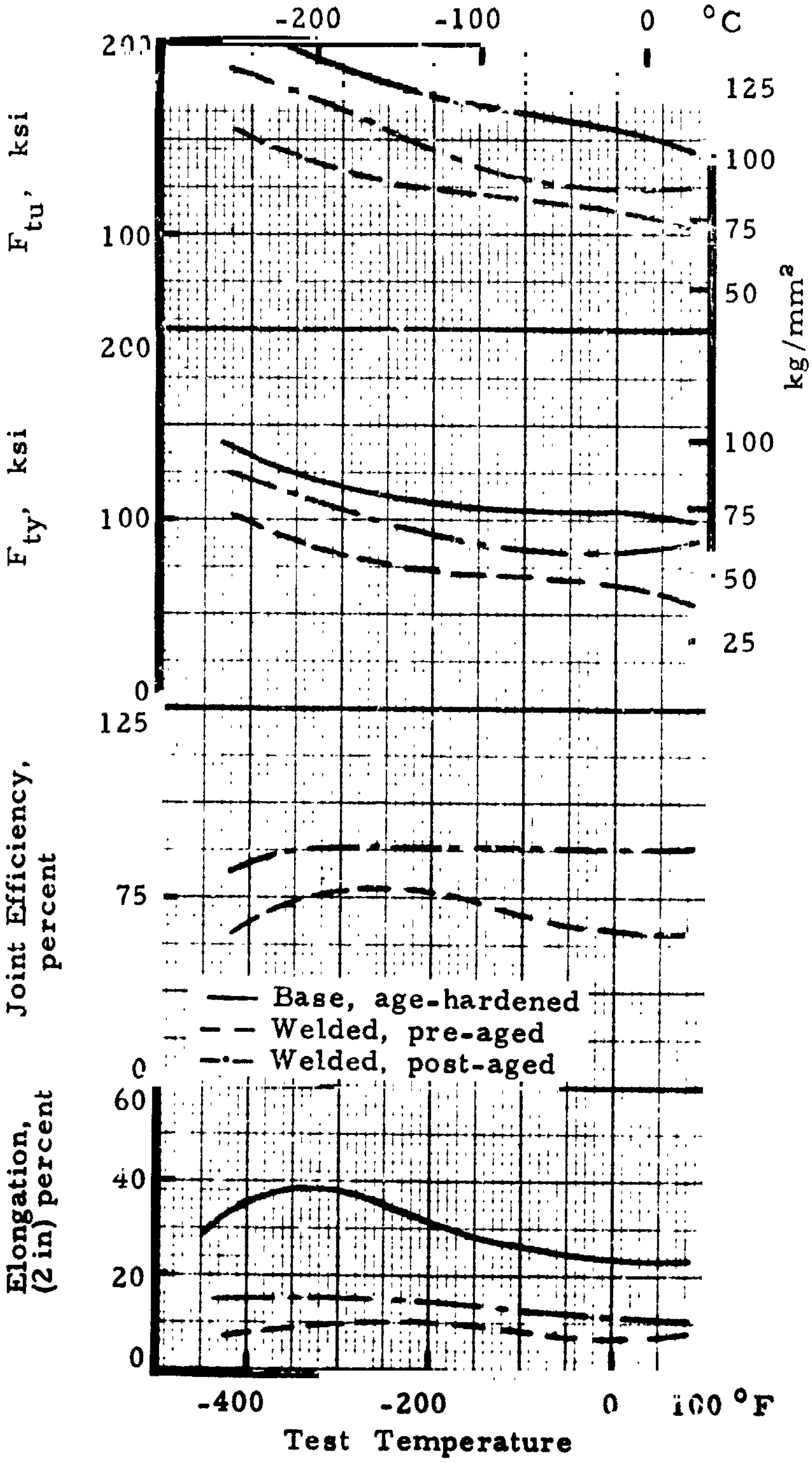

FIGURE 12.2133. — Tensile properties of TIG welds in A-286 sheet at cryogenic temperatures; thickness, 0.095 in (2.41 mm). [Aged, 1350°F (742°C), 16 hrs] (Ref. 12.10)

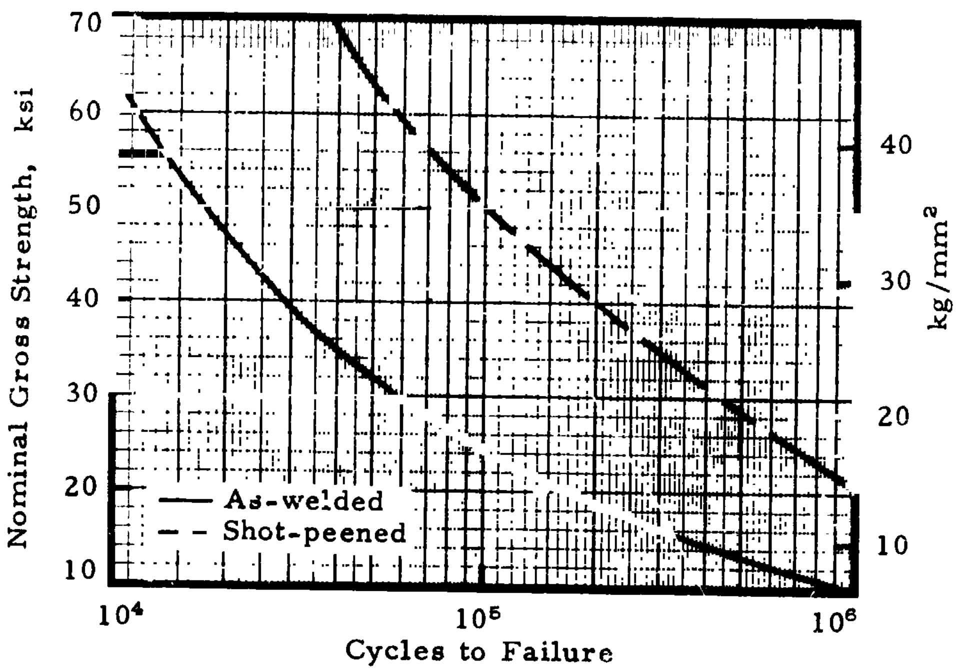

FIGURE 12.2232. — Effect of shot-peening on fatigue resistance of a 4-spot weld lap joint; 0.05-in (1.27-mm) sheet; 1800°F (982°C), 10 min, OQ + 1325°F (718°C), 16 hrs. (Ref. 12.1)

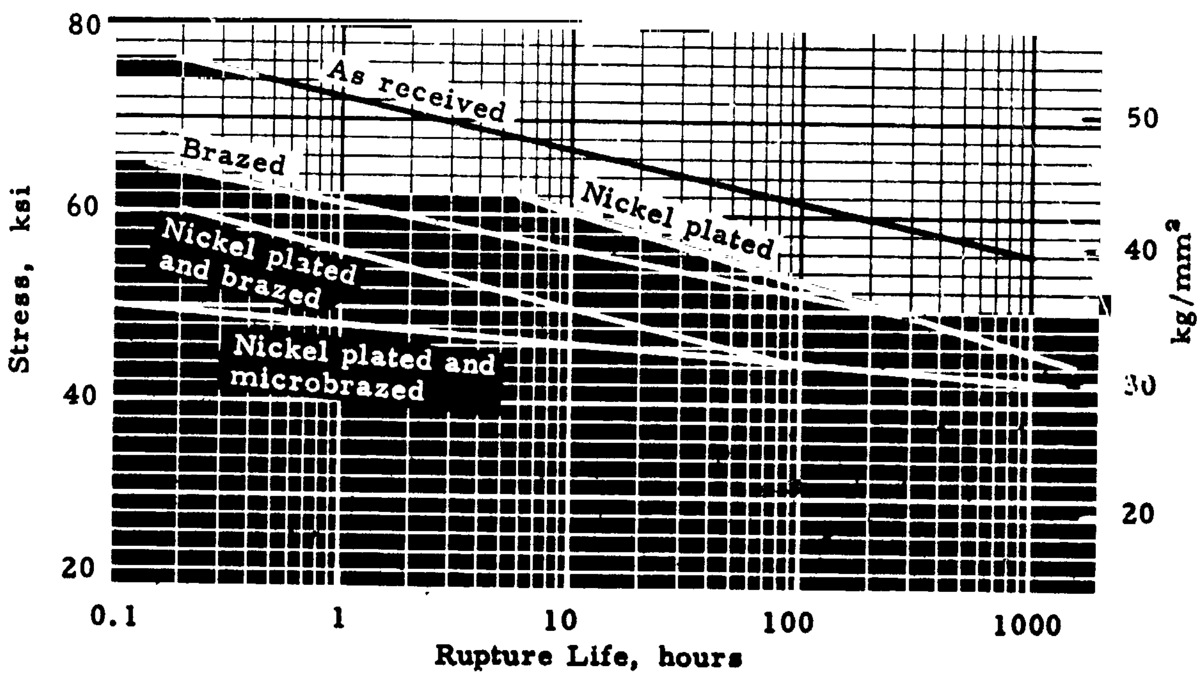

FIGURE 12.31. — Comparison of stress-rupture life of A-286 base alloy and nickel-plated alloy with that of brazed welds. (Ref. 12.13)

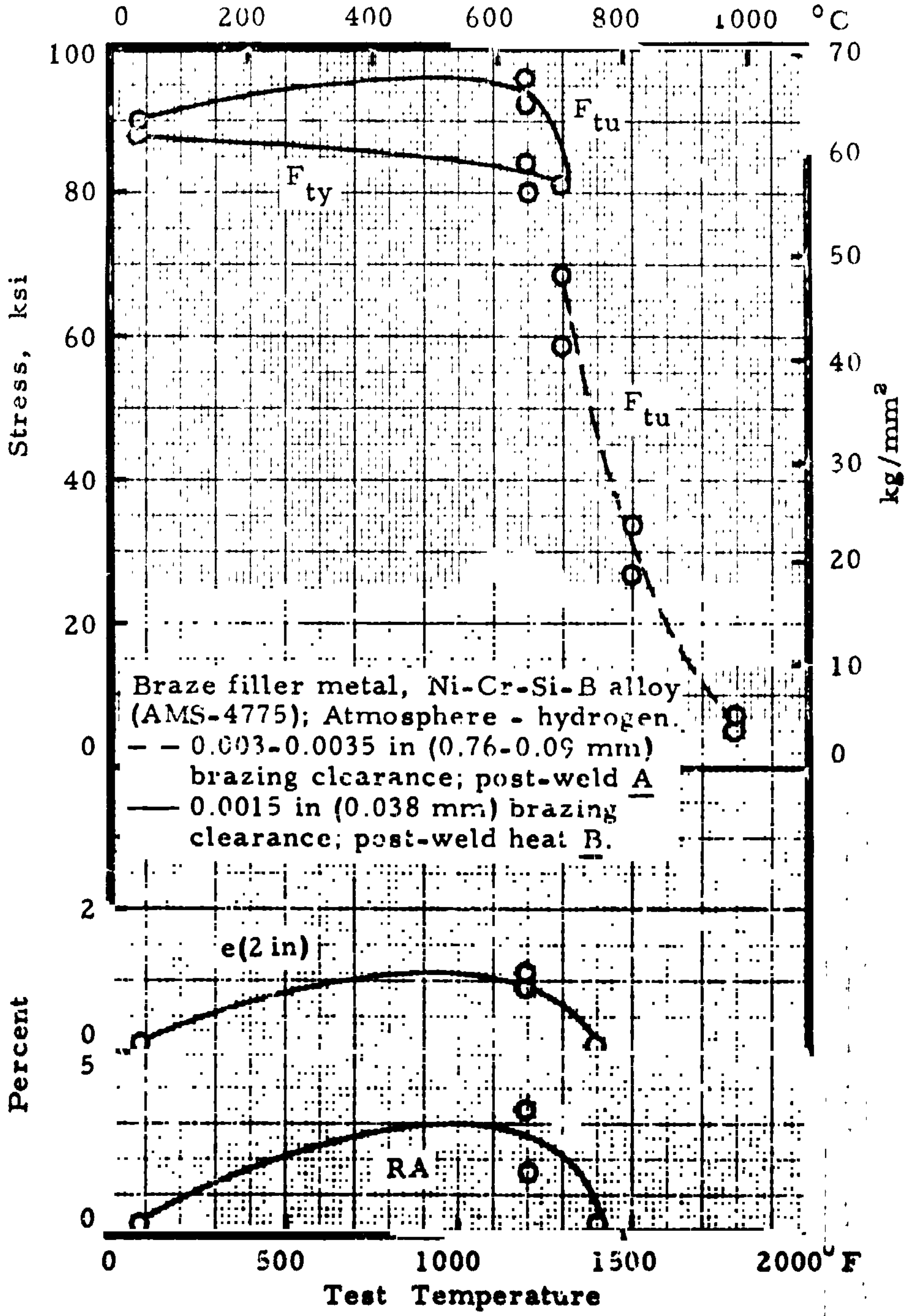

FIGURE 12.32. — Tensile properties of butt-brazed welds in A-286 at room and elevated temperatures; 11/2-in wide by 1/2-in thick (4.81 x 1.27 cm) bar; 1800°F (982°C), 1 hr, OQ, + 1325°F (718°C), 16 hrs, AC.

[A: 1325°F (718°C), 16 hrs, AC.
B: 1650°F (899°C), 1 hr, OQ, + 1325°F (718°C), 16 hrs, AC]

(Ref. 12.8)

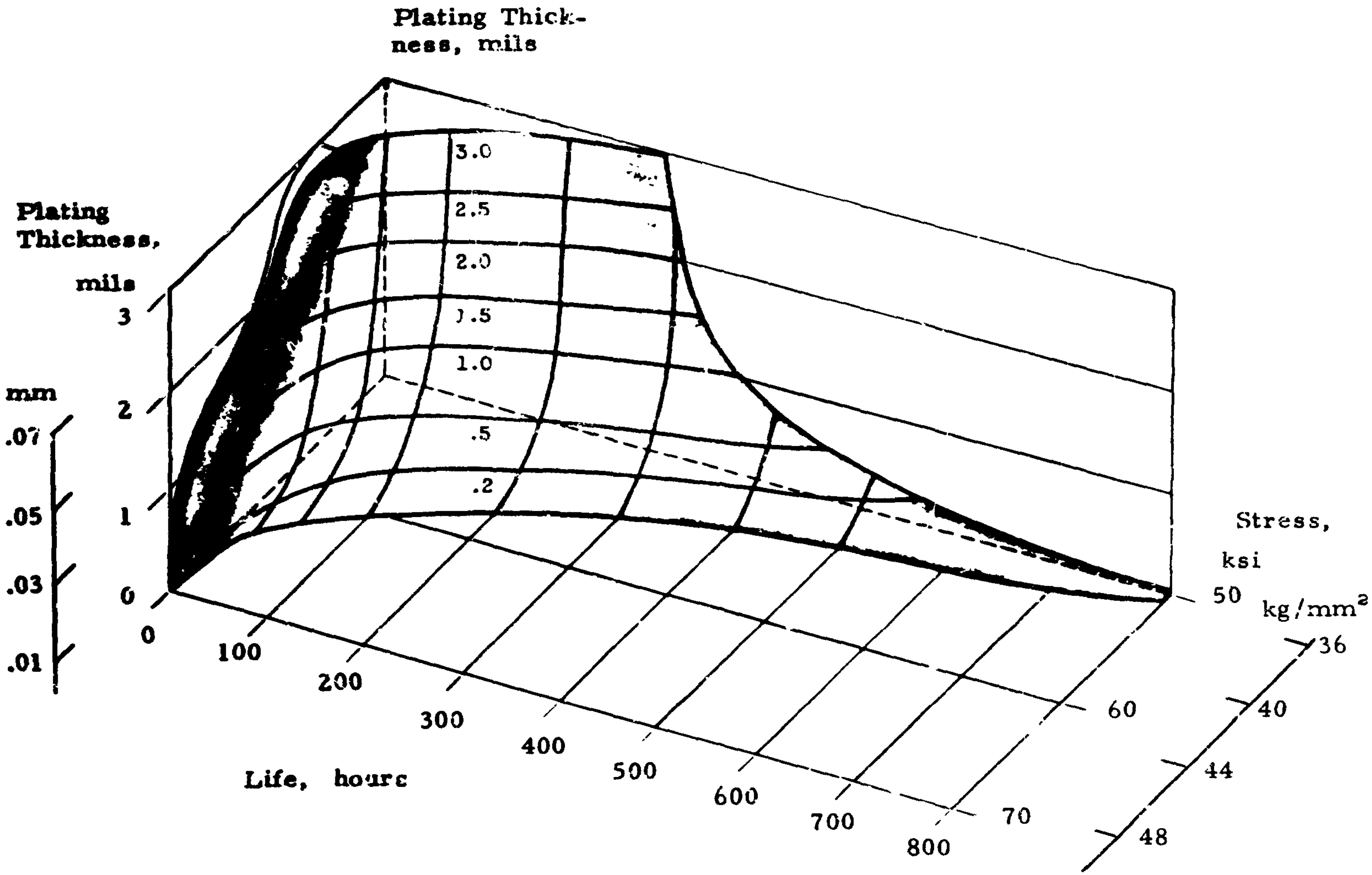

FIGURE 12.33. — Effect of nickel plating thickness on stress and life of A-286 tested in stress-rupture at 1200°F (649°C).

(Ref. 12.15)

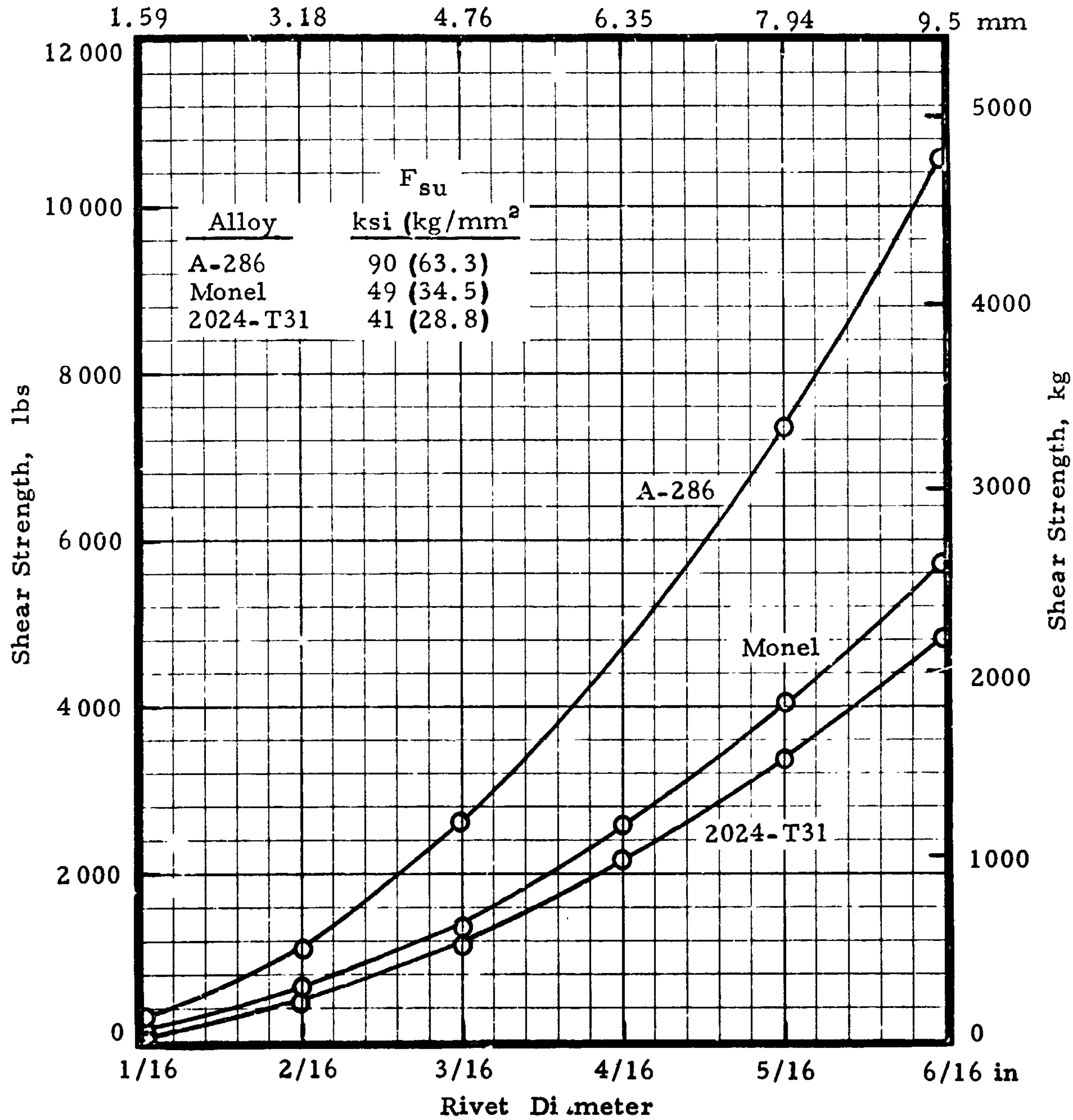

FIGURE 12.41. – Comparison of shear strengths of rivets.

(Ref. 12.16)

F

Chapter 12 - References

12.1 R. Kaltenhauser, "Weldability of Precipitation-Hardening Stainless Steels," Metals Eng. Qtr., 9 (1), 44 (1969).

12.2 Republic Steel Corporation, "Arc Welding Stainless Steel. Part I, Basics of Arc Welding," Adv. 1948a-15M-370A.

12.3 Universal Cyclops/Specialty Steel Division, "Unitemp A-286," HT 3020, 1971.

12.4 J.J. Vagi, R.M. Evans, and D.C. Martin, "Welding of Precipitation Hardening Stainless Steels," NASA SP-5087, 1968.

12.5 J.J. Vagi, R.P. Meister, and M.D. Randall, "Weldment Evaluation Methods," DMIC Report 244, August 1968.

12.6 International Nickel Co./Huntington Alloys Division, "Joining the Huntington Alloys," Technical Bulletin T-2.

12.7 Welding Handbook, Sec. 5, American Welding Society, New York, 1967, Ch. 91.

12.8 ASTM STP-226, "The Elevated Temperature Properties of Weld-Deposited Metal and Weldments," 1958, p. 19?.

12.9 I.F. Squires, "Determination of Resistance Spot-Welding Characteristics for Some Heat-Resisting Stainless Steels," British Welding J., 9 (3), 149 (1962).

12.10 Marshall Space Flight Center, "Effects of Low Temperatures on Structural Metals," NASA SP-5012, December 1964.

12.11 C.P. Smith and D.H. Love, "Development of Elevated Temperature Sheet Spot-Welded and Seam-Welded Joints," ASD TR 61-67.

12.12 P.M. Knowlson, "An Explanation of Factors Affecting the Formation of Internal Cracks in Spot Welds in Nimonic Alloys and Some Stainless Steels," British Welding J., 9 (3), 168 (1962).

12.13 Metals Handbook, 8th Ed., Vol. 1, "Selection and Properties of Metals," American Society for Metals, Metals Park, Ohio, 1961.

12.14 W.E. Russell and J.P. Wisner, "An Investigation of High-Temperature Vacuum and Hydrogen Furnace Brazing," NASA TN-3932, 1957.

12.15 J.H. Sinclair and C.A. Gyorgak, "Effect of Two Braze Coatings, Processing Variables, and Heat Treatments on 1200°F Stress-Rupture Strength of L-605, A-286, and Inconel 700 Sheet," NASA TN D-1880, November 196?.

12.16 Military Handbook 5-A, Dept. of Defense, FSC 1500, "Metallic Materials and Elements for Aerospace Vehicle Structures," February 1966; latest change order; January 1970.